

# MODELING CHALLENGES OF MODERN ENERGY MARKETS: STUDIES ON UNCERTAINTY, COMPLEXITY, AND CONSTANT CHANGE

Von der Fakultät Maschinenbau, Elektro- und Energiesysteme der Brandenburgischen Technischen Universität Cottbus-Senftenberg zur Erlangung des akademischen Grades

Doktor der Sozialwissenschaften  
(Dr. rer. pol.)

genehmigte Dissertation vorgelegt von

Master of Science  
Igor Riepin

geboren am 12.11.1990 in Zaporizhzhia, Ukraine

<b>Vorsitzender</b>	Prof. Dr. Frank Wätzold	BTU Cottbus-Senftenberg
<b>Gutachter</b>	Prof. Dr. Felix Müsgens	BTU Cottbus-Senftenberg
<b>Gutachter</b>	Prof. Dr. Luis Baringo	Universidad de Castilla-La Mancha

**Tag der mündlichen Prüfung:** 23. Juni 2022



MODELING CHALLENGES OF MODERN ENERGY MARKETS:  
STUDIES ON UNCERTAINTY, COMPLEXITY, AND CONSTANT  
CHANGE

M. SC. IEGOR RIEPIN

University:  
Brandenburg University of Technology Cottbus-Senftenberg  
Faculty:  
Mechanical Engineering, Electrical and Energy Systems  
Chair:  
Chair of Energy Economics

M. Sc. Iegor Riepin:

*Modeling challenges of modern energy markets: studies on uncertainty, complexity, and constant change*

December 2021

CHAIR OF EVALUATION COMMITTEE:

Prof. Dr. Frank Wätzold

SUPERVISORS:

Prof. Dr. Felix Müsgens

Prof. Dr. Luis Baringo

REVIEWERS:

Prof. Dr. Felix Müsgens

Prof. Dr. Luis Baringo

LOCATION:

Cottbus

SUBMISSION DATE:

January 2022

DOI:

[10.26127/BTUOpen-5976](https://doi.org/10.26127/BTUOpen-5976)

## ABSTRACT

---

This dissertation is a compilation of four self-contained research articles that focus on selected subjects in the field of energy economics.

The first article focuses on the competitiveness of offshore wind in mature markets. In this work, we harmonise auction results based on the auction design features and introduce the *harmonised expected revenue* metric. We show that offshore wind power generation can be considered commercially competitive in mature markets without subsidy. Furthermore, once auction results are harmonised, we observe similar expected revenue streams of wind farms across countries. This finding means that different auction designs can fairly reflect the actual costs of developing wind farms and thus translate cost reductions into lower bids.

The second article explores the impacts of uncertainty in integrated electricity and gas system optimization models. We address the trade-off that the energy research community faces on a daily basis, i.e., whether to neglect uncertainty when constructing an energy system model and accept a suboptimal solution or to incorporate uncertainty and increase model complexity. Our research aims to bring a systematic understanding of which parametric uncertainties most substantially affect long-term planning decisions in energy system models. Moreover, the integrated model allows us to extend single-market evaluations by tracing the effects of uncertainty across the electricity and gas markets.

In the third article, we focus on seasonal flexibility in the European natural gas market. We develop a bottom-up market optimization model to simulate the operation of the gas market over a long period. This allows us to explore structural trends in market development, which are driven by changing supply and demand fundamentals. Our work contributes to the methodological question of how to measure the contributions of different flexibility options by proposing a *scaled coefficient of variation* metric. We show that the metric improves the understanding of seasonal flexibility's market dynamics.

Finally, the fourth article investigates the value of Projects of Common Interest—gas infrastructure projects supported by EU public funds—in maintaining gas system resilience amid cold-winter demand spikes, supply shortages, and budget constraints. For this purpose, we develop the first application of adaptive robust optimization to gas infrastructure expansion planning. Our modeling approach confronts the drawbacks of mainstream methods of incorporating uncertainty into gas market models, in which the modeler predefines the probabilities and realization paths of unknown parameters. The adaptive

robust optimization problem endogenously identifies the unfortunate realizations of unknown parameters and suggests the optimal investments strategies to address them. We find that (i) robust solutions point to consistent preferences for specific infrastructure projects, (ii) the real-world construction efforts have been focused on the most promising projects from a business perspective, and (iii) most projects are unlikely to be realized without financial support.

## ZUSAMMENFASSUNG

---

Diese Dissertation ist eine Zusammenstellung von vier in sich selbstständigen Forschungsartikeln, die sich auf ausgewählte Themen aus dem Bereich der Energiewirtschaft konzentrieren.

Der erste Forschungsartikel betrachtet die Wettbewerbsfähigkeit der Offshore-Windenergie in entwickelten Märkten. In dieser Arbeit harmonisieren wir Auktionsergebnisse auf der Grundlage von Auktionsdesignmerkmalen und entwickeln die Metrik *harmonisierte erwartete Erlöse*. Wir zeigen, dass die Offshore-Windenergieerzeugung in entwickelten Märkten ohne Subventionen als wettbewerbsfähig angesehen werden kann. Sobald die Auktionsergebnisse harmonisiert sind, stellen wir außerdem fest, dass die erwarteten Erlösströme von Windparks in allen Ländern ähnlich sind. Dies bedeutet, dass unterschiedliche Auktionsdesigns die tatsächlichen Kosten für die Entwicklung von Windparks angemessen widerspiegeln und somit Kostensenkungen in niedrigere Gebote umgesetzt werden können.

Der zweite Forschungsartikel untersucht die Auswirkungen der Unsicherheit in integrierten Optimierungsmodellen für Strom- und Gassysteme. Wir befassen uns mit einem Kompromiss, mit dem die Energieforschungsgemeinschaft täglich konfrontiert ist, d. h. mit der Frage, ob man die Unsicherheit bei der Erstellung eines Energiesystemmodells vernachlässigen und eine suboptimale Lösung akzeptieren soll oder die Unsicherheit einbezieht und dadurch die Modellkomplexität erhöht. Unsere Forschung zielt darauf ab, ein systematisches Verständnis dafür zu schaffen, welche parametrischen Ungewissheiten langfristige Planungsentscheidungen in Energiesystemmodellen am stärksten beeinflussen. Darüber hinaus ermöglicht uns das integrierte Modell, die Bewertung einzelner Märkte zu erweitern, indem wir die Auswirkungen von Unsicherheiten auf den Strom- und Gasmärkten verfolgen.

Im dritten Forschungsartikel konzentrieren wir uns auf die saisonale Flexibilität auf dem europäischen Erdgasmarkt. Wir entwickeln ein Bottom-up-Optimierungsmodell, um die Funktionsweise des Gasmarktes über einen langen Zeitraum zu simulieren. Dadurch können wir strukturelle Trends in der Marktentwicklung untersuchen, die durch sich ändernde fundamentale Strukturen von Angebot und

Nachfrage bestimmt werden. Unsere Arbeit leistet einen Beitrag zur methodischen Frage, wie die Beiträge verschiedener Flexibilitätsoptionen gemessen werden können. Hierfür schlagen wir die Metrik des *skalierten Variationskoeffizients* vor. Wir zeigen, dass diese Metrik das Verständnis der Marktdynamik der saisonalen Flexibilität verbessert.

Schließlich untersucht der vierte Forschungsartikel den Wert von Projekten von gemeinsamem Interesse—Gasinfrastrukturprojekte, die mit öffentlichen EU-Mitteln gefördert werden—für die Erhaltung der Leistungsfähigkeit des Gassystems in Zeiten von Nachfragespitzen in kalten Winterzeiten, Versorgungsengpässen und Budgetbeschränkungen. Zu diesem Zweck entwickeln wir die erste Anwendung der adaptiven robusten Optimierung auf die Planung des Ausbaus der Gasinfrastruktur. Unser Modellierungsansatz überwindet die Nachteile der gängigen Methoden zur Einbeziehung von Unsicherheiten in Gasmarktmodellen, bei denen der Modellierer die Wahrscheinlichkeiten und Realisierungspfade unbekannter Parameter vorgibt. Das adaptive robuste Optimierungsproblem bestimmt endogen schlimmstmögliche Realisierungen unbekannter Parameter und schlägt optimale Investitionsstrategien vor, um diese zu berücksichtigen. Wir stellen fest, dass (i) robuste Lösungen auf konsistente Präferenzen für bestimmte Infrastrukturprojekte hindeuten, (ii) die realen Baumaßnahmen sich auf die aus wirtschaftlicher Sicht vielversprechendsten Projekte konzentriert haben und (iii) die meisten Projekte ohne finanzielle Unterstützung kaum zu realisieren wären.





## PUBLICATIONS

---

PUBLICATIONS OF THE AUTHOR THAT HAVE BEEN SELECTED TO BE PART OF THIS THESIS.

This thesis presents journal articles as originally published and reprinted with permission from the corresponding publishers. The copyright of the original publications is held by the respective copyright holders.

### Peer-reviewed journal articles:

M. Jansen, I. Staffell, L. Kitzing, S. Quoilin, E. Wiggelinkhuizen, B. Bulder, I. Riepin, F. Müsgens (2020), Offshore wind competitiveness in mature markets without subsidy, *Nature Energy*, Issue 5, 614–622.

DOI: <https://doi.org/10.1038/s41560-020-0661-2>

Supplementary Software: <https://doi.org/10.5281/zenodo.3733604>

Supplementary Data: <https://doi.org/10.5281/zenodo.3840134>

Media coverage: <https://www.altmetric.com/details/86606597/news>

I. Riepin, T. Möbius, F. Müsgens (2021), Modelling uncertainty in coupled electricity and gas systems—Is it worth the effort? *Applied Energy*, Vol. 285, 116363.

DOI: <https://doi.org/10.1016/j.apenergy.2020.116363>

Code: <https://github.com/Irieo/IntEG>

Working paper in arXiv (2020): <https://arxiv.org/abs/2008.07221>

I. Riepin, F. Müsgens (2022), Seasonal flexibility in the European natural gas market, *The Energy Journal*, Vol. 43, Issue 1.

DOI: <https://doi.org/10.5547/01956574.43.1.irie>

Code: <https://github.com/Irieo/SeasonalFlex>

Summary: [www.iaee.org/ej/ejexec/ej43-1-Riepin-exsum.pdf](http://www.iaee.org/ej/ejexec/ej43-1-Riepin-exsum.pdf)

Working paper in Cambridge Press (2019): <https://doi.org/10.17863/CAM.43923>

I. Riepin, M. Schmidt, L. Baringo, F. Müsgens (in review), European gas infrastructure expansion planning: an adaptive robust optimization approach.

Code: <https://github.com/Irieo/ARO-GasInfrastructure>

Working paper in *Optimization Online* (2021): [http://www.optimization-online.org/DB\\_HTML/2021/10/8654.html](http://www.optimization-online.org/DB_HTML/2021/10/8654.html)

## OTHER PUBLICATIONS OF THE AUTHOR

The following is the second list of publications in which the author participated either as a lead or as a co-author. These publications were carried out within the same time frame as the publications that are selected to be a part of this thesis, and may possibly be cited within this work.

### Peer-reviewed journal articles:

T. Möbius, I. Riepin, F. Müsgens, A. H. van der Weijde (in review), Risk aversion in flexible electricity markets.

Code: <https://github.com/BTU-EnerEcon/RiskAv>

Working paper in arXiv (2020): <https://arxiv.org/abs/2110.04088>

I. Riepin, S. Sgarciu, M. Bernecker, T. Möbius, F. Müsgens (in review), Grok it and use it: Teaching energy systems modeling.

Code: <https://github.com/BTU-EnerEcon/EnergySystemsModelling-course>

M. Jansen, P. Beiter, I. Riepin, F. Müsgens, V. Juarez Guajardo-Fajardo, I. Staffell, B. Bulder, L. Kitzing (in review), Policy choices and outcomes for the global competitive procurement of offshore wind.

### Conference proceedings:

T. Möbius, I. Riepin (2020), Regret analysis of investment decisions under uncertainty in an integrated energy system, IEEE EEM.

DOI: <https://doi.org/10.1109/EEM49802.2020.9221935>

I. Riepin, T. Möbius, F. Müsgens (2018), Integrated electricity and gas market modeling – effects of gas demand uncertainty, IEEE EEM.

DOI: <https://doi.org/10.1109/EEM.2018.8469790>

F. Müsgens, I. Riepin (2018), Is offshore already competitive? Analyzing German offshore wind auctions, IEEE EEM.

DOI: <https://doi.org/10.1109/EEM.2018.8469851>

R. Montenegro, I. Riepin, P. Hauser (2016), Modelling of world LNG market development: focus on US investments and supplies, IEEE EEM.

DOI: <https://doi.org/10.1109/EEM.2016.7521361>

### Magazines and science explainers:

I. Riepin, M. Jansen, I. Staffell, F. Müsgens (2020), The era of ‘negative-subsidy’ offshore wind power has almost arrived, Guest post in CarbonBrief.

URL: <https://www.carbonbrief.org/guest-post-the-era-of-negative-subsidy-offshore-wind-power-has-almost-arrived>

F. Müsgens, I. Riepin (2020), Offshore-Windenergie - subventionsfrei? e|mlw.trends.

URL: <https://www.emw-online.com/trends/artikel/205364/offshore-windenergie-subventionsfrei>



## ACKNOWLEDGMENTS

---

This thesis is the culmination of a research journey that would not have been possible without the support of many people.

First of all, I am indebted to my PhD supervisor, Prof. Felix Müsgens, for everything he did for me. Trained as an engineer, I went on a challenging and exciting journey to pursue a doctoral degree in energy economics. Prof. Müsgens introduced me to the field, supported and inspired me throughout the years, and entrusted me with absolute freedom to select and pursue the research subjects presented in this thesis. I appreciate his support very much. A long time ago we discussed a statement: *“the best economists are engineers – but so are the worst”*. Professor, I hope that I will now join the good category of engineers who become economists.

Second, I thank Prof. Luis Baringo for the effort he took to become my second PhD supervisor. I learned a lot from his research articles and books, and enjoyed the chance to work together on a collaborative research project.

Third, I recognize and appreciate my colleagues’ and co-authors’ contributions to this thesis: Thomas Möbius, Malte Jansen, Iain Staffell, Lena Kitzing, Edwin Wiggelinkhuizen, Bernard Bulder, and Matthew Schmidt.

I also am deeply grateful to all my current and former colleagues who have discussed various versions of the papers presented in this thesis with me, as well as those with whom I have shared so many happy memories of working together: Sebastian Kreuz, Daniel Scholz, Taimyra Batz, Smaranda Sgarciu, Maximilian Bernecker, Thi Ngoc Nguyen, Eddy Jalbout, and Lucien Genge. Special thanks to Prof. Madeleine McPherson for making my research stay at the University of Victoria possible.

Finally, I am grateful to my parents and my wonderful wife Kristina for supporting me at every step.

I express my sincere words of appreciation for everyone who made a direct or indirect contribution to this thesis and was not mentioned here.

## RESEARCH FUNDING SUPPORT AND FORMAL ACKNOWLEDGMENTS

Most of the publications which are now part of this thesis were carried out with the financial support of the postgraduate scholarship (GradV) awarded by the BTU. The work in Chapter 5 was partially funded by the Federal Ministry of Education and Research of Germany (*Bundesministerium für Bildung und Forschung*) under the Ariadne project [FKZ: 03SFK500], which is part of the Kopernikus program.

I am greatly thankful for this support.



# CONTENTS

---

<b>I</b>	<b>INTRODUCTION</b>	
1	INTRODUCTION	2
1.1	Thesis structure . . . . .	3
1.2	Research questions and contribution to the body of research . . . . .	3
1.3	A note on open and reproducible research . . . . .	7
<b>II</b>	<b>MODELING CHALLENGES OF MODERN ENERGY MARKETS: STUDIES ON UNCERTAINTY, COMPLEXITY, AND CONSTANT CHANGE</b>	
2	OFFSHORE WIND COMPETITIVENESS IN MATURE MARKETS WITHOUT SUBSIDY	10
2.1	Introduction . . . . .	10
2.2	Offshore wind auctions in Europe . . . . .	12
2.3	Harmonization of expected revenues . . . . .	14
2.4	Moving towards subsidy-free offshore wind farms . . . . .	17
2.5	Sensitivity to future power prices . . . . .	19
2.6	Discussion and conclusions . . . . .	20
2.7	Methods . . . . .	23
3	MODELLING UNCERTAINTY IN COUPLED ELECTRICITY AND GAS SYSTEMS—IS IT WORTH THE EFFORT?	30
3.1	Introduction . . . . .	30
3.2	Integrated and stochastic modelling of electricity and gas markets in the literature . . . . .	32
3.2.1	Integrated modelling . . . . .	32
3.2.2	Stochastic modelling . . . . .	34
3.2.3	Identifying the research gap . . . . .	35
3.3	Methodology . . . . .	36
3.3.1	Optimization approaches . . . . .	37
3.3.2	The expected cost of ignoring uncertainty . . . . .	39
3.3.3	Scenario composition . . . . .	40
3.3.4	Model formulation . . . . .	42
3.3.5	Data . . . . .	47
3.4	Results . . . . .	50
3.4.1	Deterministic solutions . . . . .	50
3.4.2	Effects of ignoring uncertainty: All parameters . . . . .	51
3.4.3	Effects of disregarding uncertainty: Isolated parameters . . . . .	53
3.5	Conclusions . . . . .	57
4	SEASONAL FLEXIBILITY IN THE EUROPEAN NATURAL GAS MARKET	60
4.1	Introduction . . . . .	60

4.2	Methodology and data . . . . .	63
4.2.1	Related work . . . . .	64
4.2.2	Model structure . . . . .	65
4.2.3	Declarations . . . . .	67
4.2.4	Model formulation . . . . .	68
4.2.5	Data . . . . .	70
4.3	Results . . . . .	72
4.3.1	Quantitative supply contributions by source . .	73
4.3.2	Measuring seasonal flexibility . . . . .	77
4.4	Conclusions . . . . .	80
5	EUROPEAN GAS INFRASTRUCTURE EXPANSION PLAN- NING: AN ADAPTIVE ROBUST OPTIMIZATION APPROACH	83
5.1	Introduction . . . . .	83
5.2	Literature review . . . . .	85
5.2.1	Methods for addressing long-term uncertainty in energy systems models . . . . .	86
5.2.2	Long-term uncertainty and its representation in natural gas models . . . . .	87
5.3	Problem formulation . . . . .	88
5.3.1	Compact formulation . . . . .	88
5.3.2	Solution procedure . . . . .	90
5.3.3	Empirical application: European gas infrastruc- ture expansion problem . . . . .	94
5.4	Results and discussion . . . . .	99
5.4.1	Robust expansion considering cold-winter gas demand spikes . . . . .	100
5.4.2	Robust expansion considering cold-winter gas demand spikes and investment options beyond the PCI list . . . . .	102
5.4.3	Robust expansion considering cold-winter de- mand spikes and supply shortages . . . . .	105
5.4.4	Robust expansion considering an investment budget . . . . .	107
5.5	Summary and outlook . . . . .	111
 <b>III APPENDIX</b>		
A	LOGARITHMIC PRODUCTION COST FUNCTIONS	114
B	GEOGRAPHICAL COVERAGE OF THE GAS MARKET MODEL	115
C	DETAILED FORMULATION OF MODEL APPLICATION	116
C.1	Deterministic model . . . . .	118
C.2	Adaptive robust optimization model . . . . .	119
C.3	Uncertainty sets . . . . .	120
C.4	Feasibility sets . . . . .	120
C.5	Solution procedure . . . . .	121
C.5.1	Master problem . . . . .	121
C.5.2	Subproblem . . . . .	122



D DEMAND AND SUPPLY UNCERTAINTY BUDGETS	125
E PROJECTS OF COMMON INTERESTS INCLUDED IN THE ANALYSIS	126
F LITERATURE REVIEW OF NATURAL GAS MODELS AND REPRESENTATION OF UNCERTAINTY	127
BIBLIOGRAPHY	129

## LIST OF FIGURES

---

Figure 2.1	Raw bids received by auctions for new offshore wind capacity in five European countries over the past eight years . . . . .	13
Figure 2.2	Harmonized expected revenues for each offshore wind farm auctioned in Europe . . . . .	16
Figure 2.3	Effective subsidy for each offshore wind farm auctioned in Europe . . . . .	18
Figure 2.4	Effective subsidy given to offshore wind farms as a function of future real-term growth in wholesale power prices . . . . .	20
Figure 3.1	A two-stage stochastic problem and an approximation (EVP) . . . . .	39
Figure 3.2	Graphical illustration of scenario composition	41
Figure 3.3	Scenarios from the 2018 TYNDP report . . . . .	47
Figure 3.4	Investments in power generation capacities [GW] and total system costs [bn € <sub>2020</sub> ] for three deterministic scenarios and an expected value problem	51
Figure 3.5	Investments in power generation capacities [GW] for the stochastic solution . . . . .	52
Figure 3.6	Total expected system costs for the SS and four EEV (markers with a solid fill) and total system costs for four DS (markers with a pattern fill) .	52
Figure 3.7	Comparing residual load after varying demand (left) and RES capacity (right) following European Network of Transmission System Operators (ENTSOs) scenarios for 2030 . . . . .	55
Figure 3.8	Variation of variable costs for four technologies due to uncertainty regarding gas demand (first column), fuel price (second column) and CO <sub>2</sub> price (third column) . . . . .	56
Figure 4.1	Monthly natural gas production at the Groningen field, January 2011 - June 2018 . . . . .	62
Figure 4.2	Nodes included in the model and capacities of gas infrastructure elements as of 2017 (in bcm p.a.) . . . . .	66
Figure 4.3	Quantitative gas supply contributions for selected countries in bcm per month. Time axis depicts calendar years . . . . .	74

Figure 4.4	Annual load duration curves for selected countries in bcm per month. Time axis depicts calendar years. Values are sorted by gas consumption levels . . . . .	76
Figure 4.5	Annual Scaled Coefficient of Variations (SCVs) for selected countries . . . . .	79
Figure 5.1	Methods for incorporating uncertainty in energy optimization problems . . . . .	86
Figure 5.2	Schematic representation of ARO model formulation . . . . .	88
Figure 5.3	Schematic representation of CCG algorithm . . . . .	94
Figure 5.4	Stylized representation of the European natural gas network . . . . .	95
Figure 5.5	Scenario projections used for the construction of the uncertainty sets . . . . .	97
Figure 5.6	PCI included in the analysis: 26 pipelines and four LNG regasification terminals . . . . .	98
Figure 5.7	Robust expansion plan considering a set of PCIs under four uncertainty budgets for gas demand (columns). The horizontal axis aggregates demand spike values per country on an annual basis. Scenarios include two CAPEX assumptions (rows) . . . . .	103
Figure 5.8	Robust expansion plan considering a set of PCIs and a 20% capacity increase option for any arc in the network (pipeline or regasification terminal) located in the EU. Scenarios include four uncertainty budgets for gas demand (columns) and two CAPEX assumptions (rows). The horizontal axis aggregates demand spike values per country on an annual basis . . . . .	106
Figure 5.9	Robust expansion plan considering a set of PCIs under different uncertainty budgets for gas demand (columns) and supply (rows). Horizontal axis aggregates demand spike values on an annual basis per country. Vertical axis presents annual supply cut per country . . . . .	108
Figure 5.10	Robust expansion plan considering a set of PCIs subject to investment budgets. Scenarios entail four annualized budgets (columns) . . . . .	110
Figure A.1	Marginal production cost functions for two selected nodes . . . . .	114
Figure D.1	Illustrative example of the worst-case demand and supply realisations subject to uncertainty budgets $[\Gamma]$ . . . . .	125

## LIST OF TABLES

---

Table 2.1	Main characteristics of the auction systems for offshore wind capacity in five European countries	15
Table 3.1	The expected costs of ignoring uncertainty: A composite mode (considering all uncertain parameters) . . . . .	53
Table 3.2	Expected costs of ignoring uncertainty: Isolated parametric uncertainty . . . . .	54
Table E.1	Projects of Common Interests included in the analysis (Chapter 5) . . . . .	126
Table F.1	Overview of natural gas studies and their respective representation of uncertainty . . . . .	127

## ACRONYMS

---

ARO	Adaptive Robust Optimization
CCGT	Combined-Cycle Gas Turbines
CCG	Column-and-Constraint Generation
CEF	Connecting Europe Facility
CHP	Combined Heat and Power
CV	Coefficient of Variation
CfD	Contract for Differences
DC	Direct Current
DG	Distributed Generation scenario
DS	Deterministic Solution
ECIU	Expected Cost of Ignoring Uncertainty
EEV	Expected result of using the Expected Value solution
ENTSO	European Network of Transmission System Operators
EUCO	European Commission's core policy scenario
EVP	Expected Value Problem
FID	Final Investment Decision
GAMS	General Algebraic Modeling System
HER	Harmonized Expected Revenues
LCOE	Levelised Cost of Electricity

LNG	Liquefied Natural Gas
LP	Linear (optimization) Problem
LTC	Long-Term Contracts
MILP	Mixed-Integer Linear Problem
NP	Naïve (optimization) Problem
OCGT	Open-Cycle Gas Turbines
PCI	Projects of Common Interest
PPA	Power Purchase Agreement
PSP	Pumped-Storage Power plant
PV	Photovoltaics
RES	Renewable Energy Sources
SCV	Scaled Coefficient of Variation
SP	Stochastic (linear) Problem
SS	Stochastic Solution
ST	Sustainable Transition scenario
TSO	Transmission System Operator
TYNDP	The Ten-Year Network Development Plan
VoLA	Value of Lack of Adequacy



Part I

INTRODUCTION

## INTRODUCTION

---

Energy systems around the globe are undergoing a major transition that involves a broad range of restructuring processes in energy resource use, energy system operation, economics, and policy. These processes include the deregulation of energy markets (i.e. replacing regulated vertically integrated monopolies with competitive energy markets to improve cost-effectiveness and bring welfare benefits to society), climate policy actions aimed toward the reduction of greenhouse gas emissions to tackle climate change, accelerating deployment of renewable energy sources, and many other developments.

The energy transition is transforming the world around us, from the prosaic—we can choose electricity suppliers via the internet based on costs and our own preferences—to the profound—governments, businesses, and research communities across the globe are working together to halt global warming. Moreover, the energy transition changes our traditional institutions, practices, and beliefs.

These transformation processes raise a multitude of economic, technical, and environmental challenges that must be researched and solved. Naturally, it is impossible to address all such energy transition challenges in a single research project, let alone in a doctoral thesis. Therefore, in this thesis, I present four research articles in which my co-authors and I focus on several selected subjects in the field of energy economics. The subjects are connected by three keywords: *uncertainty*, *complexity*, and *change*.

More precisely, the first article focuses on auctions for offshore wind and the competitiveness of this technology in mature markets. The second explores the impacts of uncertainty in integrated electricity and gas system optimization models. In the third article, we focus on the topic of seasonal flexibility in the European natural gas market. Finally, in the fourth article, we analyze the value of Projects of Common Interest—gas infrastructure projects supported by EU public funds—in maintaining gas system resilience amid cold-winter demand spikes, supply shortages, and budget constraints. In this work, we offer the first application of adaptive robust optimization to gas infrastructure expansion planning.

The rest of this Introduction proceeds as follows: section 1.1 outlines the structure of the thesis, section 1.2 gives an overview of the conducted research and contribution to the body of knowledge, and section 1.3 ends with a note on open research.



## 1.1 THESIS STRUCTURE

The main part of this thesis comprises four self-contained research articles that are presented in individual chapters. The chapters are sorted in chronological order of the articles' publication.

I am the lead author of the research articles presented in chapters 3, 4, and 5 and a co-author of the article presented in chapter 2. All four articles have a transparent authorship contribution statement, which is provided at the end of each chapter.

Three articles included in this thesis were published in *Nature Energy*, *Applied Energy*, and *The Energy Journal*, which are Q1 journals based on the Scimago Journal Ranking.<sup>1</sup> The fourth article is currently in the review stage for publication in a Q1 journal. Therefore, chapter 5 presents the working paper published on the *Optimization Online* eprints server.

The article presented in chapter 2 received remarkable public attention.<sup>2</sup> The findings discussed in the paper were mentioned by more than 120 international news outlets. Indeed, the article ranks as one of the highest-scoring outputs from the *Nature Energy* journal (#3 of 1,304). Such public attention scores in the 99<sup>th</sup> percentile of all research outputs of the same age.

The four research articles are published with a large body of supplementary data and online appendixes. I provide a description and links to these supplementary materials at the end of each chapter. The printed appendixes are provided at the end of this thesis.

## 1.2 RESEARCH QUESTIONS AND CONTRIBUTION TO THE BODY OF RESEARCH

**CHAPTER 2:** The analysis in this chapter focuses on the auctions for offshore wind and the competitiveness of this technology in mature markets without subsidy.

Although offshore wind is growing rapidly, this technology has always been considered one of the more expensive decarbonization options. Many countries have recently introduced competition-based auctions for supporting offshore wind. The results of the first auctions shocked the industry and received broad public attention. For example, more than 50% of capacity awarded in the first two German offshore wind auctions bid €0 MWh<sup>-1</sup>. These auction results suggest the prospect of offshore wind power becoming cheaper than conventional power generation. However, a direct comparison of auction results is a fruitless exercise due to a broad range of differences in the auction designs.

<sup>1</sup> See: <https://www.scimagojr.com/journalrank.php>

<sup>2</sup> See: <https://www.altmetric.com/details/86606597>

For this reason, we collate auction results from five countries<sup>3</sup> and harmonise them based on the auction-specific design features. Using this data, we define and compute the *harmonised expected revenue* metric as the discounted average revenue per megawatt hour of electricity generated over the lifetime of the project. This metric can be compared to wholesale prices or the levelized costs of electricity of other technologies as a non-subsidized benchmark. We show that offshore wind power generation can be considered commercially competitive in mature markets.

We also show that once bids are harmonised over the differences in auction designs, the expected revenue streams of wind farms are similar across countries. This important finding suggests that different auction designs can fairly reflect the actual costs of developing wind farms and thus translate cost reductions into lower bids.

Furthermore, we compute the effective level of government subsidy that is paid to each auctioned wind farm and test its sensitivity to future trajectories of wholesale electricity prices. We make an observation that might be of significant interest for energy sector stakeholders: the 2019 auction round in the United Kingdom probably delivered the world's first negative-subsidy offshore wind farm (i.e. the farm will be paying money back to society).

Overall, the chapter addresses the clear lack of academic literature on the question of whether offshore wind has reached subsidy-free status. In this context, our findings equip policymakers, academics, and the industry with evidence that offshore wind will be a low-cost, low-carbon technology in the future.

**CHAPTER 3:** This chapter explores the impacts of uncertainty in integrated electricity and gas system optimization models.

The research in this chapter is motivated by the constantly rising complexity of modern energy system models, which businesses and policymakers use to assist decision-making when addressing the challenges of the energy transition and climate change. These models comprise extensive databases, intertemporal dynamics, and a multitude of decision variables. The interdependence of electricity and natural gas markets adds another layer of complexity, as state-of-the-art models include the operation of both markets in integrated energy system optimization problems. This complexity poses a challenge for energy modelers, who must address multiple uncertainties that are prevalent in both electricity and gas markets. The operational research literature offers stochastic optimization approaches that enable an

<sup>3</sup> Countries with two or more auctions held at the time of writing.

adequate consideration of uncertainties in energy-related investment and operation planning problems. However, most previous models (and studies) dealing with the integrated optimisation of electricity and gas markets have used a deterministic approach. This is because stochastic problems—even for a single market—are complex. Therefore, while constructing integrated energy models, researchers must decide whether to neglect uncertainty and accept a suboptimal solution or to incorporate uncertainty and increase model complexity. This trade-off suggests an important question: *how inaccurate are solutions that neglect system uncertainty?*

To address this question, we develop an integrated stochastic optimization problem and parametrize it with data for European electricity and gas markets. Our analysis covers key uncertainties, such as gas and electricity demand, installed capacity of renewable energy technologies, and fuel and CO<sub>2</sub> prices. We derive the optimal investment decisions when these uncertainties are explicitly encoded (or removed) in a model and quantify the difference.

The chapter contributes to the body of literature in two ways. First, we develop a stochastic optimization problem that integrates the operation of electricity and gas systems and includes endogenous investments in power generation capacity. We use the model to explore the impacts of multiple uncertainties on the energy systems. The integrated modeling framework allows us to extend single-market uncertainty evaluations by tracing the effects of uncertainty across the integrated electricity and gas markets. Second, there is still no systematic understanding of which isolated parametric uncertainty most substantially affects long-term planning decisions in energy system models. We present an applied methodology to examine the effects of isolated parametric uncertainties on solution quality for large-scale energy system optimization models.

While our methodological contributions should be of interest to energy modelers, our findings are also relevant for industry experts and stakeholders with an empirical interest in the European energy system.

**CHAPTER 4:** This chapter focuses on seasonal flexibility in the European natural gas market.

Seasonality is a central characteristic of the European gas market. European countries manage seasonal demand swings (i.e. differences between winter and summer gas consumption) with a mix of flexibility options such as variations in domestic gas production, variations in pipeline or Liquefied Natural Gas (LNG) imports, and the operation of underground gas storage facilities.

In the years before 2018, a relative abundance of seasonal flexibility was observed in the European gas market. This was evident in low seasonal gas price spreads on gas hubs and low utilization of regasification terminals. However, this abundance of seasonal flexibility is likely not permanent. In the future, several factors will put significant downward pressure on the oversupply of flexibility options. These include (i) closures of existing seasonal flexibility options and (ii) decreasing volumes (and associated flexibility) of European domestic gas production. However, other factors work in the opposite direction. These include the continuous integration of European gas markets (i.e., the completion of new transmission and storage infrastructure), as well as the optimization of existing assets. Taken together, the future supply of seasonal flexibility remains unclear.

Previous studies have either discussed seasonal flexibility using other methodological approaches or have maintained a narrow focus, mostly on issues related to the security of supply. Furthermore, there is still no systematic understanding of how to measure the importance of a particular supply source to a seasonal demand swing.

Hence, the work presented in this chapter contributes to the literature in two ways. First, we focus our analysis on seasonal flexibility. Second, we address the problem using a bottom-up market optimization model to simulate the operation of the gas market over a long period. This allows us to explore structural trends in market development, which are driven by changing supply and demand fundamentals. Furthermore, we contribute to the methodological question of how to measure the contributions of different flexibility options by proposing a new metric. We show that a *scaled coefficient of variation* improves the understanding of seasonal flexibility's market dynamics.

**CHAPTER 5:** In this chapter, we analyze the value of Projects of Common Interest—gas infrastructure projects supported by EU public funds—in maintaining gas system resilience amid cold-winter demand spikes, supply shortages, and budget constraints. For this purpose, we develop the first application of adaptive robust optimization to gas infrastructure expansion planning.

This analysis is motivated by the ongoing discourse concerning energy supply security and appropriate business and policy decisions that involve stakeholders from public, private, and academic spheres. The EU has proactively sought to enhance its infrastructural capacity to curb vulnerabilities. Policymakers have assigned great importance to increasing the security of supply in the European gas market through Projects of Common Interest. However, these projects have been the target of signifi-

cant criticism; some contend that they are unnecessary from a supply security perspective and are at risk of becoming stranded assets.

This chapter contributes to the extant literature by suggesting an adaptive robust optimization framework for gas infrastructure expansion planning that considers long-term uncertainties. To the best of our knowledge, this constitutes the first application of adaptive robust optimization for gas infrastructure optimization problems in a real-world setting.

Our modeling framework confronts the drawbacks of mainstream methods of incorporating uncertainty into gas market models (i.e., stochastic scenario trees), in which the modeler predefines the probabilities and realization paths of unknown parameters. The model endogenously identifies the unfortunate realizations of unknown parameters and suggests the optimal investments strategies to address them. We use this feature to assess which infrastructure projects are valuable in maintaining resilience amid system stress.

In the discussion section, we highlight that robust solutions point to consistent preferences for specific infrastructure projects. Interestingly, we find that real-world construction efforts have been focused on the most promising projects from a business perspective. However, we also find that most Projects of Common Interest are unlikely to be realized without financial support, even if they would serve as a hedge against stresses in the European gas system.

The findings presented in this chapter are relevant to a broad circle of industry stakeholders with an interest in reliability issues in the European energy system. In addition, the methodological contribution will be of interest to those working on topics of decision-making under uncertainty in energy markets.

### 1.3 A NOTE ON OPEN AND REPRODUCIBLE RESEARCH

I believe that open science facilitates transparency and credibility, reduces wasteful duplications of effort, helps share ideas, and encourages further research in the field. This allows the research community to advance the frontiers of science and gain the highest benefit from scientific exploration for society. In this context, *open* means that data and code are shared using an open license and thus can be studied, modified, improved, and shared by anyone.

The four research articles included in this thesis are connected with the ideal of open science. Datasets and source codes for these research projects are available in public repositories under open licenses. I

reference these repositories at the end of each chapter. The models in these repositories reproduce the benchmarks from the papers.

## Part II

# MODELING CHALLENGES OF MODERN ENERGY MARKETS: STUDIES ON UNCERTAINTY, COMPLEXITY, AND CONSTANT CHANGE

# 2

## OFFSHORE WIND COMPETITIVENESS IN MATURE MARKETS WITHOUT SUBSIDY

---

*This chapter presents  
the journal article as  
originally published  
in Nature Energy.*  
SPRINGER NATURE  
(c) 2020

**ABSTRACT:** Offshore wind energy development has been driven by government support schemes; however, recent cost reductions raise the prospect of offshore wind power becoming cheaper than conventional power generation. Many countries use auctions to provide financial support; however, differences in auction design make their results difficult to compare. Here, we harmonize the auction results from five countries based on their design features, showing that offshore wind power generation can be considered commercially competitive in mature markets. Between 2015 and 2019, the price paid for power from offshore wind farms across northern Europe fell by  $11.9 \pm 1.6\%$  per year. The bids received in 2019 translate to an average price of  $\text{€}51 \pm 3 \text{MWh}^{-1}$ , and substantially different auction designs have received comparably low bids. The level of subsidy implied by the auction results depends on future power prices; however, projects in Germany and the Netherlands are already subsidy-free, and it appears likely that in 2019 the United Kingdom will have auctioned the world's first negative-subsidy offshore wind farm.

**PUBLISHED AS:** M. Jansen, I. Staffell, L. Kitzing, S. Quoilin, E. Wiggelinkhuizen, B. Bulder, I. Riepin, F. Müsgens (2020), Offshore wind competitiveness in mature markets without subsidy, *Nature Energy*, Issue 5, 614–622. DOI: <https://doi.org/10.1038/s41560-020-0661-2>

### 2.1 INTRODUCTION

Decarbonizing energy systems is a global necessity. Electricity from Renewable Energy Sources (RES) will be crucial for this transformation. Together with photovoltaics and onshore wind, offshore wind energy has become a major contributor of renewable electricity in Europe. With growth rates exceeding 35% a year for the last five years [1], the global installed capacity reached 28 GW by the end of 2019. A capacity of over 127 GW is forecasted by 2040 under the IEA's most conservative scenario [2] and the European Commission has announced its ambition to achieve between 250 GW and 450 GW of electricity generated using offshore wind in 2050 for Europe alone [3]. Global technical potentials exceed 10,000 GW of capacity and an annual production of 5,000 TWh in each of Europe, America and Asia [4, 5].



This historic increase came at a cost. Offshore wind energy was significantly more expensive than conventional generation, even among options for decarbonization [6, 7]. Recently, the technology has experienced rapid cost reductions, which have been widely discussed in the media and consultancy reports [8–10], with some speculating that subsidy-free offshore wind was already achieved. As with the rapid cost reductions in solar photovoltaics [11] and energy storage [12], the pace of offshore wind cost reductions has proceeded more rapidly than was widely anticipated, in contrast to the increasing capital costs during the earlier stages of development [13–16]. For example, in 2016 Wiser et al. [17] used an expert survey to forecast the cost reductions for wind power, and the prices received in recent auctions have already fallen below the expectations for 2050.

Controversy remains around how close offshore wind power is to economic competitiveness against other decarbonization options [18, 19]. The National Renewable Energy Laboratory compared auction results from the Netherlands, the United Kingdom and Denmark by adjusting values to account for grid connection, development costs and contract lengths [20]. A transparent methodology was not provided though, which limits the replicability of the results and the ability to update data in this fast-paced industry. The IEA Wind TCP Task 26 has compared country-specific impacts on the Levelised Cost of Electricity (LCOE) [21], which comprehensively covers the costs of offshore wind. While the publications mentioned in this paragraph provide a valuable background, they do not explain the bids and the pace of the underlying cost reduction. Both issues are addressed in this paper.

Competitiveness can be measured by comparing costs (usually LCOE) to other technologies or to wholesale market prices, and provides an aggregated measure of competition in the system [21, 22]. However, actual LCOE data are only available in selected countries because they are commercially valuable and sensitive [23, 24], which leads to misrepresentation [25] and the need to estimate costs. For offshore wind, estimates of investors' expected LCOE can be derived from auction results, and data on successful bids are often published openly. Although bids should correlate with costs, they cannot be directly translated, as information on expected revenues from wind power projects is unavailable.

Several important differences exist in auction design, including the length of support, whether it rises with inflation, optionality in building the project and the inclusion of development costs. Most critically, the Contract for Differences (CFD) used for remuneration can be categorized as one-sided (providing a lower-bound price below which revenues from the wind farm cannot fall) or two-sided (providing a fixed price with both lower and upper bounds). For this reason, a bid of  $\text{€}20 \text{ MWh}^{-1}$  in Germany may provide more financial revenue

for a wind farm developer than a bid of  $\text{£}50\text{MWh}^{-1}$  in the United Kingdom.

We harmonize the winning bids from 41 wind farms across auctions in five European countries between 2005 and 2019, accounting for the main features of each auction. Wind farms were selected based solely on their payment allocation scheme, that is only wind farms that were auctioned. All offshore wind technologies were considered, as were all countries that had held at least two auction rounds at the time of writing (the minimum required to detect a trend). These five countries represented 77% of the global offshore wind capacity, and the only other country to hold more than 1% of the global capacity was China, which was not included as it had only auctioned a single offshore wind farm at the time of writing [1]. This analysis provides two measures: the expected revenues (in  $\text{€}_{2019}\text{MWh}^{-1}$ ) for each wind farm, which we then compare with potential future wholesale market prices to estimate the effective subsidy, and thus the financial competitiveness of each wind farm. We aggregate data on auction settings and results, showing that current offshore wind technologies at good sites in mature markets have implied prices of less than  $\text{€}50\text{MWh}^{-1}$ , which is likely to be subsidy-free or negative-subsidy depending on future power prices.

## 2.2 OFFSHORE WIND AUCTIONS IN EUROPE

Five countries in Europe have held auctions for offshore wind capacity. In total, 17 auctions have been held, bringing forth over 20 GW of capacity. The evolution of winning bids across these auctions is summarized in Fig. 2.1. This does not reveal a clear trend and is confounded by several bids of  $\text{€}0$  (made into one-sided CfD auctions) beginning in 2017. While a declining trend can be observed, this reveals as much about the heterogeneity in auction design as it does about the reduction in wind farm costs.

All auctions for offshore wind in Europe are designed so that the wind farm operator receives a guaranteed price for a certain predefined period. This ‘strike price’, or ‘bid price’, closes the gap between the market reference price (that is wholesale electricity prices) and a guaranteed price. However, the exact payment arrangements differ between countries, and the specific design of the support scheme gives rise to significant differences in the bids received, and must be accounted for when comparing bids across different schemes. Clarification on auction design features and their influence can be found in refs. [26–29].

Several differences in implementation exist. (1) The choice of remuneration mechanism, specifically the allocation of market upside. One-sided CfDs usually pay when wholesale prices are below bid prices but do not demand money if wholesale prices are above bid

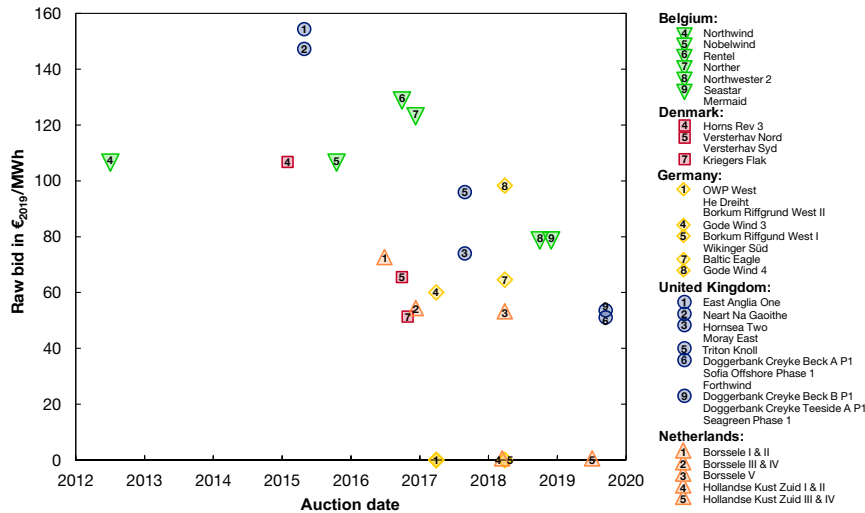


Figure 2.1: Raw bids received by auctions for new offshore wind capacity in five European countries over the past eight years

Points show the date that auctions were announced, and are converted from the local currency to €<sub>2019</sub>.

prices. With two-sided CfDs, investors must compensate for wholesale price revenues above bid prices. Further explanation can be found in [Supplementary Note 1](#). (2) Defining the support duration based on a fixed time period (years) or by the total support volume (TWh). (3) Accounting for indexation, which defines whether the guaranteed price is adjusted for inflation, choice of inflation index and base year for indexation. (4) Choice of market reference price used as the basis for comparison to the guaranteed price (for example hourly, daily, monthly average). (5) Floors of market price below which no support is being paid out (for example at negative market prices for several consecutive hours). (6) The allocation of land lease costs, (7) grid connection costs and (8) site development costs. (9) The option to capture alternative revenue streams (for example ancillary services), and (10) penalties for non-fulfilment of contracts, which could mean bids are conceived as options to build and do not necessarily reflect realistic cost estimates in all cases.

The auction schemes vary considerably across the five countries we consider, as summarized in [Table 2.1](#). All auctions provide remuneration based on produced energy (that is per kWh); however, other design aspects are not comparable between auction schemes. Further details are given in [Supplementary Data](#) and [Supplementary Table 1](#). An overview of each country's auction design and their differences is given in [Supplementary Note 2](#).

### 2.3 HARMONIZATION OF EXPECTED REVENUES

The significant differences we identify in auction and product design across countries directly influence the costs and/or revenues of projects, and thus influence the bids received. The winning bids in European auctions for offshore wind were harmonized using a monthly cashflow analysis, and account for the most significant factors identified in the previous section (see [Methods](#)). We define the ‘harmonized expected revenue’ as the discounted average revenue per MWh of electricity generated over the lifetime of the project. This gives the equivalent bid that would be offered into a support scheme with a two-sided CfD and a 25-year support duration, indexation to inflation and site development costs paid by investors.

The harmonized expected revenue incorporates all the money a wind farm can expect to earn over its lifetime, including revenues for later in the project’s lifetime when support has ended. It is therefore complementary to the widely used LCOE metric, referring to revenue rather than cost. It could therefore be a proxy to LCOE in perfectly competitive markets. The details for each wind farm that were used to determine harmonize expected revenue, including key dates and technical specification, are given in [Supplementary Data](#) and [Supplementary Table 1](#).

Comparing the harmonized expected revenues in [Fig. 2.2](#) with the raw bids reveals substantial differences: the raw bids are in the range €0 – 150 MWh<sup>-1</sup>, whereas expected revenues are €50 – 150 MWh<sup>-1</sup>, with wind farms due to begin operation after 2020 converging towards a range of €50 – 70 MWh<sup>-1</sup>. From this analysis we cannot identify one country that consistently creates lower bids than others, despite varying site conditions, auction criteria and level of competition. A capacity-weighted logarithmic regression through all auction results yields a reduction in the harmonized revenue requirement of 5.8% per year, with a standard regression error of ±1.1%. When considering the more recent auctions, with start dates from 2015 onwards, this rate increases to 11.9 ± 1.6% per year. The results for individual countries are presented in [Supplementary Table 2](#) and [Supplementary Fig. 2](#). A logarithmic fit was chosen to ensure that regression results cannot fall below zero. The increased rate of cost reduction indicates that auctions may have helped to improve efficiency in the offshore wind industry.

Large differences between auction date, Final Investment Decision (FID) and planned commencement of operation can be noted. For some zero bids in Germany, more than five years lie between the auction result and commencement of operation, whereas several wind farms in the United Kingdom made the FID on the day of winning the auction or shortly after. As a result, there is more time for turbine costs to decrease on German wind farms meaning the bids appear more in line with each other.

Table 2.1: Main characteristics of the auction systems for offshore wind capacity in five European countries

Characteristics	DK	UK	NL	DE	BE
Wind capacity (total/offshore) [GW] [30]	5.7/1.3	5.7/1.3	4.5/1.1	59.3/6.4	3.4/1.2
Date of auctions	2005-16	2015-19	2016-19	2017-18	N.A. <sup>b</sup>
Capacity awarded (all rounds) [GW]	2.2	9.8	3.0	2.7	2.3
Wind farms awarded	7	11	5	10	10
Average bid (cap.-weighted)	€84 (DKK625)	€65 (£57)	€32	€19	€104
Minimum bid	€50 (DKK372)	€46 (£40)	€0	€0	€79
Sided	2	2	1	1	1
Duration (years)	12	15	15	20	16 <sup>c</sup>
Grid costs in bid	x	✓	x	x	x <sup>d</sup>
Site costs in bid	✓	✓	x <sup>a</sup>	✓	x
Inflation adjustment	x	✓	x	x	x

<sup>a</sup> Land lease paid for by the wind farm in the latest tender round.

<sup>b</sup> Renewable obligation certificate scheme mirroring auction results of the Netherlands.

<sup>c</sup> 16 – 20 years, with 16 years for the latest wind farms.

<sup>d</sup> Financial cap on total investment.

Full details about each wind farm in these auctions are provided in [Supplementary Data](#) and [Supplementary Table 1](#). Two bids from German wind farms were undisclosed [31] and thus not analysed further. Denmark implements a new auction design for each round and support length is based on energy production. For more information on the auction design of each country refer to [Supplementary Note 2](#).

Fig. 2.2 shows that harmonized expected revenues for several projects have fallen below  $€50 \text{ MWh}^{-1}$ . This places offshore wind towards the lower end of LCOE estimates for fossil fuel generators [22]. However, such a comparison must be caveated, as these revenues will only reflect costs in perfectly competitive markets, and cost comparisons between variable renewables and dispatchable fossil fuel generators are subject to ongoing debate around integration costs [32–34].

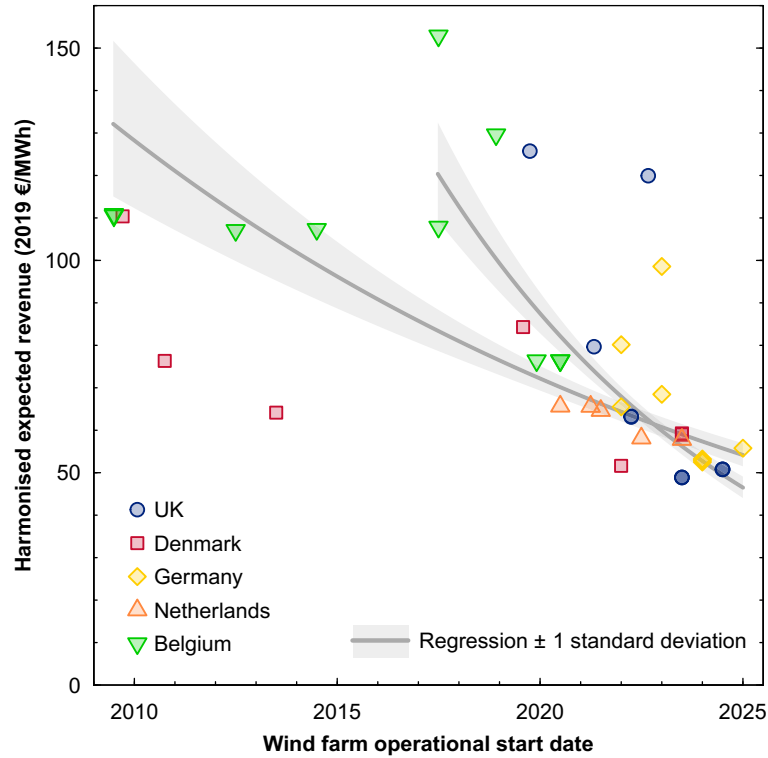


Figure 2.2: Harmonized expected revenues for each offshore wind farm auctioned in Europe

Each symbol shows the planned start date of operation against the harmonized expected revenue. The lines show the lognormal regression of expected revenue against time across all countries, covering all bids and the most recent bids (since 2015). The shaded areas depict  $\pm 1$  standard deviation on each regression. Wholesale electricity prices are assumed to remain constant in real terms when deriving revenue beyond the support duration end. Other price scenarios are shown in [Supplementary Figs. 1 and 2](#).

The harmonized expected revenue of most projects depends on the future development of wholesale prices. First, wholesale prices are directly received by projects under one-sided CfDs provided they are above the bid. Second, with an assumed technical lifetime of 25 years, all projects are expected to sell their output on the wholesale market after their auction remuneration expires. Medium- to long-term wholesale prices are therefore of particular importance to these results, but at the same time, they are highly uncertain. This is not only an academic exercise but an issue that the bidding companies must deal with, and one that the energy industry is, in general, familiar with. Estimates can be made using electricity market models to quantify the future energy system, but these depend on numerous uncertain assumptions, such as the future CO<sub>2</sub> allowance price. The fact that we find similar revenues for wind farms across several countries in the

future would, however, indicate that several bidders have arrived at a similar outlook on future power prices.

The results in [Supplementary Fig. 2](#) consider the sensitivity of these results to the future trajectory of wholesale power prices. We explore this uncertainty by presenting a range of prices derived from independent sources. First, we consider the EU Reference Scenario 2016, and scale projected prices from 50% to 150%. This accounts for structural changes in the electricity market (for example, increased penetration of renewables and higher carbon prices), but is fundamentally a theoretical modelling exercise. To complement it, we take the average power prices in each country from 2004 to 2018 and apply a constant real-term annual growth rate of between  $-2\%$  and  $+2\%$ , which more than spans the range of historical price growth observed in these countries.

We argue that the long-term prices are probably a better indicator. The prices laid out in the EU Reference Scenario 2016 are set to double electricity prices in many countries between 2010 and 2020, and therefore we exercise caution using this price forecast alone. We provide the results of all the price scenarios considered in [Supplementary Fig. 2](#), and [Supplementary Software 1](#) provides the means to test other price trajectories. From this assessment, we observe the large influence that power price has on harmonized revenues, which is a factor that each bidder will have to consider individually.

#### 2.4 MOVING TOWARDS SUBSIDY-FREE OFFSHORE WIND FARMS

The harmonized expected revenues (including the support payments expected under each wind farm's CfD contract) can be compared to the expected revenues that would be generated on the wholesale market alone (as if each wind farm were a purely merchant project). The difference between these allows us to derive the effective subsidy that is being paid to each farm, as shown in [Fig. 2.3](#). This is the difference between the discounted income stream due to the RES support payments. If the expected harmonized bid is equal to the expected wholesale market price, the effective subsidy is zero and the project is subsidy-free. These subsidies are the amount of money that will have to be refinanced through the RES support scheme.

This study does not deal with the question of whether grid construction costs should be paid by developers (the allocation-by-cause principle) or be paid by society (socialized as part of a country's infrastructure investment). [Fig. 2.3](#) therefore presents both versions, keeping in mind that, on average, grid costs account for  $\text{€}13 \text{ MWh}^{-1}$ . It must be noted that most countries have chosen the latter option, and the funding models for grid infrastructure differ widely. In the United Kingdom, socialized grid costs are borne jointly by generators and demand through transmission charges for the transmission grid,

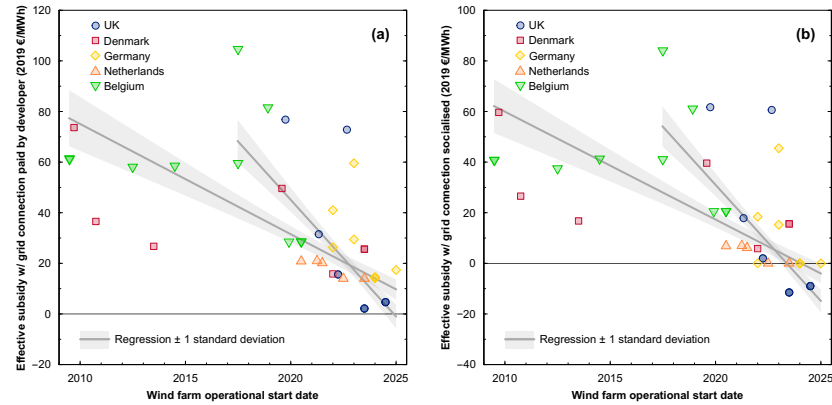


Figure 2.3: Effective subsidy for each offshore wind farm auctioned in Europe

Panel **a** assumes grid connection costs should be paid for by the developer and are thus considered part of the wind farm. Panel **b** assumes these should be socialized and considered part of the overall grid infrastructure. Each marker shows the effective subsidy for each wind farm at the planned date of operation. The lines show the effective subsidy linear regression against time across all countries, covering all bids, and recent bids from 2015 onwards. The shaded areas depict  $\pm 1$  standard deviation for each regression. Wholesale electricity prices are assumed to remain constant in real terms when calculating the support level from each CfD. Other price scenarios are shown in [Supplementary Fig. 3](#).

whereas offshore connection is paid by the wind farm only. Germany recovers grid charges (including for new offshore wind farms) solely through final consumer bills. Offshore grid connection costs remain a key uncertainty despite efforts to gather data [23, 35, 36] and model [31], these costs for each wind farm (given in [Supplementary Data](#) and [Supplementary Table 1](#)).

Using socialized grid connection costs, subsidies have reached  $-\text{€}12 \text{ MWh}^{-1}$  for the latest UK auction, with a large cluster between  $-\text{€}10 \text{ MWh}^{-1}$  and  $\text{€}20 \text{ MWh}^{-1}$ . This implies that several wind farms could expect to earn less money under the RES support scheme than under wholesale market terms alone (even with expected revenue cannibalization effects). With the grid costs being paid for by the developer, the lowest effective subsidy is  $\text{€}2 \text{ MWh}^{-1}$ , assuming real-term wholesale power price growth is 0% a year. Therefore, even slight growth in market prices (above 0.28% a year) means the cheapest wind farms are subsidy-free.

It can make sense for companies to forgo revenues in exchange for predictability. First, funding from the RES support scheme minimizes risk in several ways; notably, exposure to future market price is reduced, which in turn reduces the financial cost of  $\text{€}$  multi-billion projects and allows for a lower initial LCOE [37]. Second, in all cases, using the RES support scheme is accompanied with monetary (for



example socialized grid connection) and non-monetary privileges (for example site allocation, consent and planning) thus limiting the pre-development costs for each project.

With grid support being paid by the developer, the expected support is falling across all auctions by  $€5.30 \pm 1.00 \text{ MWh}^{-1}$  per year. Considering auction results from the last five years only, support has fallen even more dramatically (by  $€10.20 \pm 1.60 \text{ MWh}^{-1}$  per year), implying that offshore wind farms built from 2025 onwards will, on average, be subsidy-free if these cost reduction rates continue. The rates of reduction are virtually identical if grid costs are socialized, with  $€5.20 \pm 0.90 \text{ MWh}^{-1}$  (across all auctions) and  $€10.20 \pm 1.50 \text{ MWh}^{-1}$  (between 2015 and 2019) per year. Based on recent auctions, this suggests the era of subsidy-free wind farms will begin in 2023, or in 2024 when all data have been considered.

## 2.5 SENSITIVITY TO FUTURE POWER PRICES

To analyse the significance of future price developments for subsidy-free offshore wind farms, we vary future wholesale price assumptions and calculate the resulting effective subsidies. Fig. 2.4 summarizes the effect on subsidies of the real-term change in wholesale electricity prices of between  $-2.5\%$  and  $+2.5\%$  a year.

Countries which offer two-sided CfDs (United Kingdom, Belgium and Denmark) show a greater sensitivity to future wholesale prices, as higher reference prices result in farm developers paying money back to society. The minimum bids received in Germany and the Netherlands show no sensitivity to power prices (Fig. 2.4, panels a,b, horizontal lines). These one-sided  $€0 \text{ MWh}^{-1}$  bids only see support paid if wholesale prices turn negative, which is only expected for a few hours per year (see Methods). If these wind farms were required to pay for grid connections, this would be added onto the zero bid (Fig. 2.4, panel b). It is noteworthy that, with its latest auction, the United Kingdom appears to offer the lowest support payment for any wind farm, with an effective subsidy of less than  $-€12 \text{ MWh}^{-1}$ , which is in part due to the implementation of a two-sided CfD and is accompanied by predicted government power prices increases [38].

The results of the latest UK auctions indicate that if wholesale prices continue to see moderate growth of above  $0.3\%$  a year (which is below historical rates), then these farms will receive negative subsidy, and will be the first to pay money back to society. If grid construction costs are assumed to be socialized, UK offshore wind farms would be subsidy-free, even if power prices fell by more than  $1.5\%$  a year in real terms. Wind farms in Germany and the Netherlands are subsidy-free under any price scenario, whereas Belgian wind farms are trailing in terms of effective subsidies. The last auction in Denmark took place in November 2016, resulting in a comparatively high effective subsidy,

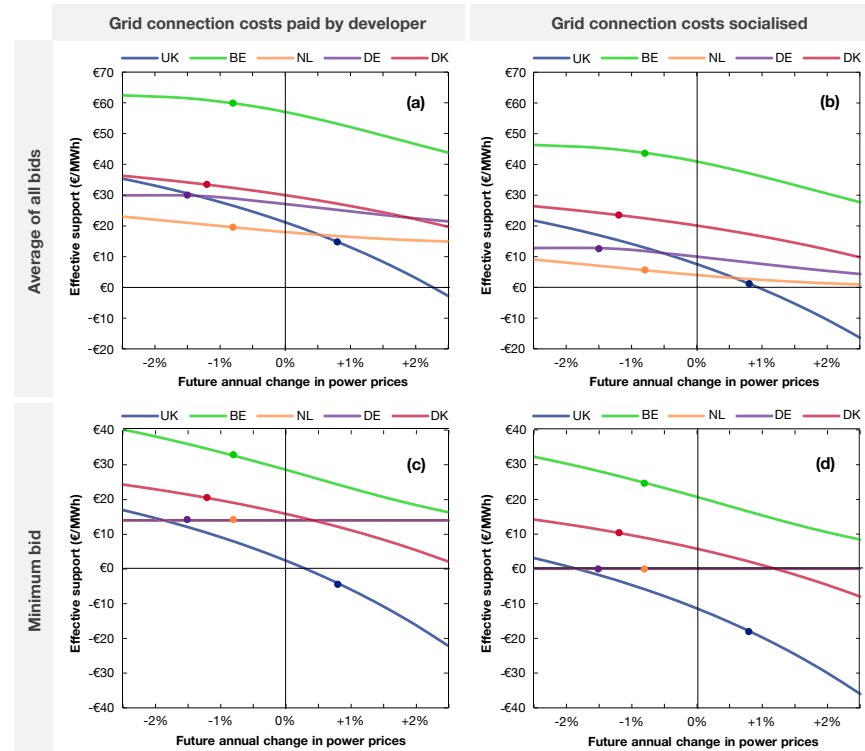


Figure 2.4: Effective subsidy given to offshore wind farms as a function of future real-term growth in wholesale power prices

The panels show four variants, considering the average bid (a,c) and minimum bid (b,d) received in each country, assuming grid connection costs are either paid by the developer (a,b) or are socialised (c,d). The circles on each line indicate the average real-term growth in wholesale power between 2004 and 2018.

but showed comparable cost progression within the industry as a whole.

## 2.6 DISCUSSION AND CONCLUSIONS

The era of subsidy-free offshore wind turbines has begun. This conclusion is founded on zero bids in the Netherlands and Germany that effectively track wholesale power prices, and bids of approximately  $\text{£}40 \text{ MWh}^{-1}$  in the United Kingdom, which will be below future wholesale prices if historical growth rates are maintained. Recent projects in the Netherlands have bid  $\text{€}0 \text{ MWh}^{-1}$  and will pay land lease fees, indicating that offshore wind farms are at the point where they are likely to pay money back into the system.

Despite significant variations in auction design, we find that once bids are harmonized the expected lifetime revenues of wind farms are homogeneous across countries, without specific outliers that would be attributable to the auction design. This implies that policymakers

have managed to design auctions that fairly reflect the actual costs of developing offshore wind farms, and that the specific auction design is not particularly influential on the outcome. This finding could aid the design of upcoming auction schemes for offshore wind farms on a global scale. It also raises the question of whether auctions are suitable policy instruments for driving down costs in less mature technologies such as wave, tidal and floating offshore wind energy. This study does not unveil whether policymakers should discontinue support for renewable energy once price parity is achieved, as the revenue stabilization offered by CfDs has been instrumental in making this possible for offshore wind [2].

Harmonizing bids into expected revenues creates a proxy for the actual costs of offshore wind, which closely relates to the LCOE plus profits for the company. We show that wind farm costs are decreasing in a uniform fashion across Europe, having recently dropped below the  $\text{€}50 \text{ MWh}^{-1}$  threshold. This makes electricity production via offshore wind a competitive option and is an extraordinary success story for a relatively young industry. It is possible that future wind farm developers will aim to build ‘merchant’ offshore wind farms without financial support, completely free of government support. However, the development costs may rise as wind farms move to less favourable locations or to less mature technologies.

There are several reasons why the harmonized expected revenues we report may diverge from underlying costs. Auction results can be seen as an ‘option to build’ that need not be realized if costs do not fall sufficiently [31]. However, the FID has already been taken for some recent bids (including the cheapest ones), including one on the day of the auction result (see [Supplementary Data](#) and [Supplementary Table 1](#)). We interpret these tangible financial commitments as a sign of developers’ intent to progress with the awarded bids. The breadth and heterogeneity of our sample (41 projects in different countries and auction rules) also suggests that such ‘option bidding’ effects are unlikely.

The presence of market power could also distort revenues away from underlying costs in either direction. If the industry is going through a shakeout period, investors may bid below cost to deter new entrants from providing competition, accepting short-term losses in return for gaining market share and higher long-term profits. This would mean the true costs are above the harmonized expected revenues we report. Alternatively, an oligopoly of large developers could exploit the lack of competition to artificially inflate auction prices. This would mean the true costs lie below our harmonized expected revenue and that offshore wind is more competitive than our analysis suggests.

To facilitate market access, electricity generated from offshore wind is often sold through Power Purchase Agreement (PPA), especially in the United Kingdom. PPAs provide long-term revenue stability

and offtaker risks are assumed by a counterparty. These could yield agreed prices below the wind-weighted average wholesale price used here, if for example limited competition between providers facilitated excess profits. This would lower the expected revenues, suggesting that offshore wind is cheaper than our results indicate. Evidence of the discounts offered in PPAs is not publicly available; therefore, we cannot establish whether they are reflective of the underlying revenue cannibalization found across the investigated countries.

Policymakers can take the rapid price decreases shown here as evidence that offshore wind will deliver in the future as a low-cost and low-carbon technology. Hence, the initial spending made on support schemes has been successful in helping to create a new industry. This opens up questions around the next steps to support the further rollout of offshore wind. This will likely entail designing schemes that move away from support payments and instead focus on planning issues, market integration, grid connection and the ease of accessing financing.

Building on the story of success, policymakers may want to extend their attention to support less mature technologies such as floating offshore wind, which would allow access to deeper waters with higher wind speeds. These technologies are currently at a less mature stage, but may prove vital in harnessing the world's best wind resources [2].

Our findings are derived from wind farms in Europe, but hold relevance for other parts of the world. Europe has been at the forefront of offshore wind as a result of its favourable conditions of relatively shallow waters and high wind speeds. This enabled cost-efficient monopile foundations to be used in most, but not all offshore wind projects. One-fifth of the capacity we consider uses jacket or gravity-based foundations. Regions of Asia and North America also benefit from shallow waters [2], and could expect some of the learning of Europe (for example, turbine size increase, construction techniques and financing) to play a key role in achieving similar results. The rates of price reduction found here may prove equally applicable to other regions of the world, and to other foundation types if a comparable scale-up is achieved, albeit from a higher starting price point. Regions that are yet to develop a supply chain and innovation system for offshore wind energy may require more time for these technologies to become subsidy-free.

As decarbonization of the world's electricity systems gains traction, attention must be given to the issues of balancing and flexibility, and to the decarbonization of heat, transport and industrial applications. With offshore wind at competitive prices, numerous sector-coupling applications that could not have been imagined as cost-competitive just a decade ago are within reach.

## 2.7 METHODS

**General principle.** Both auction and product design vary significantly between different countries. We identified major differences from a review of government literature and present these in [Supplementary Data](#) and [Supplementary Table 1](#). Many of the differences directly influence the cost and/or revenue of the projects, and thus influence the bids. This is obvious for the duration of support and also for one-sided versus two-sided support schemes, where the former has an implied option to profit in the event of future wholesale price increases. Consequently, one-sided CfDs require lower bids to make projects profitable.

The differences between auction designs were accounted for by developing a methodology to harmonize the winning bids in European auctions for offshore wind. Our harmonization accounts for the most significant factors identified in [Table 2.1](#). The bids are harmonized using a monthly cashflow analysis, which addresses seasonal variation in wind capacity factors and allows volume-based support schemes to expire part-way through a year. Hence, we define the ‘harmonized expected revenue’ as the (discounted) average revenue per MWh of electricity generated over the lifetime of the project. This can be interpreted as the bid that would give an equivalent net present value over the project life if it were offered into a hypothetical auction that offered a two-sided CfD with a 25-year duration, indexed with inflation. On this basis, we can compare the bids (and the implied expected revenues) over the entire lifetime of each wind farm, and include revenues for later in the lifetime of the project when support has ended. Details on each wind farm were primarily sourced from developer and manufacturer websites and professional databases (for example, 4C Offshore) as well as renewables and offshore wind news outlets (<https://renews.biz>; <https://www.4c offshore.com>; <https://www.offshorewind.biz>; <https://www.windpoweroffshore.com>; <https://renewablesnow.com/>).

The following sections detail how we adjust the strike price of each bid to obtain the harmonized expected revenue. Each adjustment changes the monthly cashflow, which results in monthly payments to the wind farm from the market and the ‘effective’ payments from the RES support scheme. The payment over the lifetime of the project is then aggregated. This yields the average payment per MWh received for the total (supported) payments. We also calculate the payments that would have resulted if the electricity was sold exclusively on the wholesale market. Finally, we calculate the difference between both, which represents the actual average subsidy paid.

**Harmonizing length of payments.** Support durations vary between projects. For most projects, legislation specifies an explicit time du-

ration  $d_s$ . For the Danish projects with an energy-based limit, we calculated the resulting support duration  $d_{s,DK}$  as follows, with  $d_{s,DK}$  being the support duration for Denmark,  $E_s$  the supported energy,  $P_{inst}$  the installed capacity,  $h_y$  the hours in one year and  $CF$  the capacity factor:

$$d_{s,DK} = \frac{E_s}{P_{inst} * h_y * CF} \quad (2.1)$$

The capacity factor  $CF$  is estimated using the Renewables.Ninja model with the appropriate wind turbine model for each project [39, 40]. The numbers are validated against external data points where possible [41, 42], and are found to be highly correlated. For projects using next-generation turbines we developed parametric power curves [43] if these were not publicly available. While we attempt to use representative capacity factors, these have no influence on the main results presented as both harmonised revenue and expected support are normalised per MWh. They can have second-order effects due to output-dependent support duration, but this yields minimal changes. External factors that could influence capacity factors over the farm's lifetime (such as degradation [44, 45], wake effects [46], stalling [47] or climate change [48]) are not considered as they are currently subject to much uncertainty. These could be incorporated once better understood using the cashflow models that we make available open source.

We model each wind farm's revenue over its whole lifetime, both from their strike price and the wholesale market alone. While the total lifetime of offshore wind projects is still debated, most publications estimate them between 20 and 30 years (for example, refs. [49–53]). Therefore, we assume that the lifetime  $d_l$  for all projects is 25 years. This is needed to calculate the income after RES support from the auction has run out. Variations to this assumption have limited impact on results due to the effect of discounting.

**Strike prices and market revenues.** As explained above, the annual revenue of projects are determined based on either the strike price or the market price. Before we can identify which applies in any given year for any given project, we must first derive a consistent time series for both. Among other things, we normalize currencies to Euros and all values to real monetary values for the year 2019.

We assume that wind farms sell their output on the wholesale market (or at least receive payments based on the sold electricity's wholesale market value). Historic wholesale power prices are obtained from ENTSO-E and Open Power Systems Data [54, 55]. Large uncertainties exist regarding the future of power prices, especially as we require them for more than 25 years in the future. The influence of power prices is paramount for our considerations as it significantly affects the bids. Obtaining consistent price forecast scenarios is chal-

lenging as the national price forecast would show inconsistencies on the input assumptions (fuel prices, CO<sub>2</sub> emission prices and so on).

To address the uncertainty around future power prices we choose a diversified approach. (1) The EU Reference Scenario 2016 PRIMES model provides a consistent output covering all of Europe [56], which forecasts the average annual power prices for every fifth year until 2050. It should be noted that the prices are significantly higher than today's prices. Therefore, we multiply the prices provided with factors of 0.5, 1.0 and 1.5 to create an understanding of the impact of price variations. (2) While best efforts have been made to model future power prices, we aim to mitigate the influence of modelling altogether, by using the average annual power prices to establish long-term price variations. Based on this, we use long-term price (2004 – 2018) averages and assume an annual growth of between –2% and 2% in 1% increments.

We can establish that the time-weighted average wholesale price for the time period  $t$  is dependent on the assumed price growth  $pr$ . The latter can either be given in percentage growth a year or predetermined by external inputs, such as the time series from the EU Reference Scenario 2016:

$$twp_t = twp_0 * pr^{\frac{t}{12}} \quad (2.2)$$

with  $twp_0$  being the time-weighted average wholesale price at project start,  $pr$  the rate of price growth and  $t$  the time in months since project start.

However, it is well known that electricity generation from wind does not receive the average price [57]. The price that offshore wind turbines will be able to realize on the market on average shall be called the 'capture value' (also referred to as market value factor, see ref. [58]). We derive a capture value (a multiplier that is typically below one, and thus subtracts from the average power prices) based on the linear interpolation between today's empirically determined data and the price scenarios for 2030 [58]. The capture value  $cr$  is a multiplier that determines the percentage of the time-weighted average price that the wind can capture. It is a large source of uncertainty for wind farm developers, as it is expected to decrease over time. The results from our modelling for the country-specific average values are shown in [Supplementary Table 3](#):

$$cr = \frac{\sum_h output_h * price_h}{\sum_h output_h * \overline{price}} \quad (2.3)$$

with  $output_h$  being the output in hours  $h$ ,  $price_h$  the price in hours  $h$ ,  $\overline{price}$  the time-weighted average price across all hours and  $h$  hours.

This allows us to further calculate the wind-weighted average wholesale price  $wwp_t$ :

$$wvp_t = twp_t * cr_t \quad (2.4)$$

Linear interpolation of the market value  $cr$  between today and 2030 is assumed and can be justified using the different scenarios in the UK National Grid Future Energy Scenarios annual publications [59] shown in [Supplementary Fig. 5](#). The modelling shows a roughly linear relationship between installed wind power and the merit-order effect. We can therefore also assume a linear relationship in our assessment, both for the merit-order effect as well as the capture value derived from the hourly time series analysis between today's data and the estimation for 2030.

Determination of strike price time series is relatively straightforward. In the first step, we convert strike prices to € (if applicable) using market exchange rates [60]. In the second step, we convert nominal values to real monetary values of 2019 using country-specific averages for the years 1998 to 2017 [61]. The long-term inflation for all five countries was 1.65% a year. For the UK auctions, the strike price is adjusted by the inflation rate, which is derived from the data [61] and amounts to 1.89% a year. All available inflation data is shown in [Supplementary Table 4](#). Note that the indexation measure used is based on the gross domestic product deflation index rather than consumer price indexation, as often used by central banks. This is believed to provide a more accurate representation of indexation [62]. The strike price  $SP_t$  at time  $t$  is determined by auction design to either be discounted or kept constant in real terms:

$$SP_t = \frac{SP_0}{ir^{\frac{t}{12}}} \quad (2.5)$$

with  $SP_0$  being the strike price at project start,  $ir$  the inflation rate (gross domestic product deflation) and  $t$  the time in months since project start.

**Determining revenues during support duration.** At this point, we have two normalized time series for the years of the support duration (the strike price time series and the market revenue time series, both calculated above). Which one is applicable is determined as follows:

For projects under two-sided CfDs, the strike price essentially determines a fixed payment. Hence, the relevant time series during the support duration is the strike price.

For projects under one-sided CfDs, the situation is more attractive: these projects have the right (but not the obligation) to choose the market revenues even during the support duration in case they exceed the strike price. We address this optionality in two ways. First, we select the maximum monthly strike price and market revenue as



the resulting revenue during those months. This is analogous to the option's intrinsic value. Second, the option has an additional 'time value'—reflecting the fact that the wholesale revenue described above is uncertain. It could increase—and the projects under one-sided CfDs would profit. It could also decrease, but the projects under one-sided CfDs would lose less (as they can choose not to exercise the option and sell at the strike price). Note again that, in contrast to option terminology, 'strike price' is equivalent to 'bid price' in this paper.

We further establish the uplift premia  $up$  as a function of the strike price  $sp$ . The uplift premia term describes the additional income for the generator over the market price that is caused by capturing the upside under a one-sided CfD. The uplift premium is a function of the ratio between strike price and wholesale market price and differs for every wind farm. [Supplementary Fig. 4](#) derives the value for each wind farm. It is not applicable for two-sided CfDs:

$$up(sp) = \frac{\sum_h output_h * \max\{price_h, sp\}}{\sum_h output_h * price_h} \quad (2.6)$$

**Harmonizing bids.** Having calculated one specific revenue time series for each project, we then adjust these time series to reflect the (country-specific) weighted average cost of capital. This discount rate is also called the real cost of capital (over and above inflation rate). The financing costs of wind power projects are dependent on the local funding conditions and ease of capital access. [Supplementary Table 5](#) presents the weighted average cost of capital from different sources for onshore and offshore wind, with offshore wind being more expensive. The average across these sources was used, with country-specific values in the range 6.2 – 7.9% and the average across all countries being 7.3%.

As all input parameters are now defined, the revenue for the three different cases can be calculated: (1) revenues without any RES support scheme payments  $r0_t$ , (2) revenues under a one-sided CfD  $r1_t$  and (3) under a two-sided CfD  $r2_t$ :

$$revenue = \begin{cases} r0_t = output_t * wwp_t & no\ support \\ r1_t = r0_t * up_t & one - sided\ CfD \\ r2_t = SP_t & two - sided\ CfD \end{cases} \quad (2.7)$$

with  $r0_t$  being revenue at market prices.

The Harmonized Expected Revenues ([HER](#)) for each case then results in:

$$HER = \begin{cases} \sum_t \frac{r0_t}{(1+dr)^t} & \text{no support} \\ \sum_{t \in ST} \frac{r1_t}{(1+dr)^t} + \sum_{t \notin ST} \frac{r0_t}{(1+dr)^t} & \text{one-sided CfD} \\ \sum_{t \in ST} \frac{r2_t}{(1+dr)^t} + \sum_{t \notin ST} \frac{r0_t}{(1+dr)^t} & \text{two-sided CfD} \end{cases} \quad (2.8)$$

with  $dr$  being the discount rate,  $ST$  the support time from 1 to  $sd$  and  $sd$  the support duration in years.

This allows us to calculate the effective subsidy  $ES$  as follows:

$$ES = HER - \sum_t \frac{r0_t}{(1+dr)^t} \quad (2.9)$$

In the final step, we account for the fact that some auction designs pay for grid connection and others pass the costs onto the developer. Harmonizing the effective subsidy  $ES$  by subtracting the grid costs  $CG$  accounts for the difference in the auction conditions and happens after the cashflow analysis. The implied cost differences can be regarded as a significant subsidy [31]. We have collected wind farm-specific connection costs were available in the overall data table in **Supplementary Data** and **Supplementary Table 1**, averaging country-specific data where primary data was missing. In some cases (for example, Germany) connection costs are given in  $\text{€ kW}^{-1}$  following the methodology in ref. [31], which can then be converted into  $\text{€}_{2019} \text{ MWh}^{-1}$  using capacity factors. The United Kingdom is the only country where wind farms pay in full for the grid connection. The effective subsidy with grid connection  $ES_{GridConn}$  therefore only applies to the UK auction results, as  $ES_{GridConn} = ES_{UK}$ . For all other countries  $ES_{NoGridConn} = ES_{DK,NL,BE,DE}$ . The relationships between  $ES_{GridConn}$  and  $ES_{NoGridConn}$  are

$$ES_{NoGridConn} = ES_{GridConn} - CG$$

In the results section of the paper, we show results with and without grid connection costs as equally valid options. The discussion on cost recovery of grid infrastructure will be presented in a future study.

**DATA AVAILABILITY:** The datasets used in this study are available in the ZENODO repository as Supplementary Data, DOI: <https://doi.org/10.5281/zenodo.3840134>. This includes the raw data for all results presented here and input data for Figs. 1-4. Source data are provided with this paper.

**CODE AVAILABILITY:** The cashflow model produced for this study is available in the ZENODO repository as Supplementary Software 1, DOI: <https://doi.org/10.5281/zenodo.3733604>). The

model is set up to recreate the results of this paper. Refer to the README in the instructions.

**ADDITIONAL INFORMATION:** Supplementary information is available for this paper at <https://doi.org/10.1038/s41560-020-0661-2>.

**AUTHOR CONTRIBUTIONS:** Malte Jansen, Felix Müsgens, Iain Staffell and Iegor Riepin conceived the study and developed the analysis. All authors contributed to data gathering and data analysis. All authors wrote and edited the paper.

# 3

## MODELLING UNCERTAINTY IN COUPLED ELECTRICITY AND GAS SYSTEMS—IS IT WORTH THE EFFORT?

---

*This chapter presents the journal article as originally published in Applied Energy.*  
ELSEVIER(C) 2020

**ABSTRACT:** The interdependence of electricity and natural gas markets is becoming a major topic in energy research. Integrated energy models are used to assist decision-making for businesses and policymakers addressing challenges of energy transition and climate change. The analysis of complex energy systems requires large-scale models, which are based on extensive databases, intertemporal dynamics and a multitude of decision variables. Integrating such energy system models results in increased system complexity. This complexity poses a challenge for energy modellers to address multiple uncertainties that affect both markets. Stochastic optimisation approaches enable an adequate consideration of uncertainties in investment and operation planning; however, stochastic modelling of integrated large-scale energy systems further scales the level of complexity. In this paper, we combine integrated and stochastic optimisation problems and parametrise our model for European electricity and gas markets. We analyse and compare the impact of uncertain input parameters, such as gas and electricity demand, renewable energy capacities and fuel and CO<sub>2</sub> prices, on the quality of the solution obtained in the integrated optimisation problem. Our results quantify the value of encoding uncertainty as a part of a model. While the methodological contribution should be of interest for energy modellers, our findings are relevant for industry experts and stakeholders with an empirical interest in the European energy system.

**KEYWORDS:** Energy modelling, Energy systems analysis, Sector coupling, Stochastic programming, Uncertainty

**PUBLISHED AS:** I. Riepin, T. Möbius, F. Müsgens (2021), Modelling uncertainty in coupled electricity and gas systems—Is it worth the effort? *Applied Energy*, Vol. 285, 116363. DOI: <https://doi.org/10.1016/j.apenergy.2020.116363>

### 3.1 INTRODUCTION

Modelling energy markets is immensely important for academic purposes, business decision-making and governmental projections to address energy transitions and climate change. Modern energy models

entail extensive databases, intertemporal dynamics and a multitude of decision variables, all of which are necessary to capture the complex behaviour of energy markets.

Ongoing energy transitions present new challenges for energy modellers by increasing the interconnection of energy markets. These challenges require consideration of multiple interdependencies between the models of different sectors, such as the electricity and gas sectors [63]. The growing role of gas-fired plants in renewable-based electricity markets and the increasing dependence on natural gas imports make this issue particularly important for the European energy modelling community [64]. Thus, the number of model-based studies focusing on integrated modelling of electricity and gas markets has grown in recent years. The advantages of integrated modelling come at a cost in the form of higher computational complexity stemming from simultaneous optimisation of both markets with their own intertemporal dynamics and relevant infrastructure.

Another factor troubling energy modellers is the uncertainties of input data that characterise the future development of electricity and gas sectors. These include fuel prices, technological developments (e.g. installed capacities of renewable generation), regulations and political context. Most studies focusing on the integrated optimisation of electricity and gas markets to date have been using a deterministic approach. This is likely due to the fact that stochastic models—even for a single sector—are complicated to construct and expensive to run. In many cases, however, ignoring uncertainty leads to poor decisions (see: [65, 66]).

Therefore, researchers must decide whether to neglect uncertainty and accept a suboptimal set of decisions or to incorporate uncertainty into large-scale integrated models and increase computational complexity even further. When addressing this trade-off, the natural question thus is: how inaccurate are solutions neglecting uncertainty?

Our paper answers this question. We derive the optimal investment decisions when uncertainty is explicitly encoded (or removed) in a model – and quantify the difference. Our approach is novel in two ways:

- A. To the best of our knowledge, our paper presents the first large-scale integrated electricity and gas market model with investment decisions under uncertainty. This is a methodological advancement.
- B. We quantify the impact of parametric uncertainties on the solution’s quality of the system dispatch & investment optimisation problem for widely used electricity and gas market scenarios. This is an empirical advancement.

The methodological contribution extends the existing literature stream on electricity and gas market coupling [64, 67] with consider-

ation of parametric uncertainty. It also extends the literature stream on uncertainty in either of electricity or gas sectors [66, 68] with the coupling of these sectors. Hence, our contribution provides a new stimulus for both researchers working on sector coupling as well as researchers working on stochastic optimisation – and may even foster future collaboration between the two research streams.

On the empirical side, we isolate, quantify and compare the effect of ignoring uncertainty. Our findings show which key parameters' uncertainty (electricity demand, installed renewable capacity, gas demand, fuel prices and CO<sub>2</sub> price) most substantially affects long-term investment planning decisions and total costs. Furthermore, we provide in-depth insight into how uncertainty translates into market fundamentals, e.g. residual loads and variable costs of power generation. Our analysis thus benefits future modellers facing the trade-off between model accurateness on the one hand and resource investment on the other hand. In particular, it can help them decide whether and to what extent to make their energy system models a) sector-coupled and/or b) stochastic.

We apply our model to a stylised representation of the European market. The majority of model-based studies on Europe rely on data from [ENTSO](#) for the future development of the electricity and gas sectors. We parametrise our model the same way by basing our data primarily on the The Ten-Year Network Development Plan ([TYNDP](#)) from [ENTSOs](#) [69]. Thus, we believe this research is a useful reference for a broad circle of industry experts and stakeholders with an empirical interest in the European energy system.

In order to facilitate the transparency and reproducibility of our results, as well as to encourage further research on model coupling and uncertainty, our model code, associated data and scripts for result processing are all published on the [public GitHub repository](#).

### 3.2 INTEGRATED AND STOCHASTIC MODELLING OF ELECTRICITY AND GAS MARKETS IN THE LITERATURE

#### 3.2.1 *Integrated modelling*

As already stated, interest in the representation of complex interdependencies between the electricity and gas sectors in energy models has grown in recent years. The early studies on the interplay between the two sectors were limited in their application to (i) simplified or no representations of intertemporal dynamics, (ii) toy parametrisation and (iii) soft- or hard-linking approaches.<sup>1</sup> For example, an optimisa-

<sup>1</sup> *Soft-linking* is defined as a model coupling approach in which information is processed and transferred manually by the modeller; *hard-linking* (usually associated with an iterative solution approach) is defined as a model coupling approach in which input/output information transfer is handled by an algorithm [70].

tion model on the natural gas and electricity sectors over a single time period was discussed by An, Li, and Gedra [71] and Geidl and Andersson [72]. A hard-linking approach is used by Ohishi and Mello [73], among others. These authors highlight the importance of integrated modelling for economic and secure energy system operation based on a toy system model. Bartels and Seeliger [74] use a hard-linking approach to analyse the long-term impact of CO<sub>2</sub>-emission trading on the two markets with a pan-European geographical scope. More examples are provided by Rubio et al. [75], who present a literature survey on integrated natural gas and electricity system planning literature and highlight economic and market-related aspects.

Advancements in computing power and mathematical models paired with the challenges of the energy transition process have facilitated the development of more sophisticated models. Such models address the limitations of earlier research and, thus, are characterised by (i) a larger time scope and higher time resolution with complex intertemporal dynamics, (ii) parametrisation to a regional or pan-European geographical scope and (iii) integrated (simultaneous) optimisation of both sectors. Chaudry, Jenkins, and Strbac [76] investigate the importance of gas storage in the context of integrated system stability based on the British gas and electricity network. Möst and Perlwitz [77] focus on European gas supply prospects through 2020 and their relevance for the power sector in the context of emission trading. Lienert and Lochner [78] focus on the short- and long-term dynamics between natural gas and electricity markets using the pan-European integrated model; they highlight that quantitative models that do not consider interdependencies between the two markets produce results with systematic deviations from a more realistic integrated optimisation. Abrell and Weigt [64] run several long-term gas market scenarios to capture their impact on power plant investments and short-term supply shock scenarios to analyse spatial feedback towards the electricity system. Deane, Ó Ciaráin, and Ó Gallachóir [67] construct an integrated model with a daily temporal resolution to examine the impact of gas supply interruptions on power system operation and gas flow in the European market. Several authors focus on coordinated expansion planning problems and investigate the potential for substitution effects between investments in generation and transmission across both sectors [79–81]. A number of studies have begun to examine the value of gas network infrastructure flexibility in supporting the cost-effective operation of power systems. Ameli, Qadrdan, and Strbac [82] investigate benefits of employing flexible multi-directional compressor stations as well as adopting an integrated approach to operate gas and electricity networks. Clegg and Mancarella [83] develop a novel multi-stage integrated gas and electricity transmission network model, which uses electrical Direct Current (DC) optimal power flow and both steady-state and transient gas analysis. The authors assess how the

lack of gas network's flexibility can affect the local generation and reserve constraints in the electricity network.

### 3.2.2 *Stochastic modelling*

Actors in modern liberalised electricity markets face multiple uncertainties. These are driven by the development of prices for primary energy carriers, the structural changes in the energy sector (e.g. introduction of carbon markets or nuclear phase-outs in several countries around the globe) and regulation (subsidization of renewable generation, decarbonisation policy, the introduction of the carbon price floor in the UK, etc). There are also uncertainties in natural gas markets, where many factors on the demand side (weather, decarbonisation policy) and the supply side (gas reserves) are inherently uncertain. Gas markets are also subject to structural breaks, such as recent drops in production capacity in North-Western Europe or US shale gas revolution.

It is important to understand the impact of uncertain input parameters on the model outputs, conclusions or policy recommendations. Stochastic programming, first conceived by Dantzig [84] as a framework for decision-making under uncertainty, has been successfully applied to energy models for decades. Möst and Keles [85] provide a comprehensive survey of stochastic modelling approaches for liberalised electricity markets while Egging [65] provides a structured overview of stochastic market models and algorithms for both sectors; both of these reviews show that stochastic modelling of energy markets can take on various mathematical forms with different purposes and solution algorithms. In this section, however, we focus primarily on applications of multi-stage optimisation models for short- and mid-term generation and long-term system expansion planning, which are most relevant for this paper.

Regarding electricity markets, Musgens and Neuhoff [86] use stochastic optimisation to analyse the impact of the daily wind feed-in on dispatch decisions and the value of updating wind forecasts. Benoot et al. [87] develop the MARKAL/TIMES modelling framework to integrate uncertainty about fuel prices, climate policy and price elasticity of demand in the comprehensive assessment of energy and climate change policies in the EU. Fürsch, Nagl, and Lindenberger [88] use a multi-stage stochastic programming approach to optimise power plant investments along uncertain renewable energy development paths. Weijde and Hobbs [66] use two-stage stochastic optimisation for electricity grid reinforcement planning under uncertainty; they highlight the fact that ignoring risk in transmission planning for renewables has quantifiable economic consequences while considering uncertainty yields decisions with expected costs lower than those from traditional deterministic planning methods. Seljom and Tomasgard [89], studying



the impact of stochastic wind feed-in on optimal generation capacity, conclude that the stochastic representation of intermittent renewables in long-term investment models provides more reliable results for decision-makers. Xu et al. [90] evaluate the impact of scenario tree reduction on solution quality of stochastic problem for hydropower operation. Möbius and Müsgens [91] study the impact of uncertain wind feed-in on long-term market equilibria. Schwarz, Bertsch, and Fichtner [92] present a two-stage stochastic problem for optimising investment and operation decisions in a decentralised energy system. Xu et al. [93] use stochastic programming to identify the long-term effects of using hydropower to complement wind power uncertainty.

Regarding gas markets, Zhuang [94] and Zhuang and Gabriel [95] develop an extensive-form stochastic complementarity problem and provide a small-scale natural gas market implementation. Egging [65] develops a stochastic multi-period global gas market model. The author concludes that stochastic modelling shows hedging behaviour that affects the timing and magnitude of capacity expansions, significantly affecting local market situations and prices. Fodstad et al. [68] analyse the impact of uncertainty about future European natural gas consumption on optimal investments in gas transport infrastructure and conclude that the option value of delaying investments in natural gas infrastructure until more information is available in 2020 is very limited due to the low costs of overcapacity. They also find, however, structural differences between the infrastructure investments derived from the stochastic model and those from the deterministic model.

### 3.2.3 *Identifying the research gap*

Our literature review reveals two important research gaps. First, few studies to date have combined market integration and stochastic elements. These are however, comprise toy energy systems [96, 97], focus on a single uncertainty [98, 99] or are static [80]. This observation is bolstered by Deane, Ó Ciaráin, and Ó Gallachóir [67], who state that while uncertainty in electricity and gas systems are not a recent phenomenon, their impacts on integrated systems are not well examined. Second, no study has yet to provide a framework to ignore isolated uncertain model inputs and subsequently quantify and compare their effects. Thus, there is still no systematic understanding of which isolated parametric uncertainty most substantially affects long-term planning decisions.

This paper serves to fill in these two research gaps. We present an applied methodology and an open-source model to examine the trade-off between complexity from integrated optimisation of gas and electricity systems and a wide range of parametric uncertainties.

### 3.3 METHODOLOGY

We construct and apply an integrated stochastic bottom-up optimisation model for European electricity and gas markets. The model's objective function minimises the total costs, comprising expected discounted capital and operating costs for both sectors. The optimal solution implies that all arbitrage opportunities across time and space are exhausted to the extent that the infrastructure constraints of the integrated system permit. The results of the model include spatial and temporal decisions on both investment in power generation units and the production, transportation and storage of electricity and gas. Investments in electricity and gas transmission networks are considered exogenous. The incorporation of storage and investment decisions into the optimisation problem requires (and enables) intertemporal optimisation. We opt for a linear model formulation to ensure scalability and computational tractability of the model. We introduce one-stage deterministic optimisation and two-stage stochastic optimisation approaches in Section 3.3.1. Once all model runs are complete, we analyse the results to determine whether neglecting uncertainty results in an inaccurate solution. The theoretical background for this approach is detailed in Section 3.3.2.

The gas market components in our model (input data and decision variables) have a temporal resolution of 12 consecutive months while the electricity market components are solved over 350 representative hours for each modelled year.<sup>2</sup> The temporal scope is 2020 – 2030. Model simulations are performed for three representative years: 2020, 2025 and 2030. This allows us to capture both the short-term market operations and long-term investments dynamics.

The model structure is made up by a network of nodes. A node represents a country or a group of several countries from one region. Nodes are connected by electricity and gas transmission infrastructure. The geographical scope covers most European member states, Norway, Switzerland, the United Kingdom and several non-European major gas exporters (Russia, the United States, Algeria, Libya, Nigeria and Qatar). We provide a full list of the countries considered in our model in the [Supplementary Data](#).

The markets are combined via fuel linkage; both the gas demand for the power sector and the price for gas-fired electricity generation are modelled endogenously. Fluctuations in natural gas demand from the power and non-power sectors induce gas price volatility. Thus, our modelling approach ensures endogenously defined spatial and temporal gas price patterns; as gas price is the cost input for gas-fired

<sup>2</sup> The reduced time-series is sampled by each 25th hour of a full time series, which results in a set of 350 representative hours per year. For more detail on Nth hour time reduction process, see [100].

units, its volatility affects dispatch and investment decisions in the electricity sector.

Integrated modelling has several advantages over soft- and hard-linking approaches. First, it excludes the convergence criteria used in iterative linking approaches. These criteria are usually based on the rate of change between model outputs over subsequent iterations. Large-scale energy models solved iteratively may encounter regular convergence problems [70, 101]. Second, integrated optimisation of two sectors ensures that the optimal solution includes reliable marginal cost estimators. Note that marginal electricity generation costs are derived from the dual variables of each node’s energy balance constraints. Thus, the optimal solution ensures that a relaxation of these constraints (by one MWh of gas or electricity) returns true marginal savings from producing, transporting and storing that energy unit.<sup>3</sup> Third, integrated modelling allows us to conveniently handle a large number of model runs, which are necessary to answer this paper’s research questions (see discussion of scenarios and modes in Section 3.3.3).

We provide a complete model formulation in Section 3.3.4. All of the data used are from publicly available sources. In Section 3.3.5, we discuss our assumptions on both sectors’ demand and supply structure and transmission infrastructure. The model is formulated in General Algebraic Modeling System (GAMS)<sup>4</sup> and solved with a CPLEX solver.

### 3.3.1 Optimization approaches

In this section, we introduce the one-stage deterministic optimisation and the two-stage stochastic optimisation approaches.

Consider a Linear (optimization) Problem (LP), where  $x$  represents a vector of variables,  $c$  and  $b$  are parameter vectors (i.e. known coefficients),  $A$  is a matrix of parameters, and  $T$  denotes a matrix transpose. The inequalities are the constraints that specify a convex polytope over which the objective function is to be optimised. The optimal Deterministic Solution (DS) is to find a vector  $x$  that minimises the objective under the set of relevant constraints:

$$DS = \min_x c^T x \quad (3.1a)$$

$$\text{s.t. } Ax \geq b, x \geq 0 \quad (3.1b)$$

Due to their relative simplicity, these models can be solved with a high degree of empirical detail. Hence, they are a widely used ‘work-horse’ in energy system modelling.

<sup>3</sup> Thus, marginal costs can be considered as price indicators in a competitive market.

<sup>4</sup> <https://www.gams.com/>

However, energy system forecasters face multiple uncertainties, such as primary energy carrier prices, technological developments, regulations and political context. The optimisation problem and the resulting decisions depend on these uncertainties. They are particularly relevant when analysing investment decisions in energy systems, which are largely irreversible and involve a high share of total generation costs. An approach to explicitly incorporate uncertainty is to represent the multi-stage nature of investment planning in a two-stage stochastic model. It implies that optimal *first-stage* investment decisions in power generation technologies must be made before the information on uncertain factors is revealed; while *second-stage* dispatch decisions are made after uncertainty is revealed.

The classical two-stage Stochastic (linear) Problem (SP) can be formulated as follows [102]:

$$\min_x c^T x + E_\omega[Q(x, \omega)] \quad (3.2a)$$

$$\text{s.t. } Ax = b, x \geq 0 \quad (3.2b)$$

where

$$Q(x, \omega) = \min_y q_\omega^T y \quad (3.3a)$$

$$\text{s.t. } T_\omega x + W_\omega y \geq d_\omega, y \geq 0 \quad (3.3b)$$

Where  $x$  represents the vector of first-stage variables,  $y$  is the vector of second-stage variables, and  $\omega$  is the vector of uncertain data for the second stage (i.e. the vector of possible scenarios). The parameter  $c^T$ , the matrix  $A$ , and the right-hand-side vector  $b$  of the first stage are assumed to be known with certainty. Problem 3.2 seeks a first-stage decision to minimise the costs that occur at the first stage and the *expected costs* of second-stage (recourse) decisions. Problem 3.3 seeks second-stage decisions that minimise the second-stage costs. Second-stage decisions are restricted by the first-stage decisions of  $x$ , the matrix  $T$ , the matrix  $W$ , and the right-hand-side vector  $d$ . Note that the parameters  $(q, T, W, d)$  are actual realisations of uncertain data.

By solving a stochastic problem, we obtain an optimal solution  $\bar{x}$  of the first-stage problem and optimal solutions  $\bar{y}$  of the second-stage problem for each realisation of  $\omega_n$ . Given  $\bar{x}$ , each  $\bar{y}_n$  corresponds to an optimal second-stage decision corresponding to a realisation of the respective scenario. In the context of this paper, the solution of a stochastic problem (in the sense of minimising total expected costs) defines (i) the optimal electricity generation investment (which must hold for all scenarios) and (ii) scenario-dependent optimal dispatch decisions of all assets for both electricity and gas components.

### 3.3.2 The expected cost of ignoring uncertainty

Stochastic problems are often avoided in practice because they are computationally difficult to solve. Many real-world problems are addressed with simpler approaches. For example, one can solve several deterministic programs—each corresponding to one particular scenario—and then combine solutions using a heuristic rule. The approximation problem most often discussed in the context of two-stage stochastic problems is the Expected Value Problem (EVP), a problem wherein the uncertain parameters are replaced by their expected values. Consider a two-stage stochastic problem as formulated in section 3.3.1; a Stochastic Solution (SS) is defined as follows:

$$SS = \min_x c^T x + E_\omega [Q(x, \omega)] \quad (3.4)$$

The EVP is constructed by setting  $\bar{\omega} = E_\omega \cdot \omega$ . Thus, a solution of an EVP is:

$$EVS = \min_x c^T x + [Q(x, \bar{\omega})] \quad (3.5)$$

Fig. 3.1 illustrates the modelling of an SP versus that of an EVP.

As we have already pointed out, problem 3.5 is an approximation problem, meaning it does not consider uncertainty. An alternative is to explicitly encode uncertainty into the model by setting a probability distribution for uncertain parameters, as shown in problems 3.2 and 3.3. It is crucial for us to understand whether ignoring uncertainty reduces the quality of the decisions reached. The theoretical answer to this is given in the literature by the concept of the expected costs of ignoring uncertainty (see: [102, 103]).

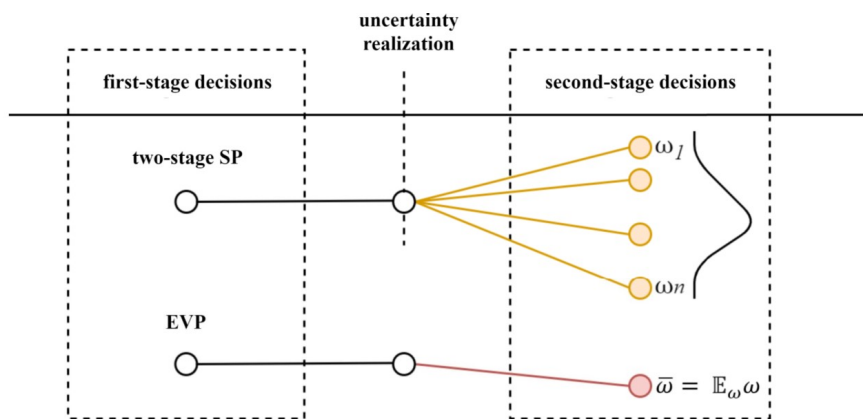


Figure 3.1: A two-stage stochastic problem and an approximation (EVP)

To reach this understanding, let  $\bar{x}(\bar{\omega})$  denote an optimal first-stage decision in an EVP. Then, constraining the stochastic problem with

the first-stage decisions of the **EVP** shows how well a decision  $\bar{x}(\bar{\omega})$  performs. The expected result of imposing  $\bar{x}(\bar{\omega})$  into a stochastic problem is denoted by Expected result of using the Expected Value solution (**EEV**):

$$EEV = E_{\omega}[\phi(\bar{x}(\bar{\omega}), \omega)] \quad (3.6)$$

The Expected Cost of Ignoring Uncertainty (**ECIU**) is defined as:

$$ECIU = EEV - SS \quad (3.7)$$

The **ECIU** is useful because it describes the value of considering the full range of uncertainties in a stochastic model rather than that of using a deterministic problem. Thus, the metric can be interpreted as *the expected cost of assuming that the future is certain*.<sup>5</sup>

### 3.3.3 Scenario composition

**Introducing scenarios.** This paper quantifies the **ECIU** relative to the **EVP** discussed above based on three scenarios from **TYNDP** (presented in Section 3.3.5). Furthermore, we compute and discuss the **ECIU**s when each of **ENTSOs'** scenarios are chosen as the reference for a deterministic model. This is done by replacing the **EVP** from problem 3.5 [ $\bar{\omega} = E_{\omega}\omega$ ] with the data for a specific scenario [ $\omega_n$ ]. Throughout the discussion, we use the term Naïve (optimization) Problem (**NP**) to refer to the set of four (each  $\omega_n$  and  $\bar{\omega}$ ) possible deterministic problems chosen by a system planner when uncertainty in data is ignored (albeit present). Thus, the Solution to an **NP** is:

$$NPS = \min_x c^T x + [Q(x, \hat{\omega} \in \{\omega_n, \bar{\omega}\})] \quad (3.8)$$

Consequently, we incorporate  $\bar{x}(\omega_n)$  into a stochastic problem to evaluate the expected result of each NPS:

$$EEV_n = E_{\omega}[\phi(\hat{x}(\hat{\omega}), \omega)] \quad (3.9)$$

This allows us to compute the scenario-specific **ECIU**s:

$$ECIU_n = EEV_n - SS \quad (3.10)$$

<sup>5</sup> An assumption we take to solve a two-stage stochastic problem is that the probability distribution for scenarios representing uncertainty of model parameters is known. This is a simplification of reality inherent to this type of optimisation problems. See Laes and Couder [104] discussing the usefulness of bottom-up energy and climate models in a light of 'deep uncertainty' that characterise the future development of energy systems.

**Introducing stochastic model modes.** We define two stochastic model modes for this study: *all parameters* and *isolated parameters*. In the first mode, a vector of uncertain data in a stochastic problem includes all five uncertain parameters. For example, scenario branch EUCCO includes gas demand, electricity demand, installed RES capacity, fuel prices and CO<sub>2</sub> prices, which all have a path as defined in the EUCCO scenario of the TYNDP. The same applies to the other two branches of a stochastic problem. Thus, optimal first-stage investment decisions in power generation technologies must be made with consideration for a composite uncertainty.

In the second mode, we provide more in-depth analysis by isolating the effects of parametric uncertainty. In this mode, a vector of uncertain data in a stochastic problem includes a single parameter. Intuitively, the development paths of the other four parameters (which are known in this set-up) have their own effects, which we capture by computing a matrix consisting of combinations of isolated parametric uncertainties and the possible development paths of known parameters.

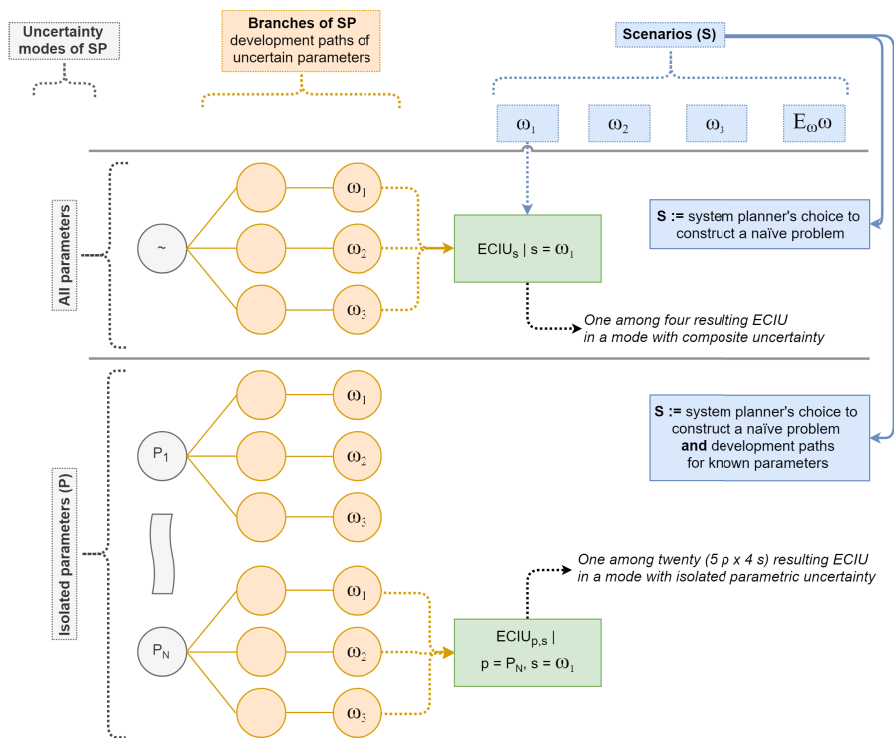


Figure 3.2: Graphical illustration of scenario composition

**Combining scenarios and modes.** The composition of modes and scenarios is illustrated in Fig. 3.2. Throughout the discussion of our results, the term *scenario branch* refers to the branches of a stochastic model (EUCCO, ST, DG) that define possible development paths of uncertain parameters; the term *scenario* refers to (i) the system planner’s

choice for solving a deterministic problem (in ‘all parameters’ mode) and (ii) the development paths for known parameters (in ‘isolated parameters’ mode).

### 3.3.4 Model formulation

#### Nomenclature (1/2)

Abbreviation	Dimension	Description
<b>Sets</b>		
gas(i)	Subset of i	Gas-fired technology
i		Technology
m		Month
n		Node
nn	Alias of n	Node
psp(i)	Subset of i	Pump storage
res(i)	Subset of i	RES technology
rwr(i)	Subset of i	Water reservoir
s		Scenario
t		(Representative) hours
tm(t)	Subset of t	Hours in month m
y		Year
<b>Variables</b>		
<i>arcflow</i>	MWh <sub>th</sub> /month	Gas flow over the arc
<i>cap</i>	MW <sub>el</sub>	Inv. in power gen. capacity
<i>charge</i>	MWh <sub>el</sub> /h	Charge by PSP
<i>flow</i>	MWh <sub>el</sub> /h	Electricity flow
<i>g</i>	MWh <sub>el</sub> /h	Electricity generation
<i>glow</i>	MWh <sub>th</sub> /month	Gas flow volume
<i>inj</i>	MWh <sub>th</sub> /month	Gas injection into storage
<i>level</i>	MWh <sub>th</sub> /month	Stock level of gas in storage
<i>pvol</i>	MWh <sub>th</sub> /month	Gas production volume
<i>shed</i>	MWh <sub>el</sub> /h	Load shedding
<i>sl</i>	MWh <sub>el</sub>	Storage level of PSP
<i>TC</i>	€	Total system costs
<i>with</i>	MWh <sub>th</sub> /month	Gas withdrawal from storage



## Nomenclature (2/2)

Abbreviation	Dimension	Description
<b>Parameters</b>		
<i>AF</i>	%	Availability factor
<i>ARCCAP</i>	MWh <sub>th</sub> /month	Transmission capacity
<i>CAP<sup>ex</sup></i>	MW <sub>el</sub>	Installed power generation capacity
<i>CC</i>	tCO <sub>2</sub> /MWh <sub>th</sub>	Carbon emission factor
<i>CHP</i>	MWh <sub>el</sub> /h	Minimum generation by <b>CHP</b>
<i>CPF</i>	h	Storage capacity-power factor
<i>EndLevel</i>	MWh <sub>th</sub>	Gas storage stock level: last period
<i>DEMAND</i>	MWh <sub>el</sub> /h	Electricity demand
<i>DF</i>		Discount factor
<i>FLH</i>	h	Full load hours of water reservoirs
<i>IC</i>	€/MW <sub>el</sub>	Annual investment costs
<i>ICAP</i>	MWh <sub>th</sub> /month	Gas storage injection capacity
<i>ICOST</i>	€/MWh <sub>th</sub>	Gas storage injection costs
<i>LTC</i>	MWh <sub>th</sub> /month	<b>LTC</b> obligation for gas deliveries
<i>NPGDEM</i>	MWh <sub>th</sub> /month	Non-power sector gas demand
<i>NTC</i>	MW <sub>el</sub>	Net transfer capacity
<i>p<sup>CO<sub>2</sub></sup></i>	€/tCO <sub>2</sub>	Carbon price
<i>PCAP</i>	MWh <sub>th</sub> /month	Available gas production capacity
<i>PCOST</i>	€/MWh <sub>th</sub>	Marginal gas production costs
<i>PF</i>	%	Production factor for <b>RES</b>
<i>SF<sup>max</sup></i>	%	Max shedding factor per node
<i>StLevel</i>	MWh <sub>th</sub>	Gas storage stock level: start period
<i>TCOST</i>	€/MWh <sub>th</sub>	Marginal gas transport costs
<i>TOP</i>	%	Take-or-pay levels
<i>VC</i>	€/MWh <sub>el</sub>	Variable power generation costs
<i>VOLA</i>	€/MWh <sub>el</sub>	<b>VoLA</b> as the cost of load shedding
<i>WCAP</i>	MWh <sub>th</sub> /month	Gas storage withdrawal capacity
<i>WCOST</i>	€/MWh <sub>th</sub>	Gas storage withdrawal costs
<i>WGV</i>	MWh <sub>th</sub>	Working gas capacity of storage
<i>η</i>	%	Storage efficiency
<i>ρ</i>	%	scenario realization probability

Objective function 3.11 minimises the total expected discounted capital and operating costs for both sectors:

$$\min TC = \sum_{s,y} \rho_s \cdot DF_y \cdot \left( \begin{aligned} & \sum_{g \setminus gas,n,t} (g_{i,n,t,y,s} \cdot VC_{i,n,t,y}) \\ & + \sum_{gas,n,t} (g_{gas,n,t,y,s} \cdot [CC_{gas} \cdot P_y^{CO_2} / \eta_{gas,n,y}]) \\ & + \sum_{n,t} (shed_{n,t,y,s} \cdot VOLA_n) \\ & + \sum_{p,n,c} (pvol_{p,n,c,m,y,s} \cdot PCOST_{p,n}) \\ & + \sum_{p,n,nn \neq n} (gflow_{p,n,nn,m,y,s} \cdot TCOST_{n,nn,t}) \\ & + \sum_c (inj_{c,m,y,s} \cdot ICOST + with_{c,m,y,s} \cdot WCOST) \end{aligned} \right) + \sum_{i,n,y} DF_y \cdot cap_{i,n,y} \cdot IC_i \quad (3.11)$$

Eq. 3.12 ensures that the market is cleared under the constraint that electricity demand in each node is satisfied at all times:

$$\begin{aligned} DEMAND_{n,t,y,s} = & \sum_{i \setminus psp} g_{i,n,t,y,s} + shed_{n,t,y,s} + g_{psp,n,t,y,s} \cdot 1/\eta_{psp,n,y} \\ & - charge_{psp,n,t,y,s} + \sum_{nn} (flow_{nn,n,t,y,s} - flow_{n,nn,t,y,s}) \quad \forall n, t, y, s \end{aligned} \quad (3.12)$$

Eq. 3.13 restricts hourly load-shedding activities to a share of the country-specific demand:

$$shed_{n,t,y,s} \leq DEMAND_{n,t,y,s} \cdot SF^{max} \quad \forall n, t, y, s \quad (3.13)$$

Eq. 3.14 define the capacity restrictions for power stations. Eq. 3.14a states that newly invested capacity in year  $y - 1$  must be present in the following year  $y$ . Eq. 3.14b limits generation to the available installed capacity. Eq. 3.14c defines the hourly RES feed-in. Eq. 3.14d considers political or technical restrictions on new investments in specific technologies (e.g. nuclear, coal):

$$cap_{i,n,y-1} \leq cap_{i,n,y} \quad \forall i, n, y \quad (3.14a)$$

$$g_{i,n,t,y,s} \leq (CAP_{i,n,y,s}^{ex} + cap_{i,n,y}) \cdot AF_{i,n} \quad \forall n, t, y, s \quad (3.14b)$$

$$g_{res,n,t,y,s} \leq CAP_{i,n,y,s}^{ex} \cdot PF_{res,t,n} \quad \forall RES \in I, n, t, y, s \quad (3.14c)$$

$$cap_{i,n,y} \leq cap_{i,n,y}^{new\ max} \quad \forall i, n, y \quad (3.14d)$$

Eq. 3.15 describe the storage mechanism. Eq. 3.15a defines the maximum storage level. Eq. 3.15b defines the state of the storage level at the end of hour  $t$ . Eq. 3.15c defines the maximum charging capacity:

$$sl_{pssp,n,t,y,s} \leq (CAP_{pssp,n,y}^{ex} + cap_{pssp,n,y}) \cdot CPF \quad (3.15a)$$

$$sl_{pssp,n,t,y,s} = sl_{pssp,n,t-1,y,s} - g_{pssp,n,t,y,s} + charge_{pssp,n,t,y,s} \quad (3.15b)$$

$$charge_{pssp,n,t,y,s} \leq CAP_{pssp,n,y}^{ex} + cap_{pssp,n,y} \cdot AF_{pssp,n} \quad (3.15c)$$

$$3.15: \quad \forall PSP \in I, n, t, y, s$$

Eq. 3.16 defines an annual limit to the generation by hydro reservoirs:

$$\sum_t g_{rvr,n,t,y,s} \leq CAP_{rvr,n,y,s}^{ex} \cdot FLH \quad \forall rvr \in I, n, y, s \quad (3.16)$$

Eq. 3.17 states that gas-fired power plants are committed to country-specific CHP requirements:

$$CHP_{n,t,y} \leq \sum_{gas} g_{gas,n,t,y,s} \quad \forall n, t, y, s \quad (3.17)$$

Eq.3.18 restricts cross-border electricity trading:

$$flow_{n,nn,t,y,s} \leq NTC_{n,nn,y} \quad \forall n, nn, t, y, s \quad (3.18)$$

Eq. 3.19 ensures that the quantity of gas imported and withdrawn from storage at each node is equal to the quantity consumed by power sectors (endogenous) and non-power sectors (exogenous) and injected into storage:

$$\begin{aligned} \sum_{p,n} pvol_{p,n,c,m,y,s} = \\ NPGDEM_{c,m,y,s} + pgdem_{c,m,y,s} + with_{c,m,y,s} - inj_{c,m,y,s} \\ \forall c, m, y, s \end{aligned} \quad (3.19)$$

Eq. 3.20a defines capacity restrictions for gas production while eq.3.20b defines those for gas transport:

$$PCAP_{p,n,y,m} - \sum_c pvol_{p,n,c,m,y,s} \geq 0 \quad \forall p, n, m, y, s \quad (3.20a)$$

$$ARCCAP_{n,nn,y} - arcflow_{n,nn,m,y,s} \geq 0 \quad \forall n, nn, y \quad (3.20b)$$

$$where: arcflow_{n,nn,m,y,s} = \sum_p gflow_{p,n,nn,m,y,s} \quad \forall n, nn, m, y, s$$

Eq. 3.21 ensures flow conservation in gas network:

$$\left[ \sum_{nn \neq n} pvol_{p,n,nn,m,y,s} - \sum_{nn \neq n} gflow_{p,n,nn,m,y,s} \right] + \left[ \sum_{nn \neq n} gflow_{p,nn,n,m,y,s} - \sum_{nn \neq n} pvol_{p,nn,n,m,y,s} \right] = 0 \quad \forall p, n, m, y, s \quad (3.21)$$

Eq. 3.22 sets a minimum amount of gas to be produced and dispatched under LTC between specific nodes:

$$\sum_p pvol_{p,n,nn,m,y,s} - TOP \cdot LTC_{n,nn,m,y} \geq 0 \quad \forall n, nn, m, y \quad (3.22)$$

Eq. 3.23a-3.23d define storage levels at the end of month  $m$  and ensure intertemporal optimisation over multiple years. Eq. 3.23e-3.23g represent constraints on storage working gas capacity, injection capacity, and withdrawal capacity:

$$level_{c,m,y,s} = level_{c,m-1,y,s} + (1 - \eta) \cdot inj_{c,m,y,s} - with_{c,m,y,s} \quad \forall c, m \setminus Jan, y, s \quad (3.23a)$$

$$level_{c,m1,y,s} = level_{c,m12,y-1,s} + (1 - \eta) \cdot inj_{c,m1,y,s} - with_{c,m1,y,s} \quad \forall c, y, s \quad (3.23b)$$

$$level_{c,m,y,s} = StLEVEL_c + (1 - \eta) \cdot inj_{c,m,y,s} - with_{c,m,y,s} \quad \forall c, s \quad [m = Jan, y = 2020] \quad (3.23c)$$

$$level_{c,m,y,s} \geq EndLEVEL_c \quad \forall c, s \quad [m = Dec, y = 2030] \quad (3.23d)$$

$$WGV_{c,m,y} - level_{c,m,y,s} \geq 0 \quad \forall c, m, y, s \quad (3.23e)$$

$$ICAP_{c,m,y} - inj_{c,m,y,s} \geq 0 \quad \forall c, m, y, s \quad (3.23f)$$

$$WCAP_{c,m,y} - with_{c,m,y,s} \geq 0 \quad \forall c, m, y, s \quad (3.23g)$$

Eq. 3.24 integrates both markets via the fuel link; gas demand of the electricity sector becomes an endogenous variable and drives gas consumption in eq. 3.19.

$$pgdem_{n,m,y,s} = \sum_{gas,t|t=tm} \frac{g_{gas,n,t,y,s}}{\eta_{gas,n,y}} \quad \forall gas \in I, t, y, s \quad (3.24)$$

## 3.3.5 Data

As already discussed, we parametrise our model primarily based on the [TYNDP](#) report from ENTSOs [69]. In this section, we detail the scenarios as defined in the report and present data for the electricity and gas sectors.

**Introduction of scenarios.** We consider scenario-dependent data for gas demand, electricity demand, installed RES capacities, fuel prices and CO<sub>2</sub> prices. Fig. 3.3 illustrates the three scenarios for the year 2030: Distributed Generation scenario (DG), Sustainable Transition scenario (ST) and the European Commission’s core policy scenario (EUCCO).

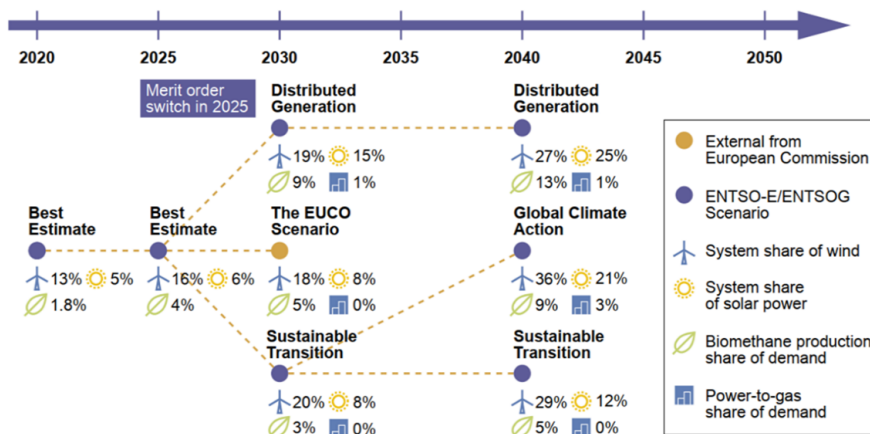


Figure 3.3: Scenarios from the 2018 [TYNDP](#) report

Source: ENTSOs [69]

The [DG](#) scenario represents a decentralised development of the energy system with a focus on end-user technologies. It assumes that consumers use smart technology and dual fuel appliances (e.g. hybrid heat pumps) to switch energy sources in line with market conditions. Additionally, in this scenario, electric vehicles see their highest penetration; Photovoltaics (PV) and batteries are both widely used in buildings. Relative to the other scenarios, [DG](#) is characterised by (i) the highest demand for electricity (both peak and total) and (ii) the highest amount of installed RES capacities.

The [ST](#) scenario represents a quick and economically sustainable reduction of CO<sub>2</sub> emissions achieved by replacing coal and lignite with gas in the power sector. Gas also replaces some oil usage in the transportation sector. The electrification of heat and transportation develops at a relatively slow pace. Relative to the other scenarios, [ST](#) is characterised by (i) the highest peak and total demand for natural gas and (ii) the highest price for CO<sub>2</sub> certificates (89.9 €<sub>2020</sub>/t in 2030).

The [EUCCO](#), which was created using the PRIMES model and the 2016 EU Reference Scenario as a starting point, is the European Commis-

sion's core policy scenario. The scenario represents the attainment of the 2030 climate and energy targets as agreed upon by the European Council in 2014, including an energy efficiency target of 30%. Relative to the other scenarios, **EUCO** is characterised by (i) the highest prices for lignite (8.8 €<sub>2020</sub>/MWh<sub>th</sub> in 2030) and hard coal (16.5 €<sub>2020</sub>/MWh<sub>th</sub> in 2030) and (ii) the lowest price for CO<sub>2</sub> certificates (28.8 €<sub>2020</sub>/t in 2030).

A detailed overview of the scenario data is provided in the **Supplementary material**<sup>6</sup>.

**Electricity sector data.** The model inputs for both sectors can be roughly divided into demand, supply and infrastructure. Electricity sector demand input, thus, encompasses scenario-dependent data on country-specific load structures and annual demand projections, which stem from ENTSOs [69].

Regarding the electricity sector supply inputs, scenario-dependent data on installed **RES** capacities (such as onshore wind, offshore wind and **PV**), fuel prices for lignite, hard coal and oil-fired power plants, and CO<sub>2</sub> prices are based on ENTSOs [69]. Prices for natural gas are endogenously derived using the integrated model. Fuel prices for nuclear power plants are based on Schröder et al. [105]. National thermal and hydro generation capacity, efficiency and decommissioning pathways come from Schröder et al. [105], Gerbaulet and Lorenz [100], Capros et al. [56] and Open Power System Data [106]. Investment costs for new power stations are taken from [105]. Additionally, we account for political and technical restrictions to investments in new technologies (e.g. the installation of nuclear, lignite or hard coal plants is only possible in countries without phase-out intentions). Run-of-river hydroelectricity, hydroelectric reservoirs, biomass and all above-mentioned **RES** are not subject to an endogenous investment decision. In order to account for country-specific Combined Heat and Power (**CHP**) utilisation schemes for gas-fired units, we implement temperature-dependent must-run conditions to meet the annual production volumes of **CHP** plants from Eurostat [107]. The storage level of a Pumped-Storage Power plant (**PSP**) is restricted by the capacity of the upper basin. A capacity-power factor connects the installed turbine capacity with the water capacity of the upper basin; it can be understood as the full load hours of a fully charged storage plant. Generation by hydroelectric reservoirs is bounded to the installed capacities and an annual water budget. To determine the annual water budget, we use empirical electricity generation data. Both empirical electricity generation data and installed capacities are taken from ENTSO-E. Transparency Platform [108]. Data on future installed capacities are derived from Capros et

<sup>6</sup> A discussion of the assumptions for each scenario and the background methodology of the **TYNDP** report can be found on the following website: <https://tyndp.entsoe.eu/tyndp2018/scenario-report/>

al. [56]. Electricity generation from intermittent renewable capacities is not dispatchable and depends on meteorological conditions. We implement hourly feed-in profiles for onshore wind, offshore wind and PV, which are derived from the ENTSO-E. Transparency Platform [108]. Given the existence of different ‘wind-years’, we assume that hourly feed-in profiles do not vary within our model horizon and only adjust capacity levels over time.

Within the model’s geographical scope, we allow for cross-border trade. Electric power transmission between nodes is restricted by net transfer capacities, which are from ENTSOs [69]. Intranational imitations on electricity flows are neglected in this study. Load-shedding activities, which are driven by a scarcity of power plant capacities, are penalised by the Value of Lack of Adequacy (VoLA), which is determined for each European country individually by Cambridge Economic Policy Associates [109]. In order to avoid an unreasonable ‘trade’ of shedding activities, we implement a maximum shedding factor that is assumed to limit hourly load shedding to 20% of respective hourly demand in a node.

**Gas sector data.** Scenario-dependent data on gas demand projections for European countries are based on scenarios from the ENTSO-G [110]. The annual gas demand levels are broken down to a monthly structure for each node. Monthly demand profiles are calculated based on historical average monthly gas consumption data from Eurostat [107].

We also use the ENTSO-G [110] for data on gas supply potential. We consider Long-Term Contracts (LTC) on an annual level, in line with Neumann, Rüster, and Hirschhausen [111], to realistically represent gas market fundamentals. In particular, we use information on contracting parties, annual contracted gas volume and contract expiration dates.<sup>7</sup> These data are used in the model as an exogenous constraint specifying the minimum bound on a trade variable between respective nodes. This constrains diversification of supplies from importing countries that would not have been captured if the long-term obligations had been omitted.

Data on the existing gas pipeline infrastructure are from the ENTSO-G [112] capacity map. Data for LNG infrastructure are based on Gas Infrastructure Europe [113] and GIIGNL [114]. Data about national storage capacities are based on Gas Infrastructure Europe [113]. All storage data are aggregated on the node level (i.e. each region has one representative storage node). Strategic storage requirements are based on an European Commission [115].<sup>8</sup> Our model incorporates exogenous gas infrastructure capacity expansions. The structure of the

<sup>7</sup> As information about take-or-pay levels is not disclosed, we assume a level of 70%.

<sup>8</sup> Thus, country-specific shares of storage capacities, which are booked for strategic storage, are exogenously fixed and excluded from the model’s decision space.

system's development is harmonised with the information from the ENTSO-G [110]. Only units with final investment decision status are included in the dataset.

We used numerous public information portals and academic studies to parametrise the cost structure of gas production [116], transmission [68, 116–118] and storage [115]. See Riepin and Musgens [119] for details on the cost structure and necessary assumptions for the gas model.

### 3.4 RESULTS

This section is organised in the following way. We begin with a brief overview of the solutions from a deterministic investment problem of an integrated electricity and gas system in Section 3.4.1. We then detail the costs of ignoring uncertainty in a composite mode in Section 3.4.2. Finally, in Section 3.4.3, we focus on the effects of single parametric uncertainty.

**TECHNICAL NOTE:** The computation was performed on a personal laptop with 2.20 GHz Intel(R) i7 – 8750H processor and 16 GB RAM system. The simulation time for different instances of a stochastic problem varied between 5 minutes (with fixed first-stage decisions) and 30 minutes (with unfixed first-stage decisions). The complete project requires computing 4 deterministic problems, 6x4 stochastic problems and 6x4 stochastic problems with fixed first-stage decisions (see Fig. 3.2). The resulting simulation time is at 11 hours.

#### 3.4.1 Deterministic solutions

We begin with a classical scenario analysis by formulating a deterministic cost-minimisation investment problem as defined in equation 3.1 and incorporating different inputs from three ENTSOs scenarios and an EVP.

Note that model's investment decision space is limited to thermal power plants (Open-Cycle Gas Turbines (OCGT), Combined-Cycle Gas Turbines (CCGT), lignite and hard coal power plants) and PSPs. Capacity installations of wind, PV, biomass, hydroelectric reservoirs and run-of-river technologies, based on data from the 2018 TYNDP, are implemented exogenously.

Fig. 3.4 breaks down the investment mix by scenario. Evidently, the different assumptions (input data) across the four scenarios result in different solutions (optimal technology mix) to the deterministic cost-minimisation problems.

The EUKO and DG scenarios are characterised by fairly similar investment mixes. A considerable amount of lignite capacities (ca. 25 GW in



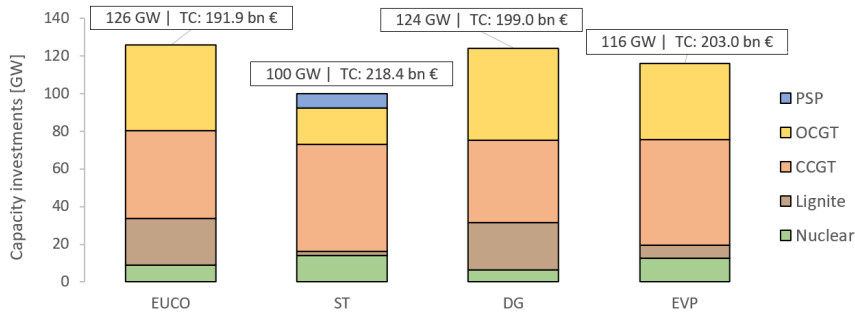


Figure 3.4: Investments in power generation capacities [GW] and total system costs [bn €<sub>2020</sub>] for three deterministic scenarios and an expected value problem

each) in these investment mixes can be explained by the middle-term 2020 – 2030 modelling horizon (i.e. we do not account for further climate policy actions after 2030). In particular, CO<sub>2</sub>-intensive capacities that are built with such foresight may end up stranded later on. In the **ST** scenario, the optimal investment decisions are based on, among other influential factors, an expectation of a high CO<sub>2</sub> price. Thus, we observe the highest degrees of investment in nuclear (14.5 GW) and **CCGT** (56.9 GW) technologies due to the high efficiency of CO<sub>2</sub> emissions per MWh<sub>el</sub>. Interestingly, in the **EVP** scenario, capacities invested in each technology are not close to a mere arithmetical mean among the scenarios. The capacities of **CCGT** and nuclear technologies are similar to those in the **ST** scenario, though just a minor amount of lignite is kept in the optimal investment mix.

Another thing that stands out in Fig. 3.4 is the difference in total system costs across individual deterministic solutions; **EUCO** has the lowest aggregated and discounted investment costs (€ 202.6 bn) followed by **DG** (€ 209.9 bn), **EVP** (€ 214.0 bn) and, the most expensive, **ST** (€ 230.0 bn). These cost differences are, again, driven by scenario-specific assumptions. The high total system costs in the **ST** scenario are driven by the high variable costs of power generation, which, in part, are driven by the scenario’s relatively high CO<sub>2</sub> price.

As already discussed, an alternative to such a scenario analysis is to explicitly encode uncertainty as a part of the model by setting a probability distribution for uncertain parameters, as shown in eq. 3.2 and 3.3. Comparing the two approaches—ignoring uncertainty versus explicitly modelling uncertainty—is crucial for us understand the degree to which modelling uncertainty affects decision quality.

### 3.4.2 Effects of ignoring uncertainty: All parameters

In this section, we continue to solve the stochastic problem defined in eq. 3.2 and 3.3 by using a vector of uncertain data that includes all five correlated uncertain parameters (see section 3.3.3). The optimal

first-stage decision for this problem is illustrated in Fig. 3.5. It includes a mix of technologies that hedges against a composite uncertainty (as the stochastic model, by definition, minimises the expected costs by accounting for all possible scenarios).

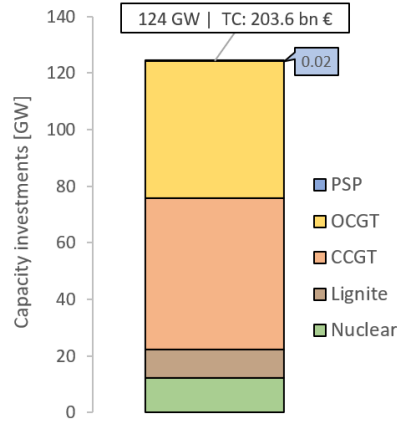


Figure 3.5: Investments in power generation capacities [GW] for the stochastic solution

Fig. 3.6 highlights how the scenario-specific deterministic first-stage investment decisions perform in a stochastic setting. The expected total system costs of stochastic problems with fixed first-stage decisions are defined in eq. 3.9 as  $EEV_n$  (markers with a solid fill). It is thus intuitive that  $EEV_n$  can be below/above the total system costs of corresponding deterministic solutions (markets with a pattern fill), as a stochastic problem by definition accounts for the *expected costs* across all considered scenarios. Interestingly, the optimal investment mix for the stochastic problem is not optimal for any individual scenario despite the fact that the stochastic solution has the lowest expected costs overall.

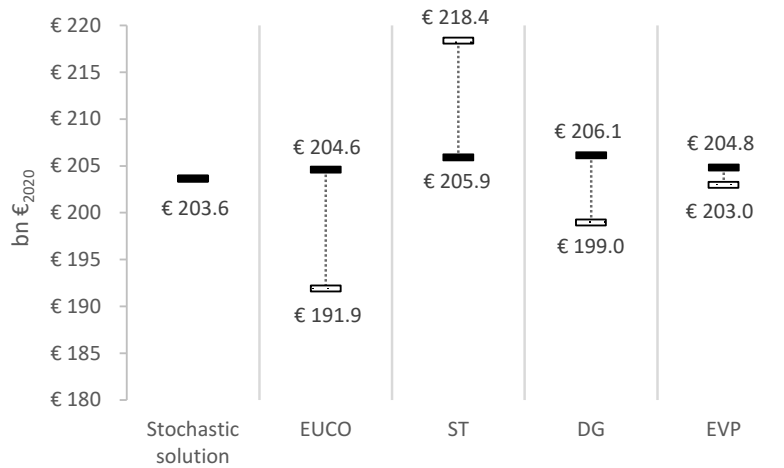


Figure 3.6: Total expected system costs for the SS and four EEV (markers with a solid fill) and total system costs for four DS (markers with a pattern fill)

The difference between the  $EEV_n$  and the SS is denoted as  $ECIU_n$  (as shown in equation 3.10). Table 3.1 depicts the results for the  $ECIU$  calculation. Evidently, the  $ECIU$  varies by scenario. The  $ECIU$  values range from € 1,005.2 M (EU scenario) to € 2,131.3 M (DG scenario).

For comparison, this accounts for 10.1 – 21.3% of all power generation investment costs in the stochastic solution. Note that **ECIU** cannot be negative, as recognising the correct probabilities cannot worsen the expected costs [66].

In contrast to intuition, the **ECIU** in the **EUCO** scenario is lower than that in the **EVP** scenario. This is likely due to load-shedding activities, which are driven by the allocation of scenario-specific maximum residual load levels. A closer inspection of **ENTSOs** data for electricity demand reveals there are several country subsets (i.e. nodes in our model) that face maximum residual load levels in each of the three scenarios. Hence, no investment plan based on a deterministic scenario is dominant with regard to minimising load-shedding activities in the stochastic problem. A detailed analysis of this issue is provided in the [Supplementary Data](#).

Table 3.1: The expected costs of ignoring uncertainty: A composite mode (considering all uncertain parameters)

	EUCO	ST	DG	EVP
<b>ECIU</b> [€ <sub>2020</sub> ]	€ 1,005.2 M	€ 1,620.5 M	€ 2,131.3 M	€ 1,125.4 M
<b>ECIU</b> [% of investment costs]	10.1%	16.2%	21.3%	11.3%

Costs are computed for three representative years: 2020, 2025 and 2030.

### 3.4.3 Effects of disregarding uncertainty: Isolated parameters

This section addresses isolated uncertainties. For this, we set a vector of uncertain outcomes in a stochastic problem to include only one unknown parameter, allowing us to compute the isolated effects of parametric uncertainty (see Section 3.3.3 for details on scenario composition). Table 3.2 presents the results which are backed up with a detailed analysis below.

**Electricity demand and installed RES capacity.** As shown in Table 3.2, **ECIU** for electricity demand is significant across all four scenarios. **ECIU** is the highest, among all parameters, for electricity demand in three of the four scenarios. This is likely because investment decisions are sensitive to peak demand levels. Underestimating this effect leads to under-investment that cause higher load-shedding activities while overestimating it leads to over-investments and, in turn, higher investment costs.

Under the condition of uncertain electricity demand, investment decisions derived using deterministic scenarios, compared to the stochastic problem, lead to higher shedding costs in the **EEV** prob-

Table 3.2: Expected costs of ignoring uncertainty: Isolated parametric uncertainty

Isolated parameter	EUCO	ST	DG	EVP
Electricity demand	€ 577.3 M	€ 695.8 M	€ 1,112.6 M	€ 674.7 M
Installed RES capacity	€ 89.9 M	€ 83.0 M	€ 389.5 M	€ 104.5 M
Gas demand <sup>1</sup>	€ 50.2 M	€ 45.9 M	€ 3.0 M	€ 0.4 M
Fuel price <sup>2</sup>	€ 245.8 M	€ 9.3 M	€ 51.0 M	€ 1.0 M
CO <sub>2</sub> price	€ 864.2 M	€ 661.4 M	€ 11.5 M	€ 41.9 M

Costs in [€<sub>2020</sub>] are computed for three representative years: 2020, 2025, 2030.

<sup>1</sup> Gas demand reflects uncertainty in non-power sector gas demand.

<sup>2</sup> Fuel price reflects uncertainty in lignite, hard coal and oil prices.

lems (see Table 5 in the [Supplementary Data](#)). This is due to the fact that scenario-specific demand developments differ between European countries. Thus, all deterministic capacity expansion plans show under-investment in some nodes and, therefore, increased shedding activities. The DG scenario, for example, has the highest electricity demand, which results in an investment level higher than that of the stochastic solution. This, in turn, leads to lower load-shedding activities relative to other scenarios. However, certain nodes' demand levels reach their maximum in other scenarios (e.g. in the UK node, maximum demand is observed in the EUCO scenario; thus, constraining the stochastic problem with the investment mix from the DG scenario results in increased shedding activities in the UK node).

As with electricity demand, electricity generation from RES capacities eventually affects the residual load. Hence, the mechanism how uncertainty in RES installed capacities affects the investment decisions is similar to that in electricity demand (i.e. a system planner optimises a capacity mix that varies by scenario- and country-specific residual load levels). However, when analysing uncertain development in RES capacity, the ECIUs are lower than those for electricity demand. This is likely due to the influence of parametric uncertainty on the residual load.

Fig. 3.7 shows boxplots for hourly residual load levels for each scenario in 2030 after varying after varying electricity demand and RES capacity levels. The necessary assumption to depict residual load levels for electricity demand variation is to fix the RES feed-in to one of four scenarios (and vice versa for RES feed-in variation). We use the EUCO scenario for both illustrative examples in Fig. 3.7 but the impact on the residual load is within the same magnitude for the other scenarios. Residual load boxplots for all scenarios are in the [Supplementary Data](#).

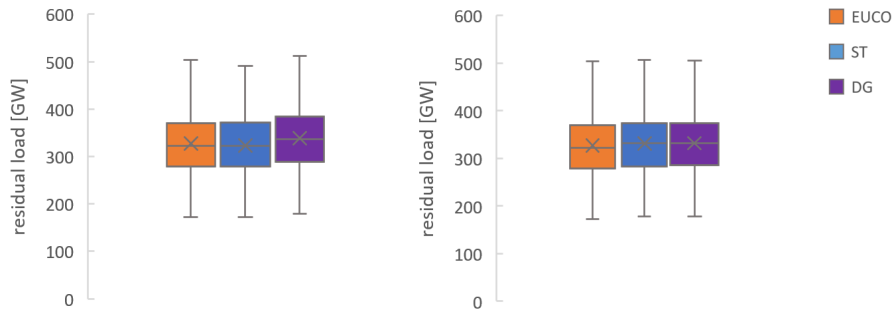


Figure 3.7: Comparing residual load after varying demand (left) and RES capacity (right) following [ENTSOs](#) scenarios for 2030

It is clear that the difference in maximum residual level between scenario branches is significantly higher when implementing demand variation. The maximum residual load level ranges within the three branches from 491.2 GW to 512.0 GW when electricity demand is varied but only from 503.6 GW to 506.2 GW when RES capacity is varied.

**Gas demand, fuel price and CO<sub>2</sub> price.** As shown in Table 3.2, [ECIU](#) for gas demand is at a negligible level across all four scenarios. [ECIU](#) for fuel price is negligible in all but one scenario ([EUCO](#)). The effect of CO<sub>2</sub> price uncertainty strongly varies by scenario from high to negligible. We back up these observations with a detailed analysis of the impact that parametric uncertainties have on the integrated system.

Our analysis is supported by Fig. 3.8, which comprises convex hull plots depicting variable costs for four technologies: lignite, hard coal, [CCGT](#) and [OCGT](#). Nuclear and biomass are excluded because their costs do not differ across [ENTSOs](#) scenarios. The abscissa represents years. The ordinate represents variable costs in €/MWh. Each column represents an uncertainty driver—gas demand, fuel price and CO<sub>2</sub> price—while each row represents a scenario path for the other four known parameters. Each hull is built around nine dots—three dots per year. The three dots represent variable costs for each technology evaluated at gas, fuel, and CO<sub>2</sub> prices observed in each of the three branches in a relevant stochastic model. Thus, convex hull width conveys ranges of variable costs per technology caused by parametric uncertainty. These plots are useful because they visualise how parametric uncertainty affects variable costs of power generation and provide an intuition for the resulting [ECIU](#) measures.<sup>9</sup>

In the first column of Fig. 3.8, convex hull width depicts the sensitivity of variable costs to gas demand uncertainty. The impact of gas demand uncertainty on the variable costs of [CCGT](#) and [OCGT](#) is small. Predictably, the impact on lignite and hard coal is null. We conclude

<sup>9</sup> More detail on constructing convex hull plots can be found on the following link: <https://github.com/Irieo/IntEG/tree/master/HullPlots>

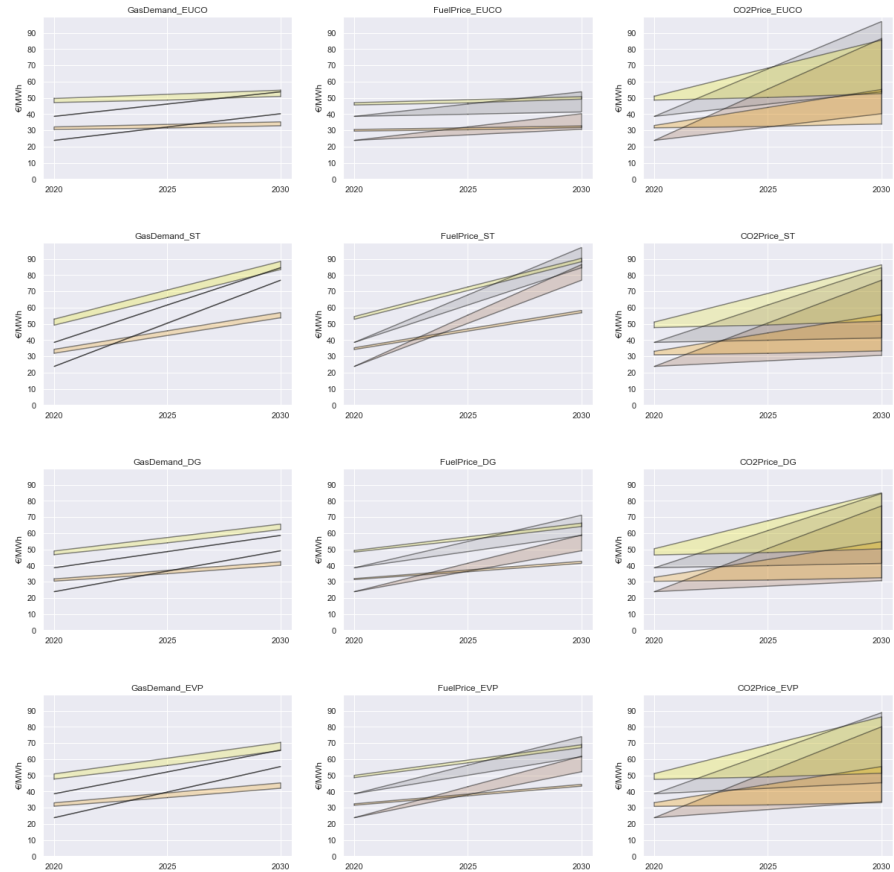


Figure 3.8: Variation of variable costs for four technologies due to uncertainty regarding gas demand (first column), fuel price (second column) and CO<sub>2</sub> price (third column)

Colour codes: lignite [brown]; hard coal [grey]; CCGT [orange]; OCGT [yellow].

that the differences in gas prices driven by the uncertainty of gas demand do not significantly change installed capacities of electricity generation technologies. This result is driven by the substantial European gas infrastructure, which is sufficiently capable of meeting the range of future gas demand scenarios defined in TYNDP. The negligible ECIU measures for gas demand uncertainty reflect this observation.<sup>10</sup>

The second column of Fig. 3.8 depicts the sensitivity of variable costs to the uncertainty of lignite and hard coal prices. It is notable that the intersection of lignite and CCGT significantly varies by underlying fuel price assumption. For example, with uncertain fuel prices and

<sup>10</sup> Riepin, Möbius, and Müsgens [98] illustrate the reallocation of gas-fired technologies as the effect of gas demand uncertainty on electricity sector investments. However, they also point out that the value of a stochastic solution (the ECIU) is small. Similar results are revealed by Fodstad et al. [68], who study the effect of gas demand uncertainty on investments in gas sector infrastructure. They find structurally distinct infrastructure solutions in stochastic and deterministic models but report a negligible value of a stochastic solution.

the high CO<sub>2</sub> price in the *ST* scenario, generation with *CCGT* becomes cheaper than that with a lignite plant in all branches of the stochastic model by 2025. Isolating fuel price uncertainty reveals that the cost structures of the *ST*, *DG* and *EVP* scenarios ensure that there are null or minor investments in lignite power plants. Thus, uncertainty in lignite prices has a negligible effect. In the *EUCO* scenario, with a low CO<sub>2</sub> price, lignite remains cheaper than *CCGT* all over the modelling horizon in some branches of a stochastic problem. Consequently, the optimal solution contains a moderate amount of lignite capacity in the investment mix. In this case, lignite price uncertainty has a notable effect, which is reflected by the *ECIU* measure.

The third column of Fig. 3.8 depicts the sensitivity of variable costs to the uncertainty of CO<sub>2</sub> prices. The hull widths (ranges of variable costs) are higher than in the other two parametric uncertainties. In order to explain values for CO<sub>2</sub> price uncertainty in Table 3.2, it is important to note that hull width illustrates the potential for high costs of ignoring uncertainty. This is driven by the stochastic problem hedging against the large differences in variable costs established by the extreme CO<sub>2</sub> price values (the ‘higher’ and ‘lower’ hull edges). The deterministic solution, by definition, disregards this variation and seeks to optimise investments for a particular CO<sub>2</sub> price realisation. The width of hulls (i.e. variety of cost structures) highlights this mismatch. This is illustrated by the results in the *EUCO* and *ST* scenarios (characterised by the high and low CO<sub>2</sub> prices, respectively), resulting in considerable *ECIU* measures. The optimal capacity mix for deterministic solutions in these two scenarios significantly differs from the optimal mix for the stochastic problem, which accounts for a full range of scenarios. Therefore, evaluating the performance of these deterministic solutions in a stochastic setting results in considerably higher expected system costs.

### 3.5 CONCLUSIONS

This paper investigates the trade-off between complexity from integrated optimisation of gas and electricity systems and parametric uncertainty. To do this, we use a combination of deterministic and stochastic optimisation approaches. The methodological contributions of combining integrated and stochastic optimisation problems and comparing the isolated effects of parametric uncertainty shall be of interest for energy modellers. We parametrise our model and derived scenarios from data in the 2018 *TYNDP* report published by *ENTSO*s. We believe that our findings are of interest to industry experts and stakeholders with an empirical interest in the European energy system. In order to enhance the transparency and reproducibility of our results, we have published the data and source codes for the entire research

project online. Beyond these broad methodological and empirical contributions, we recognise five key take-aways.

First, the expected costs of ignoring uncertainty can constitute a significant share (up to 20%) of cumulated costs from investments in power generation capacity. Although our results are obtained under restrictive assumptions and do not reflect all real-world planning complexities, this number is impressive given that it is obtained just by adjusting the planning approach.

Second, concerning the underestimation of required capacity and the resulting load-shedding activities, our results suggest that no capacity expansion plan based on a deterministic scenario is dominant in terms of minimising load-shedding activities. Energy modellers should recognise that, in a framework of European [TYNDP](#) data, choosing the scenario with the highest aggregated demand does not result in the absence of load shedding on account of country-specific load peak variation.

Third, our analysis of isolated parametric uncertainties revealed that the effect of ignoring electricity demand uncertainty is significant across all four scenarios in our modelling scope. For installed [RES](#) capacities, the effect is notably low. The magnitude of the effect for these parametric uncertainties is mainly driven by residual load peak variation. This observation should be seen in light of the ten-year modelling horizon we included; however, it strongly suggests incorporating electricity demand uncertainty into research items that focus on the expansion plans of power generation in the context of increasing capacities of renewable energy sources.

Fourth, the expected costs of disregarding gas demand uncertainty are low across all considered scenarios. The take-away for energy modellers is two-fold. One, our findings suggest that there is a small value for incorporating stochastic optimisation under gas demand uncertainty into large-scale integrated electricity and gas system models. Two, when focusing on the impacts of long-term uncertainty in single-sector models for electricity and gas, the effect of capturing interactions between the two sectors seems limited; this could justify the choice of future modellers to focus resources on a single sector when analysing uncertainty. It is worth noting that this finding should be seen in the light of our modelling scope and [TYNDP](#) scenario data for gas demand uncertainty.

Fifth, the effect of CO<sub>2</sub> price uncertainty strongly varies by the scenario path of other parameters. In the context of the 2018 [TYNDP](#) scenarios, the effect is negligible when the [DG](#) scenario realises. In contrast, ignoring CO<sub>2</sub> price uncertainty leads to expensive decisions if the [EUCO](#) or [ST](#) scenarios play out, as investments made in anticipation of these scenarios poorly match with system needs after uncertainty is revealed. Our concluding suggestion for the energy modelling community focused on long-term system planning problems is to



consider including CO<sub>2</sub> price uncertainty into model formulations—at least during test runs. Investigating the interactions between assumed future CO<sub>2</sub> price ranges (or, alternatively, emission caps) and scenario assumptions for the other parameters can bring significant benefits over naïve modelling practices.

**DATA & CODE AVAILABILITY:** Datasets related to this article and a source code for the entire project are available in the public GitHub repository: <https://github.com/Irieo/IntEG>. The code reproduces the benchmarks from the paper.

**SUPPLEMENTARY DATA** Supplementary data to this article can be found online at <https://doi.org/10.1016/j.apenergy.2020.116363>.

**CREDIT AUTHORSHIP CONTRIBUTION STATEMENT** **Igor Riepin:** Conceptualization, Methodology, Data curation, Software, Validation, Investigation, Visualization, Writing - original draft. **Thomas Mobius:** Conceptualization, Data curation, Software, Investigation, Visualization, Writing - original draft. **Felix Müsgens:** Conceptualization, Writing - review & editing, Supervision.

# 4

## SEASONAL FLEXIBILITY IN THE EUROPEAN NATURAL GAS MARKET

---

*This chapter presents  
the journal article as  
originally published  
in The Energy  
Journal.*  
IAEE (C) 2022

**ABSTRACT:** This paper focuses on seasonal demand swings in the European natural gas market. We quantify and compare the role of different flexibility options (domestic production, gas storage, and pipeline and LNG imports) to assess European demand fluctuations in monthly resolution. We contribute to the existing literature on seasonal flexibility by addressing the problem with a mathematical gas market optimization model. Our paper provides valuable empirical insights into the decline of gas production in northwestern Europe. Furthermore, we focus on how specific flexibility features differ between pipeline supplies and LNG supplies and between gas imports and storage dispatch. In terms of methodology, we construct a bottom-up market optimization model and publish the complete source code (which is uncommon for gas market models). Furthermore, we propose a new metric—the scaled coefficient of variation—to quantify the importance of supply sources for seasonal flexibility provision.

**KEYWORDS:** European gas market, Market modeling, Seasonality

**PUBLISHED AS:** I. Riepin, F. Müsgens (2022), Seasonal flexibility in the European natural gas market, *The Energy Journal*, Vol. 43, Issue 1. DOI: <https://doi.org/10.5547/01956574.43.1.irie>

### 4.1 INTRODUCTION

Seasonal demand swings (i.e. differences in gas consumption across seasons) constitute a fundamental element of the European gas market. Heating demand, which is primarily driven by temperature, is high in the winter but low in the summer, causing strong seasonal demand swings—the aggregated European gas demand is typically more than twice as high in the winter than it is in the summer.<sup>1</sup> European countries balance the demand variation with a mix of flexibility options, such as varying domestic gas production, varying pipeline or LNG imports, and operating of underground gas storage facilities.

These options differ in terms of both cost and availability. Varying domestic gas production requires free domestic production capacity. Varying imports requires free foreign production capacity and free ca-

---

<sup>1</sup> Between 2010 and 2017, natural gas consumption in the EU-28 was, on average, 2.2 times higher during the three winter months than it was during the three summer months [107].

capacity in transportation infrastructure. LNG imports are only available to certain European countries, as they require regasification terminals; however, increasingly integrated European gas markets allow cross-border gas transfers. Gas storages provide seasonal flexibility by shifting gas demand from the winter to summer; utilization of gas storages is also subject to available capacities and technical characteristics of storage facilities.

The years leading up to 2018 saw a relative abundance of flexible capacity in the gas market. This was largely due to (i) low gas demand in almost all European countries over the past decade, (ii) investment in additional assets,<sup>2</sup> and (iii) the integration of European gas markets driven by the optimized utilization of existing assets. This abundance of flexible capacity was reflected by low seasonal gas price spreads at European gas hubs and the low utilization of European regasification terminals.

However, this abundance of seasonal flexibility is not permanent. In the future, several factors will put significant downward pressure on the availability of flexibility options. First, market forces reflect an oversupply of such options amid lower price spreads between summer and winter months. Lower spreads make investments in additional flexibility less attractive and may even cause a shutdown of existing flexibility options. Second, both the Netherlands and the United Kingdom—the European Union’s two largest gas producers—will provide less flexibility in the future. In response to seismic activity, the Dutch government announced a series of directives to limit maximum annual production from the Groningen field;<sup>3</sup> the annual-production cap of 42.4 bcm p.a., which had been in place since January 2014, was reduced to 21.6 bcm p.a. for the 2017 – 2018 gas year with the ultimate goal being to completely shut down the Groningen field by 2030 [121, 122]. Furthermore, in 2016, the Dutch government established regulations to spread out natural gas production as evenly as possible throughout the year. In terms of monthly fluctuations, this regulation fixes gas extraction from the Groningen field each month to a range of plus or minus 20% [121]. Taken together (Fig. 4.1), these two changes reduce the Groningen field’s seasonal flexibility by around 85% (from a swing of 4 – 5 bcm between the winter and the summer in 2011 – 2013 to one of just 0.6 bcm in 2017 – 2018).<sup>4</sup> The UK government also indicates that there will be a rapid decline in domestic gas production.<sup>5</sup> The projected 2030 production volume is 17.8 bcm p.a., which constitutes a drop of more than 50% from the 2015 production

<sup>2</sup> ENTSO-G [110] reports that 42 infrastructure projects were completed between 2015 and 2018.

<sup>3</sup> REKK [120] estimates that total European production flexibility was 213 mcm/day in 2012, of which 163 mcm/day was from the Groningen field.

<sup>4</sup>  $21.6 \text{ bcm p.a.} / 12 = 1.8 \text{ bcm per month}$ ;  $0.6 \text{ bcm} = 1.8 \text{ bcm} * (1 + 20\%) - 1.8 \text{ bcm} * (1 - 20\%)$ .

<sup>5</sup> See: <https://www.gov.uk/guidance/oil-and-gas-uk-field-data>

volume. Consequently, gas import dependency is expected to increase significantly—from 44% in 2015 to 74% in 2030 [123]. Europe must respond to this drop in domestic production and the associated decline in flexibility with alternative options and find a new cost-optimal way to cover seasonal demand swings.

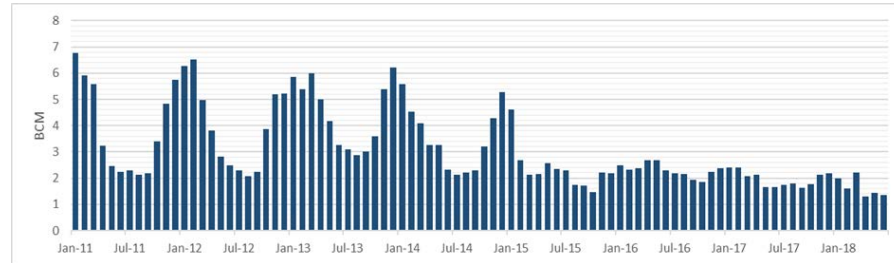


Figure 4.1: Monthly natural gas production at the Groningen field, January 2011 - June 2018

Data is based on NAM <https://www.nam.nl/gas-en-oliewinning/groningen-gasveld.html>

On the other hand, new infrastructure projects are expected to enter the market. The ENTSO-G [110] identifies plans for around 120 transmission and compressor stations, 27 LNG terminals, and 9 underground storage facilities. Forty-six of these projects have been approved for investment; almost 75% of the submitted initiatives are expected to be commissioned no later than 2022.

Overall, the future need for seasonal flexibility remains unclear. Assessments must consider both regulatory and economic changes in the gas market structure. The application of an economic modeling framework can reveal market fundamentals and the evolving structure of flexibility options.

This paper analyzes seasonal gas demand swings and the flexibility necessary to cover them using a fundamental modeling framework. We analyze how various flexibility options (domestic production, gas storage, and pipeline and LNG imports) cover European demand fluctuations in monthly resolution. We contribute to the existing discussion on seasonal flexibility by addressing the problem with a mathematical gas market optimization model. Our paper provides valuable empirical insights into the decline of gas production in northwestern Europe, much of which stems from the Groningen event and recent developments in the UK. Such structural breaks are optimally addressed by fundamental models. Furthermore, we differentiate between LNG and pipeline imports to analyze the specific flexibility features of pipeline and LNG supplies. In terms of methodology, we construct a gas market model and publish the complete source code.<sup>6</sup>

<sup>6</sup> While there is almost a decade of open modeling initiatives in European energy research (e.g. <https://wiki.openmod-initiative.org> listing numerous open models for the electricity, heat, and mobility sectors), publishing input data and

Furthermore, we propose a new metric to improve the quantification of supply sources' provision of seasonal flexibility. This metric extends the well-established coefficient of variation.

The remainder of this paper is organized as follows. Section 4.2 details the methodology employed for this study. We present our modeling framework as well as a mathematical description of our market optimization model and its associated data. Section 4.3 presents and interprets the modeling results. We begin by illustrating modeling results in the form of monthly gas demand profiles to lay a background for the analysis. We continue with an investigation into supply sources' quantitative contributions to cover gas demand and determine which supply source offers the most flexibility in covering seasonal demand fluctuations. Finally, Section 4.4 concludes with major findings and outlines our ideas for future work.

## 4.2 METHODOLOGY AND DATA

We construct and apply an optimization model covering the European gas market and its neighboring regions. The model is formulated as a deterministic linear programming problem with perfect foresight. This allows us to solve the large-scale optimization model with intertemporal constraints and high temporal granularity over a large timespan. As such, decision variables (e.g. gas production, trade, and storage) have a time resolution of 12 consecutive months for each modeled year. We simulate market operations over a long time period (from 2018 to 2030). This enables us to explore future market developments driven by changing supply and demand fundamentals. The model's spatial coverage encompasses European countries and major non-European gas exporters (Norway, Russia, United States, Algeria, Libya, Nigeria, and Qatar). The dataset, which includes all necessary economic and technical data, is taken from publicly available sources. We discuss our assumptions regarding gas demand and supply structures as well as transmission infrastructure elements below. The model is formulated in GAMS v25.17 and solved with a CPLEX solver with default solver settings.<sup>8</sup> The applied GAMS code, associated input data, and processing of the results are available in a public GitHub repository: <https://github.com/Irieo/SeasonalFlex>

---

source code is still uncommon among studies on the gas sector. A recent update to this is made by Egging and Holz [124] who published code and data documentation for the Global Gas Model.

<sup>7</sup> more details at: <https://www.gams.com/>

<sup>8</sup> An instance of this problem for 27 nodes and 204 time periods (17 years x 12 months) has 2,868,379 single variables and 552,599 equations.

#### 4.2.1 *Related work*

The mathematical modeling of gas markets has a long history. Mathiesen, Roland, and Thonstad [125] were among the first to model the European gas market. Interest in model-based analysis of the European gas market increased significantly at the end of the 1990s when the European Commission initiated liberalization policies. The growth of computing power and the advancement of mathematical models—paired with the challenges of energy transitions—facilitated the widespread employment of elaborated mathematical models in this field. Since then, a considerable amount of research has been oriented to the economic modeling of the European gas market.

Most of the studies in this research stream have adopted one of two methodological approaches. Studies using the first approach analyze the operation of the gas market using mixed complementarity-based equilibrium models, which allow for the incorporation of individual players' strategic decisions [65, 116, 126–130]. Those that use the second approach employ bottom-up optimization models in which the whole system is optimized with regard to the costs of the gas supply and relevant constraints. While these models must rely on the assumption of perfectly competitive market operation, they benefit from the use of optimization solvers that allow for the incorporation of a high level of spatial and temporal resolution as well as more detailed representation of complex gas infrastructure (e.g. [64, 111, 131–134]).

Most recent studies that use a bottom-up optimization model to analyze flexibility in the European gas market focus on short-term flexibility, often dealing with supply security (e.g. the ability of the gas system to sustain operation under shock scenarios). REKK [120] analyzes the flexibility of the European gas market with a focus on how interconnectivity, gas storage, and demand-side adjustments impact the resilience of the gas system during supply shocks. Tóth et al. [135] examine the infrastructure priorities of the EU's LNG and underground gas-storage strategies in various short-term supply/demand shock scenarios. While these studies include seasonal representation of the European gas market operation in their models, they do not focus on seasonal flexibility.

The literature on seasonal flexibility has adopted other methodological approaches. For example, Höffler and Kübler [136] conduct a simple top-down analysis of supply flexibility, in which they project future additional demand for gas storage in northwestern Europe. Correlje [137] provides another outlook on seasonal flexibility in northwestern Europe and addresses the issue of supply capacity adequacy to meet gas demand during a potential severe winter. They propose and compare several statistical methods to evaluate the required amount of seasonal flexibility needed for 2011 – 2020. A comprehensive empirical investigation of the role of gas storage in the European gas market

is provided in a report issued by the European Commission [115]. The report, which looks at 2013 and 2014, discusses the competition between gas storage and alternative sources of flexibility and suggests the use of a variation coefficient to measure supply sources' contributions to demand swing. Our work adds a detailed analysis of seasonal flexibility through 2030 with a fundamental model of the European gas market; furthermore, it suggests improving the methodology by measuring the provision of seasonal flexibility (see Section 4.3.2).

To sum up, previous studies either discussed seasonal flexibility using top-down or statistical approaches or they maintained a narrow focus, dealing mainly with short-term flexibility. The literature still lacks a systematic understanding of how to measure the importance of a particular supply source's contribution to seasonal demand swings. Hence, this study contributes to the literature by conducting a long-term analysis of seasonal flexibility with a large-scale gas market model. Furthermore, we contribute to the methodological question of how to measure the contributions of different flexibility options by proposing a new metric.

#### 4.2.2 Model structure

The model structure consists of a network of nodes, each of which represents a country or a region. This paper incorporates 27 nodes representing the countries and regions that are most relevant in the European gas market (Fig. 4.2). Nodes are connected by gas transmission infrastructure, including (i) cross-border interconnection pipelines within the EU, (ii) cross-border pipelines with non-EU parties (such as Nord Stream), and (iii) liquefaction and regasification terminals. All forms of gas transmission infrastructure are represented via one-directional arcs.<sup>9</sup> Bidirectional flows are displayed using two parallel one-directional arcs. The model neglects friction and pressure drops in the gas network.<sup>10</sup>

The model includes the following activities that can occur within each node: production, consumption, storage (injection and withdrawal), and both exporting and importing via pipelines or LNG routes. The only exception to this rule is that, in the case of non-EU gas exporters, we model only the supply side using residual supply curves (i.e. gas supply potential available to European markets).<sup>11</sup>

<sup>9</sup> We use entry and exit point capacities at the transmission level. Data about gas distribution networks is scarce and has not been included.

<sup>10</sup> The nonlinear dynamics of gas flow in transportation networks are usually ignored in the literature on natural gas markets. Of course, there are some exceptions, including Midthun [138], Herrán-González et al. [139], and Qiu et al. [140]. Although interesting and insightful, the models presented in these studies do not scale up to a large-scale representation of the European natural gas market.

<sup>11</sup> A modeling exercise incorporating the operation and development of domestic markets in these nodes would require a global gas model.

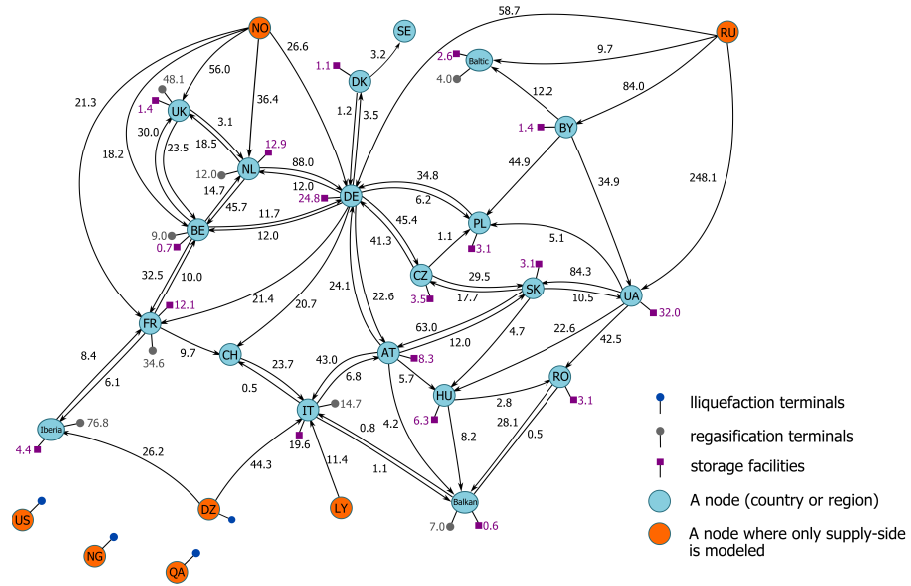


Figure 4.2: Nodes included in the model and capacities of gas infrastructure elements as of 2017 (in bcm p.a.)

We provide a full list of the countries and regions included in our model in Appendix B.

It is important to note that gas production for export is optimized endogenously for both the non-EU gas exporters and the European domestic gas producers. The demand side consists of exogenous gas consumption levels. To account for seasonality, annual consumption is transformed into monthly consumption based on historical average demand profiles for each country (or region). Demand-side response is not considered in our analysis, as data on country-specific potentials are generally not available. Furthermore, the European Commission [115] argues that the role of demand-side response as a flexibility tool in the European gas market is limited. We incorporate long-term contracted volumes (minimum take-or-pay levels) as lower bounds for gas deliveries between respective nodes to ensure a realistic representation of gas supply flexibility options. Additionally, we apply a special constraint for Dutch production to incorporate the impact of regulation on the Groningen field's flexibility.

The model algorithm receives exogenous input data and searches for the decision vectors matching gas demand and supply with respect to minimizing the total cost function. The optimal solution is that in which all arbitrage opportunities across time and space are exhausted to the extent that infrastructure (i.e. production, transportation, and storage) permit. The results of the model include spatial and temporal decisions on production, transportation, and storage. The incorporation of gas storage into the model requires and guarantees intertemporal optimization.



It is important to note that the model is designed to provide a quantitative assessment of possible future developments by capturing the economic aspects of decision-making in a competitive gas market.<sup>12</sup> The model can simulate market operation based on the supply and demand equilibrium; additionally, it accounts for dynamic factors. The results largely depend on the quality of the input data. Our assumptions on these are based on publicly available sources from 2018 to early 2019, when the paper was written. Of course, data quality varies; some parameters (e.g. uncertain future developments and unavailable data) are estimates. However, to ensure transparency, we are providing input data in the [public GitHub repository](#). Furthermore, our methodology can be used with more accurate data once it is available.

### 4.2.3 Declarations

The following notations are valid for the gas market model formulation used in this paper. We use subscripts for indexation. For readers' convenience, we use upper-case letters for exogenous variables (parameters) and lower-case letters for endogenous variables.<sup>13</sup> For example, the parameter  $PRODCAP_{p,n,t}$  sets an upper constraint for the gas production from each facility  $p$  located in a node  $n$  for a time period  $t$ .

#### Nomenclature (1/2)

Element	Description
<b>Sets</b>	
$n, m \in N$	nodes in the network
$c \in N$	nodes where consumption activity occurs
$p \in P$	gas production facilities <sup>a</sup>
$t \in T$	time periods (months) <sup>b</sup>

<sup>a</sup>Elements of set  $P$  come from linear piecewise approximation of the logarithmic production cost function per node.

<sup>b</sup>The temporal structure in the model consists of sets of consecutive months and years. The tracking of the year index is not shown for clarity.

<sup>12</sup> Our model relies on the assumption of perfect competition. See, for example, Chyong and Hobbs [116], Hecking and Panke [127], and Holz [128], who discuss strategic aspects of the European gas market.

<sup>13</sup> Throughout the remainder of this paper, we follow established conventions and refer to exogenous variables (i.e. model inputs) as "parameters" and endogenous variables (which are determined during optimization) as "variables."

## Nomenclature (2/2)

Element	Description
<b>(Positive) Variables</b>	
$prodvol_{p,n,m,t}$	gas production from $p$ 's facility in node $n$ and export to node $m$
$expph_{p,n,m,t}$	gas flow volume over arc $n \Rightarrow m$
$arcflow_{n,m,t}$	total gas flow volume over arc $n \Rightarrow m$
$level_{n,t}$	stock level of working gas storage in node $n$
$inj_{n,t}$	gas injection volume into storages in node $n$
$with_{n,t}$	gas withdrawal volume from storages in node $n$
<b>Parameters</b>	
$PRODCOST_{p,n}$	marginal production costs of $p$ 's facility in node $n$
$PRODCAP_{p,n,t}$	production capacity of $p$ 's facility in node $n$
$ARCCAP_{n,m,t}$	transmission capacity <sup>c</sup> for arc $n \Rightarrow m$
$TRANSCOST_{n,m,t}$	marginal transmission costs for arc $n \Rightarrow m$
$CONSUM_{n,t}$	gas consumption in node $n$
$WGV_{n,t}$	working capacity of gas storage in node $n$
$INJCAP_{n,t}$	storage injection capacity in node $n$
$WITHCAP_{n,t}$	storage withdrawal capacity in node $n$
$INJCOST$	storage injection costs
$WITHCOST$	storage withdrawal costs
$LOSS$	gas losses per storage cycle
$LTC_{n,m,t}$	take-or-pay levels of gas deliveries under <b>LTC</b> from node $n$ to node $m$

<sup>c</sup>It includes **LNG** routes and exogenous infrastructure capacity expansions.

#### 4.2.4 Model formulation

Objective function 4.1 represents the total system costs that include aggregated gas production costs, gas transmission costs over pipeline and **LNG** routes<sup>14</sup>, and gas storage costs.

<sup>14</sup> The costs of liquefaction are modeled as costs of using the "virtual arc" between gas production and liquefaction activities. Similarly, the costs of regasification are modeled as costs of using the "virtual arc" between gas regasification and consumption activities.

$$\min TC = \sum_t \left( \begin{array}{l} \sum_{p,n,c} (prodvol_{p,n,c,t} \cdot PRODCOST_{p,n}) \\ + \sum_{n,m \neq n} (arcflow_{n,m,t} \cdot TRANSCOST_{n,m,t}) \\ + \sum_c (inj_{c,t} \cdot INJCOST + with_{c,t} \cdot WITHCOST) \end{array} \right) \quad (4.1)$$

The objective function is subject to the following set of technical and balance constraints. Equation 4.2 limits the quantity of gas produced and exported by each production facility to its production capacity.

$$PRODCAP_{p,n,t} - \sum_c prodvol_{p,n,c,t} \geq 0 \quad \forall p, n, t \quad (4.2)$$

Equation 4.3 ensures that arc capacity constrains the total gas flow over each arc.

$$ARCCAP_{n,m,t} - arcflow_{n,m,t} \geq 0 \quad \forall n, m, t \quad (4.3a)$$

$$where : arcflow_{n,m,t} = \sum_p expph_{p,n,m,t} \quad (4.3b)$$

Equation 4.4 ensures that the entire quantity of gas imported and withdrawn from storage by each node equals the entire quantity consumed and injected into storage.

$$\sum_{p,n} prodvol_{p,n,c,t} = CONSUM_{c,t} + with_{c,t} - inj_{c,t} \quad \forall c, t \quad (4.4)$$

Equation 4.5 ensures flow conservation throughout the network; for each node, gas trade variables (imports/exports) must equal physical flow variables (inflows/outflows).<sup>15</sup>

$$\left[ \sum_{m \neq n} prodvol_{p,n,m,t} - \sum_{m \neq n} expph_{p,n,m,t} \right] + \left[ \sum_{m \neq n} expph_{p,m,n,t} - \sum_{m \neq n} prodvol_{p,m,n,t} \right] = 0 \quad \forall p, n, t \quad (4.5)$$

Equation 4.6 establishes minimum production and export levels under long-term contracts between nodes.

<sup>15</sup> Note that  $n$  and  $m$  are aliases for nodes in the system.  $n, m$  denotes a flow from  $n$  to  $m$ ; while  $m, n$  denotes a flow from  $m$  to  $n$ .

$$\sum_p \text{prodvol}_{p,n,m,t} - LTC_{n,m,t} \geq 0 \quad \forall n, m, t \quad (4.6)$$

Equation 4.7 defines the storage level at time period  $t$ .<sup>16</sup>

$$\text{level}_{c,t} = \text{level}_{c,t-1} + (1 - \text{LOSS}) \cdot \text{inj}_{c,t} + \text{with}_{c,t} \quad \forall c, t \quad (4.7)$$

Equations 4.8a, 4.8b and 4.8c represent storage capacity, injection capacity, and withdrawal capacity constraints, respectively.

$$\text{WGV}_{c,t} - \text{level}_{c,t} \geq 0 \quad \forall c, t \quad (4.8a)$$

$$\text{INJCAP}_{c,t} - \text{inj}_{c,t} \geq 0 \quad \forall c, t \quad (4.8b)$$

$$\text{WITHCAP}_{c,t} - \text{with}_{c,t} \geq 0 \quad \forall c, t \quad (4.8c)$$

Finally, equation 4.9 sets a production flexibility constraint for the Netherlands.

$$0 \leq \frac{\sum_{p,m} \text{prodvol}_{p,n,m,t}}{\sum_{p,m} \text{prodvol}_{p,n,m,t-1}} \leq 0 \quad \forall t \geq \text{Jan16}, n = \text{NL} \quad (4.9)$$

#### 4.2.5 Data

Data for the existing cross-border interconnection pipelines is based on the ENTSO-G [141]. Data for LNG liquefaction and regasification terminals was acquired from Gas Infrastructure Europe [113] and GIIGNL [114]. The model also incorporates exogenous capacity expansions of gas infrastructure (including transmission, storage, and regasification). The structure of the system's development is harmonized with the ENTISOs [69] TYNDP report. Only units with final investment decision status are included in the dataset.<sup>17</sup> This study does not include endogenous capacity expansions.

We also use the ENTISOs [69] TYNDP for data on gas supply potential.<sup>18</sup> Gas demand projections for European countries are based on the EUCO demand scenario from the same source. EUCO is a core

<sup>16</sup> At the start of the first month, storage levels are fixed at 60%; at the end of the last month, storage levels must reach 60%. This prevents the "finite time horizon" problem, which would mean that the model's algorithm tends to withdraw all gas from storage facilities by the end of the last year (to maximize profit by using the value of gas stored).

<sup>17</sup> New infrastructure is typically added to the model dataset each January. Thus, all units that are planned to be commissioned in 2020 will be "launched" by the model in January 2020.

<sup>18</sup> Supply potential is defined as "the capability of a supply source to supply the European gas system in terms of volume availability."

policy scenario originally produced by the European Commission. It projects a nearly constant annual EU gas demand over the next decade (451 bcm in 2020 and 453 bcm in 2030). Country-specific projections, however, vary considerably (e.g. over the same decade, annual gas demand increases by 50% in Poland and 36% in Belgium but decreases by 12% in the UK). Annual gas demand is transformed into monthly levels for each node. Monthly demand profiles are calculated based on historical average monthly gas consumption data from Eurostat [107]. We provide the results for two additional scenarios for gas demand developments in the [Online Appendix](#).

We analyzed public information portals, open-source literature, and relevant academic papers to parametrize the cost structure of gas production, transmission, and storage. Production costs are calculated as linear piecewise approximations to logarithmic cost functions, which are calibrated based on Chyong and Hobbs [116].<sup>19</sup> Transmission costs are calculated as linear functions of pipeline length. Following the literature on natural gas modeling [68, 116] and publicly available estimates [117], transmission costs are assumed to be 1.2 €/MWh per 1000 km. For all underwater transmission routes, transmission costs are 2.0 €/MWh per 1000 km. Liquefaction and regasification costs are assumed to be 3.7 €/MWh and 0.7 €/MWh, respectively [68, 142]. LNG shipping costs are calculated as a function of the distance between nodes,<sup>20</sup> average vessel speed (18 knots), average vessel capacity (150.000 m<sup>3</sup>), and charter rates (69.000 €/day) based on GIIGNL [114] and Rogers [143]. Information about average vessel speed and capacity paired with information on charter costs allows us to compute cost per voyage (0.1 €/MWh per 1000 km). This data, combined with distance between nodes, gives shipping costs in €/MWh per route. For example, the shipping cost between the Qatar and UK nodes (approximate distance of 9,875 km) is estimated to be 1.95 €/MWh. Hence, the delivery cost (including liquefaction, regasification, and shipping) of one MWh via the LNG route between these two nodes amounts to € 6.35. Due to the limited information available on the actual price paid by storage users, we assume variable costs to be uniform at 2.0 €/MWh across all storage nodes. This cost level represents the marginal operation costs and transport fees between storage sites and virtual trading points [115].

Data on national storage capacities and maximum monthly injection and withdrawal rates is from Gas Infrastructure Europe [113]. This data was aggregated on the node level (i.e. each region has one representative storage node). We assume storage losses to be 1.5% per cycle.<sup>21</sup> We incorporate European strategic storage requirements

<sup>19</sup> Please note that marginal production costs vary over the modeling horizon because they are a function of  $PRODCAP_{p,n,t}$  (see Appendix A).

<sup>20</sup> We use <https://sea-distances.org/>

<sup>21</sup> This assumption is in line with Egging [65], who finds that storage losses vary between 1% and 1.5% depending on storage operator information and local characteristics.

based on data from CEER [144] and European Commission [115].<sup>22</sup> As such, country-specific shares of storage capacity, which are reserved for strategic storage, are exogenously fixed and not included in the model's decision space. In turn, storage obligations are not included in the model.<sup>23</sup> Thus, in our modeling framework, gas storage utilization is driven solely by price signals.<sup>24</sup> Related short-term flexibility measures (e.g. management of gas stored in the pipeline network) are not included in the model due to this paper's seasonal focus.

Our model incorporates existing long-term contracts based on data from a study by Neumann, Rüster, and Hirschhausen [111], which contains a literature survey on existing global long-term contracts covering both pipeline and LNG deliveries.<sup>25</sup> In particular, we use information on contracting parties, annual contracted gas volumes, and contract expiration dates. As information about take-or-pay levels is not disclosed, we assume a uniform level of 70%. This data is used in the model as an exogenous constraint specifying the minimum bound on a trade variable between nodes. This constrains the diversification of supply by importing countries that would not have been captured if long-term obligations had been omitted.

### 4.3 RESULTS

This section discusses the numerical results of our model. The first subsection investigates the quantitative contributions of supply sources to cover gas demand. We focus on competition between different flexibility options to cover seasonal swings. The second subsection introduces a novel quantitative metric that measures the contribution of different flexibility options to meet seasonal demand swings. We apply this metric to determine which supply source offers the most flexibility in covering seasonal demand fluctuations and how the contribution changes over time.

<sup>22</sup> *Strategic storage* refers to a mechanism under which a portion of storage capacity is removed from the market, generally by the Transmission System Operator (TSO), for use only in extreme circumstances.

<sup>23</sup> *Storage obligations* require market participants (mainly gas suppliers) to secure storage capacity and ensure that a certain amount of gas is stored and available at a specified time.

<sup>24</sup> Gas storage has multiple functions aside from addressing seasonal flexibility needs, e.g. covering short-term flexibility needs and system security needs. This paper, however, focuses exclusively on seasonal flexibility. Note that we do not deduct storage capacity that is used for short-term flexibility needs. Thus, we establish an upper limit of flexibility available for seasonal needs from gas storage. However, benchmarking our results with historical data suggests that modeled injection and withdrawal volumes are in line with history in the European and country-specific cases.

<sup>25</sup> The data covers 426 long-term (five years or more) gas supply contracts, of which 127 are for pipeline deliveries and 299 are for LNG shipments.

#### 4.3.1 Quantitative supply contributions by source

Gas supply profiles follow the seasonal structure of demand. A certain “base load” must be covered throughout the year. In addition, heating demand increases gas consumption during the winter. We distinguish between four options for providing natural gas to European consumers: domestic gas production, pipeline imports, LNG imports, and storage withdrawals.<sup>26</sup>

Since our modeling setup aims to determine the market-clearing that minimizes the total cost, the simulated supply mix at every node is formed each month based on a “merit order” principle (i.e. in ascending order of marginal costs). One strength of our approach is that it considers intertemporal constraints with respect to storage. As a result, supply sources with the lowest value-chain costs are the first to be dispatched to meet gas demand. More expensive supply sources are used to satisfy “peak load.” However, intertemporal optimization adds complexity to this picture (e.g. importing and storing gas in the summer to decrease imports during the winter).

Fig. 4.3 illustrates the modeling results for quantitative gas supply contributions to cover monthly gas demand. We show the European aggregated demand profile, as well as that of three selected nodes: Germany, the UK (the two countries with highest gas consumption in Europe), and the Netherlands (due to significant expected production changes). Another reason these countries are particularly interesting for our analysis is that Germany and the Netherlands maintain one-third of all gas storage in the EU-28 (21% and 13% accordingly), while the UK historically has a relatively low level of gas storage (1% following the closure of the Rough storage facility [113]). For the historical outlook, we plot data from Eurostat [107] (January 2014 - December 2017) next to the model simulation results (from January 2018). It is important to note that the data from Eurostat does not differentiate between pipeline imports and LNG imports. However, we are able to differentiate between the two in our model. Hence, Eurostat’s aggregated net imports (i.e. imports minus exports) should be compared to the sum of pipeline imports and LNG imports. In addition, Dutch domestic production includes gas volumes used for exports (therefore, for the period of 2014 – 2017, Dutch production exceeds Dutch consumption).

It is clear that base load is largely covered by domestic production (e.g. the Netherlands until 2018), pipeline imports (e.g. Germany), or a combination of the two (e.g. the UK). Seasonal demand swing is covered by country-specific combinations of all four sources. Such combinations depend on geographical position, domestic production

<sup>26</sup> Note that while withdrawals from storage can be a supply source for one month, the gas must first be injected in the form of increased consumption in a prior month. Overall, gas storage is a net consumer (due to losses) but an important source of flexibility.

volumes, flexibility, the availability of transmission infrastructure (including pipeline and LNG routes), and the production capacity of gas exporters.

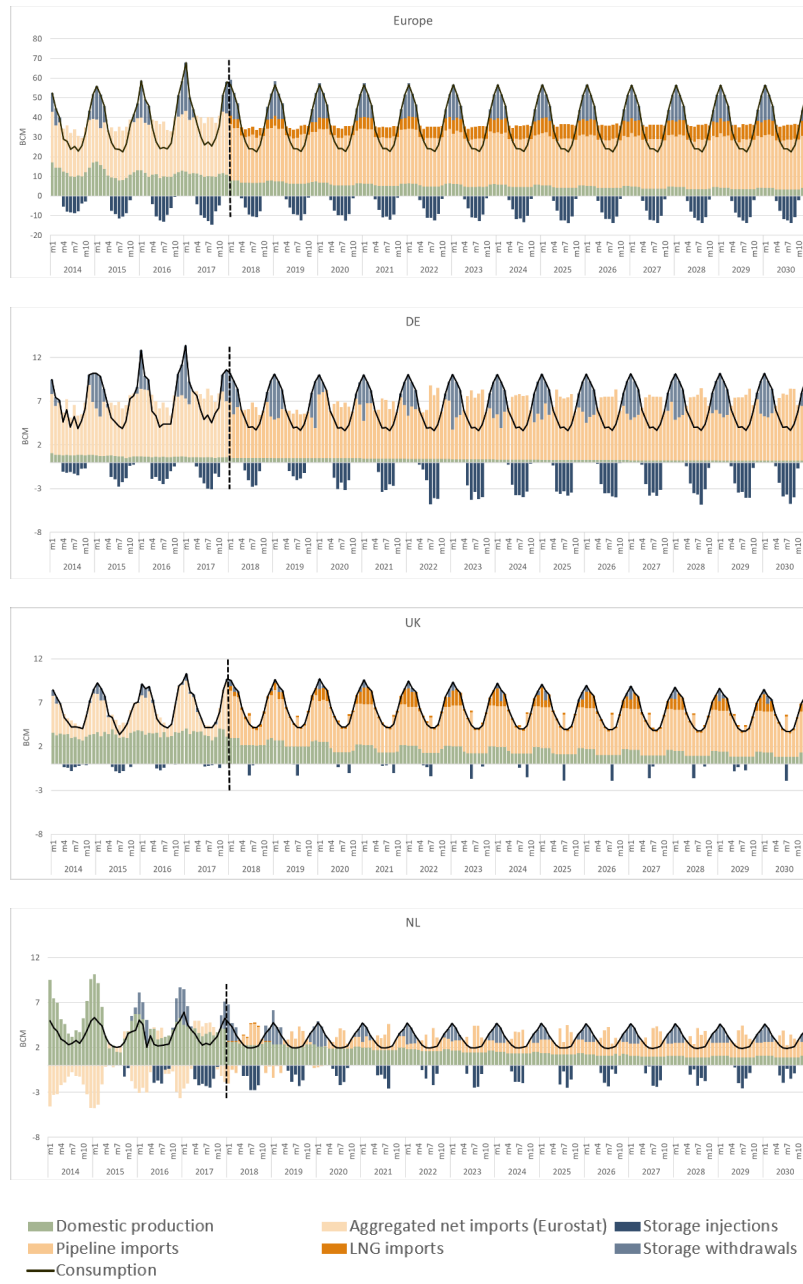


Figure 4.3: Quantitative gas supply contributions for selected countries in bcm per month. Time axis depicts calendar years

Fig. 4.3 also illustrates how the two major European domestic producers, the UK and the Netherlands, compensate for their decreases in production volumes. The Netherlands, which became a net gas importer in 2017, increasingly relies on pipeline imports and storage



to cover seasonal fluctuations.<sup>27</sup> In the UK, however, while annual domestic production decreases in the future, it still allows for seasonal flexibility. The latter is partially driven by a relative lack of alternative flexibility sources (in particular storage; see Fig. 4.4 below for detailed discussion).

To further enhance the visualization of the usage of seasonal flexibility options, we also present monthly demand levels in descending order of magnitude to form load duration curves.<sup>28</sup> Fig. 4.4 presents load duration curves for selected nodes on a monthly resolution, starting with the highest demand month on the left, for 2020, 2025, and 2030. The figure provides insight into the utilization levels of gas supply sources, their seasonality, and their role in the future of gas storage.

On the European level, the results reinforce what we pointed out in the discussion of Fig. 4.3.

First, storage provides the most flexibility on the European level. Storage withdrawals during peak demand remain high over the modeling horizon.

Second, the share of pipeline gas imported (relative to gross consumption) does not change significantly over the modelling period. LNG is increasingly filling in the gap in European consumption left by the drop in domestic European production. Up from 42 bcm of LNG imported by Europe in 2014 and 60 bcm in 2017, the volume of LNG imported in our model simulation is 61 bcm in 2020 and 91 bcm in 2030. Thus, LNG has a growing role in the European import mix—but it does not become the game-changer that some expect it to be. However, higher quantities of potential LNG imports are available to Europe. The maximum supply available to Europe (assumed in the model) is 103.2 bcm in 2020 and 158.3 bcm in 2030.<sup>29</sup> It is worth noting that the share of LNG in European imports depends not only on availability of global liquefaction capacities and cost chain, but also on the availability and costs of alternative supply sources and European gas demand.

Third, the model forecasts significant free seasonal flexibility remaining in the European system over the modeled period. Regarding storage capacity, only 49 – 60 bcm—out of about 110 bcm of working gas storage capacity—is withdrawn annually.<sup>30</sup> With regard to

<sup>27</sup> Please note that an important update on Dutch domestic production was published while this paper was in the peer-review process. The Groningen field is expected to be closed in 2022 with a possible extension up to 2026 to prevent supply issues [145]. Analyzing the effects of this supply shift on gas market in northwestern Europe would be a fruitful area for further research.

<sup>28</sup> While the term is mostly used in the context of electricity markets, the underlying idea is useful for visualising the use of gas market flexibility sources.

<sup>29</sup> Please note that we parametrize the model with the estimates for LNG supply potentials that were available in 2018.

<sup>30</sup> This observation reconfirms that reserving a certain share of storage for short-term flexibility needs would likely not affect results in the context of our analysis.

LNG, the annual utilization of terminals increases from 29% in 2020 to 43% in 2030. The same applies to pipeline infrastructure; while some cross-border interconnection points to Europe (e.g. RU  $\Rightarrow$  DE, NO  $\Rightarrow$  UK) or within Europe (e.g. DE  $\Rightarrow$  NL after 2021) are utilized at full capacity during the winter, a large amount of available pipeline capacity remains unused. This indicates that there is significant excess pipeline and LNG import potential. Nonetheless, events not analyzed in this paper (e.g. supply interruptions and exceptionally cold and long winter periods) require additional flexibility and more detailed analysis.

An analysis of country-specific results reveals further insights.

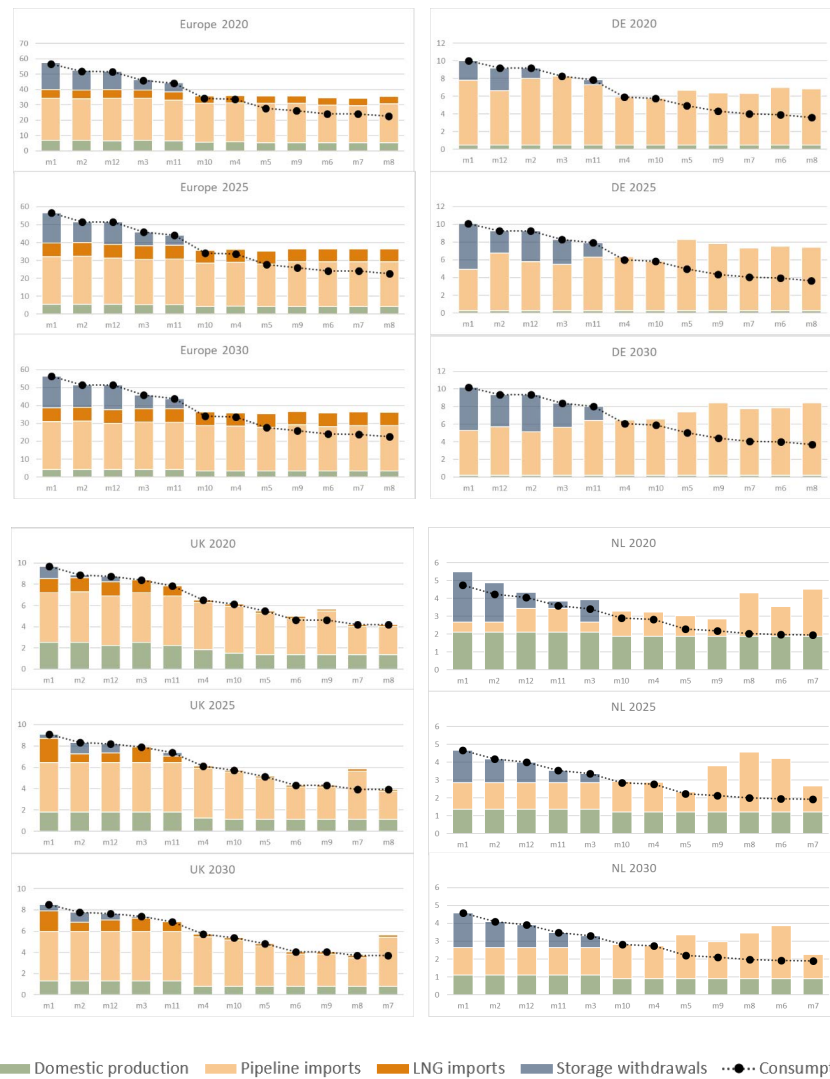


Figure 4.4: Annual load duration curves for selected countries in bcm per month. Time axis depicts calendar years. Values are sorted by gas consumption levels

The UK has historically had a relatively low level of gas storage (for more details, see Le Fevre [146]). The working capacity dropped even further in 2017 after the permanent stop of Rough storage operations, which had 3.3 bcm of working capacity (approx. 70% of all UK storage capacity). As a result, the working capacity of gas storage in the UK was reduced to 1.4 bcm p.a.—a remarkably low value compared to the country’s 2017 gross national consumption of 77.6 bcm [107]. According to our modeling results, the remaining storage is utilized at full capacity. Additional flexibility in the UK is provided by LNG, which primarily covers winter demand, thus taking the role of seasonal peak supplier. The importance of LNG for the UK gas supply increases over time. Furthermore, it is noteworthy that even declining national production will contribute to flexibility for the UK. Fig. 4.4 shows this clearly.

The results in Germany and the Netherlands are substantially influenced by Russian gas. In the case of Germany, the Nord Stream 2 pipeline project (which is included in our model from January 2020) immediately started to influence storage utilization.<sup>31</sup> Fig. 4.4 reveals that pipeline imports partially substitute storage withdrawals for the first half of the calendar year 2020. This substitution drives fewer storage injections in the preceding summer, though more injections occur in the following summer;<sup>32</sup> as a result, storage utilization recovers in winter 2020/2021. In the medium term, the effect of Nord Stream 2 on the utilization of German storage is limited. More detail on this effect is provided in the [Online Appendix](#). In the case of the Netherlands, the share of gas imports from Russia in a consumption mix increases from 2021 onwards, substituting the drop in domestic production. Norwegian export volumes decrease over time, reflecting our assumptions on decreasing production capacity. Our results are in line with the argument of Honore [121] that the only possibility of increasing the delivery of Norwegian gas to the Netherlands would be to re-direct some volumes at the expense of other European importers. The take-away message is that Norwegian exports cannot be seen as a solution to substitute the drop in Dutch production gas volumes and associated flexibility.

#### 4.3.2 *Measuring seasonal flexibility*

In this section, we analyze the contributions of different flexibility options to seasonal flexibility on both the country-specific and European level. Flexibility is analyzed on a monthly level, and both monthly

<sup>31</sup> During the peer-review process, information emerged that the completion of the project is delayed until Q4 2020 or Q1 2021.

<sup>32</sup> This effect is possible because Nord Stream 1 is utilized at full capacity (transport costs via the Ukrainian route are higher). The actual Nord Stream 1 utilization neared 93% in 2017

and seasonal conclusions are derived.<sup>33</sup> Consequently, all of our input data is in a monthly resolution to be consistent. Furthermore, our gas market model is optimized to analyze seasonal flexibility with a monthly time resolution. Thus, a key metric to measure and compare technologies' flexibility contribution should also be optimized for the research question and constructed with a monthly resolution.

With this aim, we develop a new metric that extends the Coefficient of Variation (CV) used in a report by the European Commission [115]. The authors introduce the CV to determine which supply source provides the most swing required to meet demand fluctuations. The CV is defined as a variable's standard deviation in relation to its mean 4.10:

$$CV = \frac{\sqrt{\frac{1}{n} \sum_1^n (x_i - \bar{x})^2}}{\bar{x}} \quad (4.10)$$

We propose adjusting the CV to remove two potential pitfalls of applying it in the context of seasonal gas market flexibility analysis. First, problems likely arise when the mean value is close to zero. With the mean in the denominator, the CV becomes sensitive to small changes of the mean near zero. For example, a small volume of LNG imported by a country with little LNG in its import mix in a specific year may cause the CV parameter to approach a relatively high number for that year. Second, the importance of a supply source in the provision of seasonal flexibility cannot be measured solely by CV. Following our earlier example, a small volume of imported LNG imported in a month of peak demand may have a high CV value (if the imported LNG volumes are low in most other months); however, the actual contribution of LNG imports to covering seasonal demand may be minuscule compared to a high volume of flexible pipeline imports. Hence, to fix both of these problems, we propose scaling the CV with the annual share of a specific supply source in covering gas demand 4.11:

$$SCV_i = CV_i \cdot AS_i = \frac{\sqrt{\frac{1}{12} \sum_{m1}^{m12} (S_{i,m} - \bar{S}_i)^2}}{\bar{S}_i} \cdot \frac{\sum_m S_{i,m}}{\sum_{i,m} S_{i,m}} \quad (4.11)$$

where

$CV_i$  annual coefficient of variation for flexibility option  $i$

$AS_i$  annual share of gas demand covered by flexibility option  $i$

$S_{i,m}$  gas quantity supplied by flexibility option  $i$  in month  $m$

The intuition for this SCV metric can be derived from its components. The CV is zero when supply is constant throughout the year (i.e. standard deviation is zero). It only increases once the supply pattern forms a seasonal structure.  $AS_i$ , as specified in equation 4.11, reflects

<sup>33</sup> An analysis of short-term flexibility on the daily or weekly level requires a different set-up.

a supply source’s aggregated annual contribution to demand and has an interval of  $[0, 1]$ . Therefore, the CV’s first problem does not apply to the SCV metric, as a low  $AS_i$  value compensates for the CV’s tendency to spike in cases where the mean is close to zero. The second problem is also addressed, as a supply source with even small-to-moderate seasonal variation is noted by the SCV metric if it has a relatively high  $AS_i$  value. Alternatively, a supply source with high seasonal variation but a small  $AS_i$  value would have a small SCV value. Overall, the SCV constitutes an effective measurement for the contributions of different flexibility options to covering seasonal demand swings.

We calculate SCVs based on our modeling results for the representative nodes on an annual basis (Fig. 4.5). We include Eurostat data for 2015 – 2017 to provide a historical reference. On the European level, the results show that compared to other flexibility sources, gas storage contributes most to seasonal flexibility. We find no evidence that gas storage facilities may be displaced from this position of prominence by pipeline or LNG imports in the long term.

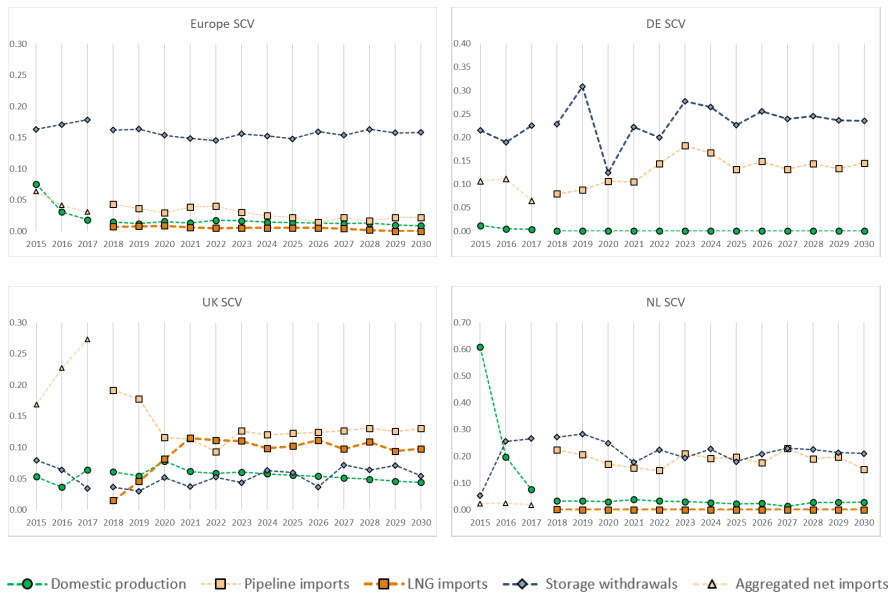


Figure 4.5: Annual SCVs for selected countries

Regarding country-specific results, Fig. 4.5 again shows the relative lack of storage in the UK market. In all other regions presented in the figure, storage is the most significant provider of flexibility based on the SCV. In the UK, storage makes the lowest average contribution over the period of observation. Furthermore, the contribution of domestic production to seasonal flexibility decreases over the modeling horizon. This is driven by declining domestic production volumes in the UK. The low volume of storage working capacity and the decline in domestic production can potentially be compensated by pipeline interconnections with continental Europe, a direct pipeline intercon-

nection with Norway, and high-capacity regasification terminals. The sharp increase in seasonal flexibility provided by LNG between 2018 and 2022 is driven by increasing LNG volumes during the winter.

In Germany, the SCV for domestic production is low on account of low volumes and a constant production pattern. Gas storage, in contrast, covers the bulk of its seasonal demand swings. The SCV metric also captures the above-mentioned (see Section 4.3.1) short-term effect of Nord Stream 2 displacing German storage as the key provider of seasonal flexibility, especially in the year 2020. The results also highlight that the role of pipeline imports in covering German seasonal demand swings increases after 2021, largely due to the higher volume of gas imports brought about by the eventual completion of the Nord Stream 2. The abundant volume of German working gas storage capacity permits significant storage of gas imports during the summer; therefore, it should be noted that seasonal flexibility provided by storage requires sufficient capacity of pipeline interconnectors.

The SCVs in the bottom-right chart of Fig. 4.5 quantify the drop in seasonal supply flexibility provided by domestic production in the Netherlands. Since 2017, Dutch production has played a minor role in covering demand swings, delivering a nearly constant amount of gas (see Section 4.3.1). Increasing SCVs for gas storage and pipeline imports, both based on historic and model-generated values, quantifies their role as replacements for domestic production.

#### 4.4 CONCLUSIONS

This paper quantifies and compares the roles of various flexibility options in the European gas market using a fundamental modeling framework. We contribute to the ongoing discussion of this topic with (i) a thorough analysis of seasonal flexibility and (ii) an optimization model to simulate long-term market operations. This allows us to explore structural trends in market development, which are driven by changing supply and demand fundamentals. Furthermore, we propose a new metric to quantify the provision of seasonal flexibility.

Our findings provide several insights into changes in the utilization of gas supply sources. In particular, the results illustrate that (i) European domestic production faces a dramatic decrease in volume; (ii) while LNG makes up a growing share of the European import mix, it does not constitute a game-changer; (iii) Europe continues to rely heavily on pipeline imports from Russia. Norwegian export volumes will not fill the gap, as Norway's production is expected to decrease steadily over the next few decades. Russia, in contrast, has enough free production and transportation capacity to substantially increase its exports to Europe. Our findings show that the bulk of the decline in Dutch production is substituted by pipeline imports from Russia while Norwegian gas is mainly imported to cover seasonal demand

swings; (iv) storage utilization at peak demand levels will remain high on both the national and European level.

We show that our methodologically enhanced **CV**—the scaled coefficient of variation—allows for a better understanding of how market dynamics affect seasonal flexibility. For example, the **SCV** captures the effects caused by the decline in Dutch domestic production and flexibility, the closure of the Rough storage facility in the UK, and the completion of new transmission infrastructure projects (e.g. Nord Stream 2). Our results indicate that gas storage contributes most to European seasonal flexibility across all years in the modeling horizon. Even following the completion of Nord Stream 2, pipeline imports rarely displace storage in meeting seasonal gas demand swings. Instead, additional interconnection is used with relatively low variations over the year. The contribution of **LNG** to seasonal flexibility is small on the European level; however, it may play a more important seasonal role on the national level (e.g. the UK). Taken together, we find no evidence that gas storage facilities will be displaced by pipeline or **LNG** imports from its role as the key seasonal flexibility provider in the long term.

Several questions remain for further research. In terms of methodology, our work can serve as the foundation for future work that quantifies the value of flexibility options, especially gas storage. In this paper, the new **SCV** metric was computed and interpreted exclusively with monthly data. Time resolution could be increased further to introduce short-term market dynamics (e.g. diurnal seasonality). Consequently, future investigations might differentiate between types of storage facilities (e.g. seasonal storage and fast-cycle storage). Paired with an analysis of the short-term factors most responsible for extrinsic optionality (which is not part of this study), assets in the gas sector could be evaluated. Furthermore, it would be interesting to see further studies that, while inspired by our methodology, focus on other product markets (e.g. electricity).

Further modeling work must be conducted to determine the impacts of demand and supply shocks on seasonal flexibility. Such analysis could determine the critical transport infrastructure projects and contribute to a comprehensive understanding of gas system safety needs and the insurance value associated with gas storage facilities. A further study with a focus on the gas market in northwestern Europe could include data on L-gas and H-gas production fields and transmission infrastructure. An increased geographical scope of the model would allow researchers to study the impacts of global **LNG** trends on the European gas market; this would facilitate a more thorough analysis of the competition between **LNG** supplies and alternative seasonal flexibility options. A progression of this work with a focus on southeastern Europe could be developed by incorporating the Caspian Sea region into its geographical scope. As this study adopted a deterministic approach, further research could explore the effects of parametric

uncertainty on the role of different flexibility options in the European gas market. Additionally, further modeling work could explore the potential of flexibility on the demand side. While the price elasticity of natural gas demand is difficult to estimate, sector demands could be analyzed in more detail by coupling sector models. Thus, an integrated electricity and gas sector model could be used to analyze the potential role of demand response by gas-fired power generation. Finally, the **SCV** metric could be used in further research to facilitate a vulnerability analysis of gas networks.

**DATA & CODE AVAILABILITY:** Datasets related to this article and a source code for the entire project are available in the public GitHub repository: <https://github.com/Irieo/SeasonalFlex>. The code reproduces the benchmarks from the paper.

**ONLINE APPENDIX** We provide modelling results for two additional scenarios and other supplementary data to this article in the Online Appendix at <https://github.com/Irieo/SeasonalFlex>.

**EXECUTIVE SUMMARY** A non-technical summary for this paper is available at [www.iaee.org/ej/ejexec/ej43-1-Riepin-exsum.pdf](http://www.iaee.org/ej/ejexec/ej43-1-Riepin-exsum.pdf).

**CREDIT AUTHORSHIP CONTRIBUTION STATEMENT** **Igor Riepin:** Conceptualization, Methodology, Data curation, Software, Validation, Investigation, Visualization, Writing - original draft. **Felix Müsgens:** Conceptualization, Writing - review & editing, Supervision.



## EUROPEAN GAS INFRASTRUCTURE EXPANSION PLANNING: AN ADAPTIVE ROBUST OPTIMIZATION APPROACH

---

**ABSTRACT:** The European natural gas market is undergoing fundamental changes, fostering uncertainty regarding both supply and demand. This uncertainty is concentrated in the value of strategic infrastructure investments, e.g., Projects of Common Interest supported by European Union public funds, to safeguard security of supply. This paper addresses this matter by suggesting an adaptive robust optimization framework for the problem of gas infrastructure expansion planning that considers long-term uncertainties. This framework confronts the drawbacks of mainstream methods of incorporating uncertainty in gas market models (i.e., stochastic scenario trees), in which the modeler predefines the probabilities and realization paths of unknown parameters. Our mathematical model endogenously identifies the unfortunate realizations of unknown parameters, and suggests the optimal investments strategies to address them. We use this feature to assess which infrastructure projects are valuable in maintaining system resilience amid cold-winter demand spikes, supply shortages, and budget constraints. The robust solutions point to consistent preferences for specific projects. We find that real-world construction efforts have been focused on the most promising projects from a business perspective. However, we also find that most projects are unlikely to be realized without financial support, even if they would serve as a hedge against stresses in the European gas system.

**KEYWORDS:** Adaptive robust optimization, Capacity planning, European gas market, Uncertainty

**PUBLISHED AS:** I. Riepin, M. Schmidt, L. Baringo, F. Müsgens (in review), European gas infrastructure expansion planning: an adaptive robust optimization approach. Working paper in *Optimization Online* (2021): [http://www.optimization-online.org/DB\\_HTML/2021/10/8654.html](http://www.optimization-online.org/DB_HTML/2021/10/8654.html)

*This chapter presents the working paper as originally published in Optimization Online eprint server. The journal article is in review stage.*

### 5.1 INTRODUCTION

Natural gas is a key energy source in modern economies, as it is used for heating, for generating electricity, and as a combustion fuel for industrial processes. Despite increasing global demand, recent years

have seen the production of natural gas steadily decline in traditional European supply countries, such as Norway, the Netherlands, and the U.K. Hence, European dependence on natural gas is set to rise alongside rising competition for foreign resources. These two simultaneous developments entail heightened geopolitical risks, potentially triggering supply disruptions [147]. While gas demand in Europe is expected to drop dramatically in the long term—under the assumption that policy objectives will be met—its trajectory in the medium term is subject to significant uncertainty, with scenarios anticipating a peak in 2030 [148]. This uncertainty poses planning challenges for the European transmission system.

Since the initial foray of European Union (EU) into energy market liberalization, the issue of supply security has been a priority on the policy agenda [149]. The EU has proactively sought to enhance its infrastructural capacity in order to curb vulnerabilities. An official European energy security strategy instituted in 2014 tackles two policy priorities: first, boosting the short-term resilience of the natural gas network as a mechanism against supply interruption; second, reducing dependence on prevailing suppliers in the long term [150]. Policymakers have lent great importance to heightening supply security through the development of new gas pipelines and LNG receiving terminals. European Projects of Common Interest (PCI) have been supported by public funds to advance market reform and further integrate and strengthen transnational gas infrastructure. Recently, these projects have been the target of significant criticism, with some arguing that they are unnecessary from a supply security perspective and are at risk of becoming stranded assets [151].

In order to evaluate the impacts of uncertainties on European natural gas infrastructure and assess which infrastructure projects are critical to maintaining system resilience, this paper employs an Adaptive Robust Optimization (ARO) approach [152]. Several features of ARO make it particularly suitable for this purpose. First, ARO does not rely on the assumption of a finite number of uncertainty realizations with respective (known) probabilities. This feature confronts the drawbacks of mainstream methods of incorporating uncertainty in gas market models (i.e., stochastic scenario trees based on discrete probability distributions) [102, 153]. ARO requires only basic information about underlying uncertainty (e.g., the range of the uncertain data). Second, ARO is preferable when solutions exhibit strong sensitivity to minor changes in assumptions or input data. This feature is valuable in systems like the European natural gas market with complex spatial and intertemporal dynamics and numerous infrastructure assets. Finally, ARO has gained attention as a mechanism with which to model uncertainty in applications with high reliability requirements. Solution robustness in the context of energy systems is extremely valuable, as the penalty associated with infeasible solutions is exorbitant [152].

This paper addresses the following research questions:

- How can an adaptive robust optimization approach be employed to assess the impact of supply and demand uncertainties on infrastructure development in the European gas market?
- What implications do different levels of uncertainty have on specific infrastructure projects in the context of supply security?

ARO has gained prominence in the field of electricity systems analysis; however, in the field of gas network modeling, the applications has largely been restricted to testing distribution networks and stationary models [154, 155]. This paper contributes to the extant literature by applying ARO to model uncertainties in a real-world setting. To the best of our knowledge, this constitutes the first application of ARO in gas infrastructure expansion planning. Furthermore, we make an empirical contribution to the literature by assessing the implications of demand and supply uncertainty in 2030 on European natural gas infrastructure.

To facilitate transparency and encourage future research in this field, the source code of the model and the associated input data for each scenario is published in a public GitHub repository: [github.com/Irieo/ARO-GasInfrastructure](https://github.com/Irieo/ARO-GasInfrastructure). The code reproduces the results presented in the paper.

The remainder of the paper is organized as follows. Section 5.2 provides a brief overview of the methods used in this paper. Section 5.3 presents the formulation of the adaptive robust optimization problem, a representation of the employed uncertainty sets, and their empirical application to the European natural gas market. Section 5.4 reports and discusses the results and their implications. Section 5.5 concludes the paper with a summary of our analysis and a brief outlook on the potential for future research. Appendix C provides the detailed formulation of the adaptive robust optimization model for gas infrastructure expansion planning. Appendix D provides an illustrative example of the worst-case demand and supply realisations subject to uncertainty budgets. Appendix E lists PCI included in our analysis. Appendix F complements literature review section and lists research papers that focus on natural gas markets and address parametric uncertainty.

## 5.2 LITERATURE REVIEW

This section briefly reviews common approaches to model long-term uncertainties in the extant literature. In Section 5.2.1, we discuss methods for addressing long-term uncertainty in energy system models. In Section 5.2.2, we narrow our focus to natural gas market models.

### 5.2.1 Methods for addressing long-term uncertainty in energy systems models

The subject of long-term uncertainty in the context of model-based policy analysis has been vigorously discussed in the academic literature for decades [156]. Assessments of the impact of long-term systematic uncertainty in energy systems models commonly employ one of the three methods illustrated in Figure 5.1.

The vast majority of analyses incorporate uncertain parameters via deterministic scenarios (Figure 5.1a), often coupled with ex-post sensitivity analyses [157].

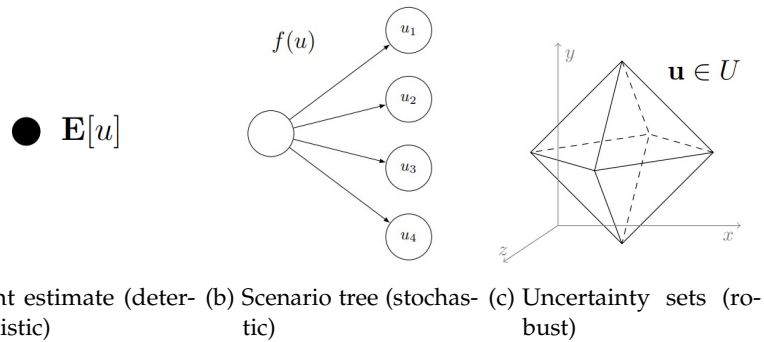


Figure 5.1: Methods for incorporating uncertainty in energy optimization problems

Another prominent method of incorporating uncertainty involves multi-stage stochastic optimization (Figure 5.1b). In this method, uncertain information is modeled by scenario trees (i.e., sequences of observable data vectors over the planning horizon). The branches (possible realizations of uncertain data) follow a probability distribution, which is assumed to be known to the decision-maker. At each stage, a decision must be irrevocably fixed based on the currently available information. One drawback of applying stochastic optimization to real-world problems is the fact that the realization probabilities of the random variables are mostly unknown [158]. Detailed reviews of the use of stochastic methods in energy system modeling are available in Wallace and Fleten [159], Möst and Keles [160], and Collins et al. [161]. However, a simple stochastic representation of uncertainty is not always viable when the probabilities of possible events are uncertain, knowledge of all possible events (unknown unknowns and black swans) is unavailable [162], or uncertainty is not purely exogenous.

The third method employs robust optimization (Figure 5.1c), which dates back to Soyster [163]. An *adaptive* robust optimization implements different techniques to improve on the original static robust optimization by incorporating multiple stages of decision into the algorithm [164]. As noted above, ARO is well-suited for applications

where distributional information about a given uncertainty is limited or where solution feasibility is the ultimate evaluation metric. ARO renders solutions that exhibit feasibility for all possible realizations of uncertainty within a range defined in an uncertainty set. The set should be constructed to capture correlations among certain parameters. Although one can derive such sets based on probabilistic data, well-defined probability distributions are not required to construct uncertainty sets. Various types of uncertainty sets (e.g., box, polyhedral, ellipsoidal, cardinality-constrained budgets) have been employed in the extant literature [165]. Original box-type uncertainty sets were only able to accommodate the most conservative uncertainty manifestations. More recently, polyhedral uncertainty sets have been developed and employed [166]. Their uncertainty budgets can constrain the degree of uncertainty attached to a parameter. An in-depth review of its applications and methodological foundations can be found in Yanikoglu, Gorissen, and Hertog [167]. In terms of its applications in the analysis of energy systems, ARO has been utilized to evaluate both short- and long-term uncertainties. Short-term analyses predominantly focus on electricity markets with unit commitment problems under uncertainty (e.g., intermittent wind power feed-in) [152, 168, 169]. Fewer short-term analyses involve natural gas, and most that do focus on scheduling problems in coupled electricity and gas markets (e.g., [154, 170]). In terms of long-term uncertainties, a substantial strand of literature has applied variations of ARO to transmission-expansion planning models (e.g., [171–174]). There have yet to be any such ARO approaches to gas market modeling.

### 5.2.2 Long-term uncertainty and its representation in natural gas models

The subject of medium- to long-term uncertainty in natural gas markets has received considerable attention. The prevailing strand of analysis is deterministic in nature, deploying scenario and sensitivity analyses or (n-1) stress tests to incorporate uncertainty. More recently, model-based analyses have begun to adopt a stochastic approach in order to handle ranges of uncertain manifestations of relevant parameters (e.g., [68, 175–177]). A tabular overview of such studies and their individual structures and representations of uncertainties is provided in Table F.1 in Appendix F.

The overview highlights that extant literature has explored developments in natural gas supply and demand. Prospective demand trajectories, supply interruptions, and infrastructural bottle-necks have been in the focus of recent work. Research on the European market has focused on supply interruptions and infrastructure resilience on account of past geopolitical discord associated with transit negotiations regarding Russian gas supplied via Ukraine [129, 176, 178–181]. Given the uncertainty on the use of natural gas in medium-term trajectory,

the prudence of impending investments in the resource remains in center of researchers' attention.

Our analysis contributes to the growing literature on this subject by employing a novel methodological approach to evaluate the resilience of European natural gas infrastructure under the worst-case combinations of uncertain demand and supply developments.

### 5.3 PROBLEM FORMULATION

This section details the formulation of the ARO model. For the sake of clarity, we first introduce an ARO problem in a compact form in Section 5.3.1. Afterward, in Section 5.3.2, we present a decomposition algorithm for the ARO problem. Finally, we apply the ARO model to a gas infrastructure expansion planning problem in Section 5.3.3. In this section, we also parameterize the problem with the respective input data for the European natural gas market.

#### 5.3.1 Compact formulation

The methodology takes stock of the ARO problems developed for energy markets (primarily electricity markets) [171, 174, 182–184]. These problems are formulated as three-level optimization problems. The robust problem can be written in compact matrix form, as illustrated in Figure 5.2.

$$\begin{array}{l}
 \min_x C_I^T x \\
 \text{s.t.} \\
 x \in \mathbb{Z}^n \\
 h(x) = 0 \\
 g(x) \leq 0
 \end{array}
 \quad
 \begin{array}{l}
 \max_u \\
 \text{s.t.} \\
 u \in U
 \end{array}
 \quad
 \begin{array}{l}
 \min_y [C_O(x, u)]^T y \\
 \text{s.t.} \quad y \in \Xi(\cdot)
 \end{array}$$

Figure 5.2: Schematic representation of ARO model formulation

Authors' illustration based on Baringo, Boffino, and Oggioni [174] and Mínguez and García-Bertrand [184]

The problem in Figure 5.2 includes three nested optimization layers:

1. The first level represents a *planning strategy* prior to the uncertainty realization (i.e., binary variables in vector  $x$  representing

- investment in transmission infrastructure projects with an investment cost vector  $C_I$ ).
2. The second level represents the worst-case *uncertainty realization* (in the sense of cost maximization) within an uncertainty set (i.e., variables in vector  $u$ ).
  3. The third level represents the *corrective actions* made to mitigate the effect of the uncertainty realization (i.e., variables in vector  $y$  with the vector including operating costs  $C_O$ ).

Thus, the problem illustrated in Figure 5.2 involves both a preventive and a curative component. Hence, in many respects, it mirrors the nature of infrastructure planning processes (i.e., project planning subject to uncertainty realizations, for which subsequent mitigation measures are deployed) [171]. In the problem,  $\Xi$  and  $U$  are the feasibility and uncertainty sets, respectively. Set  $\Xi$  identifies the feasible space of the third-level optimization variables, as explained in subsection 5.3.1.1, while uncertainty set  $U$  is described in subsection 5.3.1.2.

#### 5.3.1.1 Definition of feasibility sets

Set  $\Xi$  models the feasible space of third-level optimization variables given the first- and second-level decisions:

$$\begin{aligned} \Xi(x, u) = \{y : \\ A(x, u) \cdot y = b(x, u) : \lambda \\ D(x, u) \cdot y \geq e(x, u) : \mu \\ \} \end{aligned} \quad (5.1)$$

where  $A, b, D$ , and  $e$  are matrices with constant parameters depending on the problem configuration, and  $\lambda$  and  $\mu$  are the dual variable vectors associated with inequality and equality sets of constraints, respectively. Note that the feasibility set  $\Xi$  is parameterized in terms of first- and second-level decision variables.

#### 5.3.1.2 Definition of uncertainty sets

This paper employs a specific type of polyhedral uncertainty sets. Bertsimas et al. [152] were among the first to apply such uncertainty sets for the energy network transmission expansion problem. The applicability of polyhedral uncertainty sets to modern energy research paired with the challenges of energy transitions facilitated intensive research and elaborated descriptions of the uncertainty in the literature.

In particular, cardinality-constrained uncertainty sets are advantageous, as they enable the description of uncertainty in the energy markets alongside the improved convergence characteristics of the

ARO problems. In such a formulation, the worst-case uncertainty realization corresponds to the vertex of the polyhedron representing the uncertainty set. Thus, polyhedral uncertainty sets can be equivalently characterized by solely modeling the finite set of extremes or vertices of the polyhedron. This approach has been employed by many researchers (e.g., [174, 184–187]), with binary variables being used to model the extreme-based equivalent for the original cardinality-constrained uncertainty set.

The problem in Figure 5.2 includes the second-stage decision variable  $u$ , which takes values within the known confidence bounds:

$$u \in [\tilde{u} - \hat{u}, \tilde{u} + \hat{u}] \quad (5.2)$$

where  $\tilde{u}$  and  $\hat{u}$  represent the vectors of the forecast and fluctuation levels of the uncertain variables, respectively. The corresponding cardinality-constrained uncertainty set, as defined in Baringo, Boffino, and Oggioni [174], assumes the following form:

$$U = \{u = \tilde{u} + \text{diag}(z^+) \hat{u} - \text{diag}(z^-) \hat{u}, \quad (5.3a)$$

$$z^+, z^- \in \{0, 1\}^m, \quad (5.3b)$$

$$\sum_{k=1}^m (z_k^+ + z_k^-) \leq \Gamma, \quad (5.3c)$$

$$z_k^+ + z_k^- \leq 1, \quad \forall k \} \quad (5.3d)$$

Eq. (5.3a) defines the value of the uncertain variable  $u$  based on the forecast and fluctuation levels. Eq. (5.3b) defines the vectors of binary variables  $z^+$  and  $z^-$ . Eq. (5.3c) defines the uncertainty budget  $\Gamma$ , which enables us to control the robustness of the solution.  $\Gamma = 0$  implies that all instances of the uncertain variable  $u$  are equal to their forecast values (i.e., uncertainty is disregarded). Any positive value of  $\Gamma$  implies that the variable  $u$  can deviate from its forecasted value.  $m$  indicates the size of the vector of variable  $u$ . Eq. (5.3d) ensures that the uncertain variables in vector  $u$  cannot simultaneously be at both their upper and lower bounds.

### 5.3.2 Solution procedure

The three-level optimization expressed in Figure 5.2 is solved via a decomposition technique. Here we again follow past research in the field of robust optimization for power systems. Specifically, we rely on the research of Baringo, Boffino, and Oggioni [174] and Mínguez and García-Bertrand [184], who employ an efficient coupling method for second- and third-level problems, as well as that of Bertsimas et al. [152], Mínguez and García-Bertrand [184], and Conejo et al. [188],



who develop, benchmark, and illustrate a Column-and-Constraint Generation (CCG) algorithm, which is efficient for ARO problems.

The CCG algorithm involves iterative solutions for the master problem and subproblem through the exchange of information provided by the primal decision variables.<sup>1</sup> Finite convergence to the optimal solution is guaranteed given the convexity of the problem [152, 164]. The algorithm consists of the following three major steps:

1. First, the master problem is solved. The master problem is mainly based on the first-level problem in Figure 5.2. The master problem uses the solution from the subproblem as input data (i.e., uncertainty realization variables in vector  $u$ ).
2. Second, the subproblem comprising the second- and third-level problems is solved. The subproblem incorporates input data from the master problem (i.e., the infrastructure expansion decisions in binary vector  $x$ ).
3. Third, the master problem and the subproblem are iteratively solved until they reach convergence to the optimal solution (i.e., a convergence tolerance is fulfilled).

The following sections provide detailed explanations of the master problem, the subproblem, and the solution procedure.

#### 5.3.2.1 Master problem

The master problem, in a compact form at iteration  $\nu$ , is as follows:

$$\min_{x, \eta, y^{(\nu)}} Z^M = C_I^T x + \eta \quad (5.4a)$$

subject to

$$h(x) = 0 \quad (5.4b)$$

$$g(x) \leq 0 \quad (5.4c)$$

$$\eta \geq [C_O(x, u^{(\nu)})]^T \cdot y^{(\nu)} \quad \forall v' \leq \nu \quad (5.4d)$$

$$A(x, u^{(\nu)}) \cdot y^{(\nu)} = b(x, u^{(\nu)}) \quad \forall v' \leq \nu \quad (5.4e)$$

$$D(x, u^{(\nu)}) \cdot y^{(\nu)} \geq e(x, u^{(\nu)}) \quad \forall v' \leq \nu \quad (5.4f)$$

where variables in set  $\Phi^M = [x, \eta, y^{(\nu)}, \forall v' \leq \nu]$  are the optimization variables of the master problem (5.4).

Overall, the master problem (5.4) is a relaxed version of the three-level problem in Figure 5.2, in which the auxiliary variable  $\eta$  iteratively approximates the worst-case value of the second-level objective function. Note that Eqs. (5.4d)–(5.4f) are formulated for all realizations of

<sup>1</sup> For this reason, the algorithm is sometimes referred to as “primal Benders’ decomposition”.

$u^{(v')}$ , which refers to the optimal values of variables  $u$  obtained in the subproblem at iteration  $(v')$ . This procedure is the basis for the term “column-and-constraint generation”.

### 5.3.2.2 Subproblem

The subproblem is formulated in two steps.

In the first step, we follow the approach used by Baringo, Boffino, and Oggioni [174] and Mínguez and García-Bertrand [184] to couple the second- and third-level problems depicted in Figure 5.2. We do this by taking the third-level problem:

$$\min_y [C_O(x^{(v)}, u)]^T y \quad (5.5a)$$

subject to

$$A(x^{(v)}, u) \cdot y = b(x^{(v)}, u) : \lambda \quad (5.5b)$$

$$D(x^{(v)}, u) \cdot y \geq e(x^{(v)}, u) : \mu \quad (5.5c)$$

and deriving the corresponding dual problem:

$$\max_{\lambda, \mu} [b(x^{(v)}, u)]^T \lambda + [e(x^{(v)}, u)]^T \mu \quad (5.6a)$$

subject to

$$[A(x^{(v)}, u)]^T \lambda + [D(x^{(v)}, u)]^T \mu = C_O(x^{(v)}, u) \quad (5.6b)$$

$$\lambda : \text{free}, \mu \geq 0 \quad (5.6c)$$

In the second step, we rely on the strong duality equality, which allows us to merge the dual form of the third-level problem (5.6) with the second-level problem. As a result, the subproblem is formulated as a single-level optimization problem:

$$\max_{u, \lambda, \mu} Z^S = [b(x^{(v)}, u)]^T \lambda + [e(x^{(v)}, u)]^T \mu \quad (5.7a)$$

subject to

$$[A(x^{(v)}, u)]^T \lambda + [D(x^{(v)}, u)]^T \mu = C_O(x^{(v)}, u) \quad (5.7b)$$

$$\lambda : \text{free}, \mu \geq 0, u \in U \quad (5.7c)$$

where variables in set  $\Phi^S = [u, \lambda, \mu]$  are the optimization variables of the subproblem (5.7). Note that at each iteration of  $v$ , the master problem (5.4) provides the expansion decision  $x$ , which is fixed in the subproblem:  $x = x^{(v)}$ . In turn, the subproblem determines the worst-case uncertainty realizations in variable vector  $u$ , which are

passed to the next iteration of the master problem. Thus, the size of the master problem increases alongside the number of iterations, as a new instance of uncertainty realization is added to the master problem constraints in each iteration.

At this stage, there is only one detail left unfulfilled in formulating the subproblem. The bilinear term  $[b(x^{(\nu)}, u)]^T \lambda$  included in the objective function (5.7a) must be linearized. We follow the example of Mínguez and García-Bertrand [184] by replacing the bilinear term with the mathematically exact reformulation, which is provided in Appendix C.

### 5.3.2.3 Algorithm

At this point, the master problem (5.4) and the subproblem (5.7) have been defined. The problems are iteratively solved via the exchange of information provided by the primal decision variables. The CCG algorithm functions as follows:

1. **Input:** Select the uncertainty budgets  $\Gamma^G$  and  $\Gamma^D$ , and the convergence tolerance  $\varepsilon$ . These data are selected by the decision-maker.
2. **Initialization:** Initialize the iteration counter ( $\nu = 0$ ) and set the lower bound (LB) and the upper bound (UB) to  $-\infty$  and  $+\infty$ , respectively.
3. Solve the master problem (5.4).
4. Update the lower bound:  $LB = Z^{M^*}$ .
5. The solution to the master problem contains decision variable vector  $x^*$ ; set  $x^{(\nu)} = x^*$ .
6. Solve the subproblem (5.7).
7. Update the upper bound:  $UB = \min\{UB, C^T x + Z^{S^*}\}$ , where  $S^*$  is the optimal value of the subproblem objective function.
8. If  $UB - LB < \varepsilon$ , the algorithm stops. The optimal decision is  $x^*$ . Otherwise, go to Step 9.
9. Update the iteration counter as follows: ( $\nu = \nu + 1$ ).
10. Set  $u^{(\nu)} = u^*$ , where  $u^*$  is the optimal decision variable vector of the subproblem obtained in Step 6.
11. Go to Step 3.

Figure 5.3 presents a visual depiction of the algorithm:

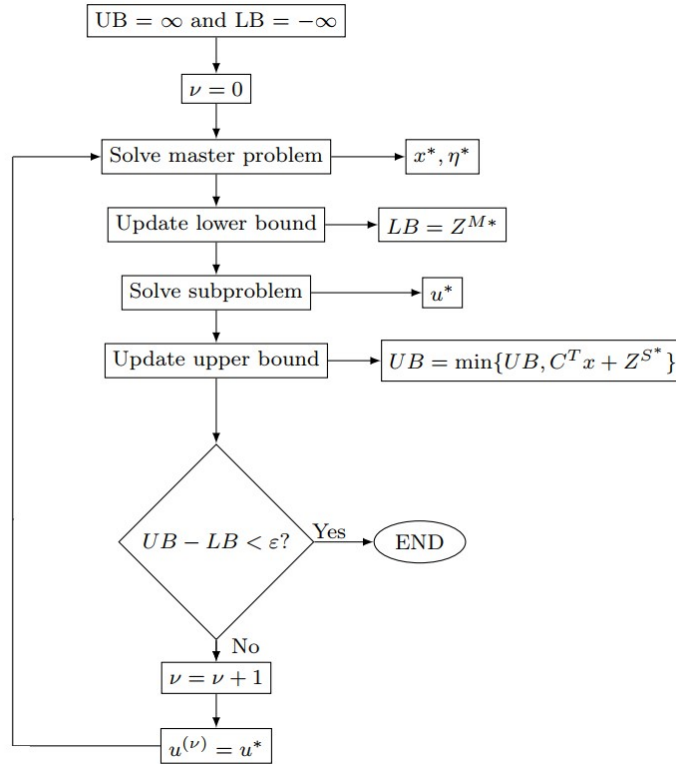


Figure 5.3: Schematic representation of CCG algorithm

Authors' illustration based on Conejo et al. [188].

### 5.3.3 Empirical application: European gas infrastructure expansion problem

In this section, we apply the ARO method described above to empirically analyze infrastructure expansion needs in the European gas system under unfortunate realizations of demand and supply for 2030.

The resulting model is formulated as a Mixed-Integer Linear Problem (MILP). The model endogenously determines the worst-case stress for the gas system that falls within the confidence bounds (see section 5.3.1.2) and iteratively finds the optimal infrastructure expansion plan to address that stress. The objective function aims to minimize the costs of constructing the new infrastructure assets and the operational costs of supplying natural gas under unfortunate realizations of parametric uncertainty subject to the appropriate techno-economic constraints.

The remainder of this section is structured as follows. First, we provide a brief description of the gas network in Subsection 5.3.3.1. Second, we take a deeper look at the key elements of our analysis: (i) an empirical parametrization of uncertainty budgets in Subsection 5.3.3.2 and (ii) the set investment options (PCIs) in Subsection 5.3.3.3. Finally, we discuss the model's other data inputs in Subsection 5.3.3.4. The formulation of the expansion planning problem for the European gas market is provided in Appendix C.

### 5.3.3.1 Gas network

The model structure consists of a network of nodes, each of which represents a country or region. Overall, the gas network (shown in Figure 5.4) comprises 37 nodes representing the countries and regions that are most relevant in the European gas market.

Nodes are connected by gas transmission infrastructure assets, including (i) cross-border pipe-lines within the EU, (ii) cross-border pipelines with non-EU parties (such as the Nord Stream), and (iii) regasification terminals for LNG imports. Overall, the gas network includes 96 individual pipeline arcs and 11 regasification terminals. Bi-directional pipelines are modeled as two distinct arcs. In our analysis, we model a single representative LNG producer that serves the European market and can ship liquified gas to individual countries based on its total domestic regasification capacity. Regasification terminals included as part of the PCI investment options are similarly modeled as arcs available to be built between the LNG supplier and the destination country. The model neglects friction and pressure drops in the gas network.

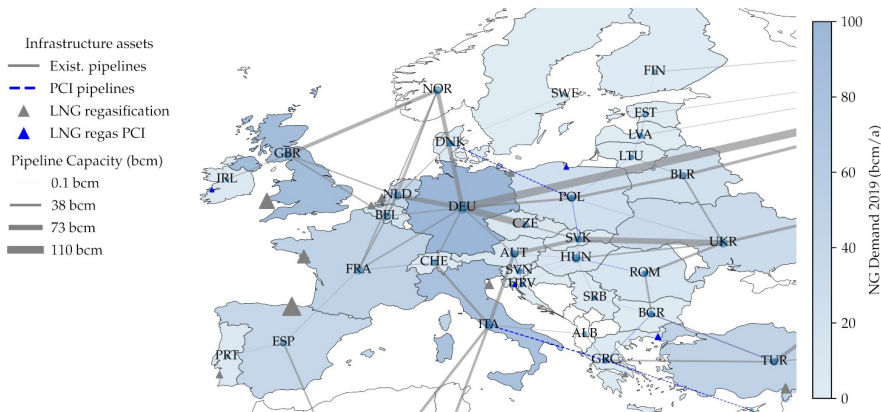


Figure 5.4: Stylized representation of the European natural gas network

Authors' illustration.

### 5.3.3.2 Long-term uncertainty characterization: Uncertainty set

Here, in line with Section 5.3.1.2, we present the parametrization of the uncertainty sets with the data instance relevant for the European gas market. In this paper, we focus on uncertainties surrounding natural gas demand and supply. Both of these sources of uncertainty are characterized by cardinality-constrained uncertainty sets, which are represented mathematically as follows:

$$\Omega = \left\{ \bar{g}_{dt}^D = \tilde{G}_{dt}^D + z_{dt}^D \cdot \hat{G}_{dt}^D \quad \forall d, \forall t \right. \quad (5.8a)$$

$$\bar{g}_p^P = \tilde{G}_p^P - z_p^P \cdot \hat{G}_p^P \quad \forall p \quad (5.8b)$$

$$\sum_{d \in D, t \in T} z_{dt}^D \leq \Gamma^D \quad (5.8c)$$

$$\sum_{p \in P} z_p^P \leq \Gamma^P \quad (5.8d)$$

$$z_{dt}^D \in \{0, 1\} \quad \forall d, \forall t \quad (5.8e)$$

$$z_p^P \in \{0, 1\} \quad \forall p \quad (5.8f)$$

Constraints (5.8a) and (5.8b) express the uncertain variables—the demand and supply vectors—with respect to projected reference values and their deviations, resulting in system stress. In Eq. (5.8a),  $\bar{g}_{dt}^D$  denotes the uncertain demand in each node and time step,  $\tilde{G}_{dt}^D$  denotes the reference value, and  $\hat{G}_{dt}^D$  denotes the possible deviation from the reference value. Eq. (5.8b) corresponds similarly to the network supply. Note that the unfortunate realization of supply is modeled on an annual basis. Thus, Eq. (5.8b) does not feature a time step index. This reflects the temporal nature of parametric uncertainty in the model: cold-winter gas demand spikes on the one hand; policy- and technology-driven development of annual gas supply potentials on the other hand. Constraints (5.8c)–(5.8f) follow the explanation in Section 5.3.1.2.

Data-driven approaches to constructing suitable uncertainty sets are the common tools used in ongoing research [171]. Such approaches incorporate available data to devise uncertainty sets that ensure that the random variables under investigation are contained in defined probability distributions. We construct the uncertainty sets for natural gas demand and supply volumes based on scenario projections for 2030, which stem from the scenario framework adopted in the TYNDP [189].<sup>2</sup> The reference values adopted for the uncertainty sets correspond to the optimistic scenario projections regarding supply security (i.e., mild winter demand levels and the highest available supply volumes). The uncertainty sets enable the investigation of unfortunate realizations with respect to 2030 supply security. The demand and supply volumes covered by the cumulative budgets are displayed in Figure 5.5. The bar graphs comprise the scenario-specific demand and supply projections for the individual countries and/or suppliers in the model.

In line with the analysis of the PCIs' contributions to supply security, the demand uncertainty budgets are constructed to reflect the realization of a cold-winter peak demand event across Europe. The demand budgets considered are allocated across five winter months

<sup>2</sup> Projections are sourced from the National Trends and Global Ambition scenario.

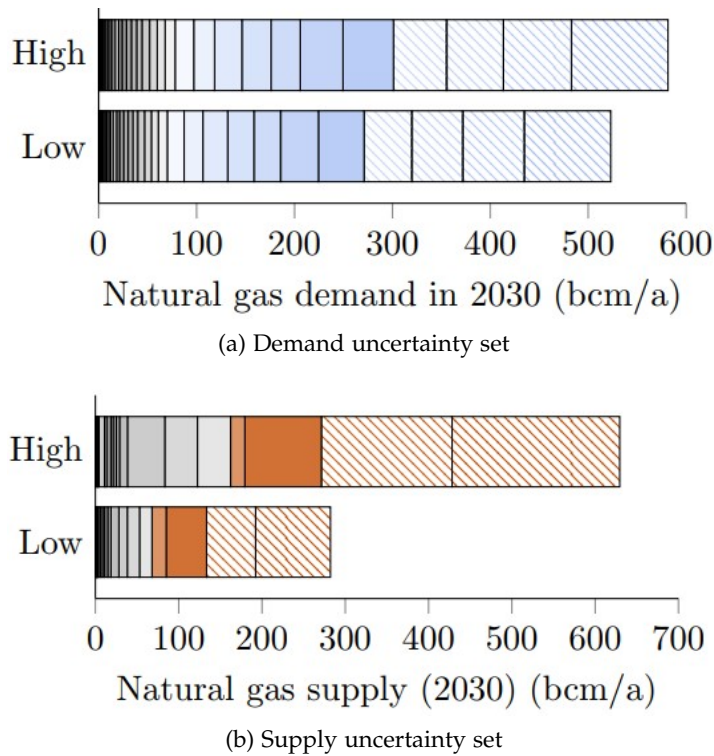


Figure 5.5: Scenario projections used for the construction of the uncertainty sets

Each segment represents the annual demand level (top panel) and supply potential (bottom panel) of an individual country. Source: ENTSO-G [189]

(November–March). Deviations per month incorporated are based on historical peaks of gas demand in each modeled country over the last decade [190]. To provide a more explicit illustration of how the uncertainty budgets are employed in the model, Figure D.1 in Appendix D illustrates the worst-case demand realizations given the uncertainty budget of  $\Gamma^D = 10$ . The demand spikes materialize in a way that represents the worst-case scenario in terms of the gas system operational costs.

Regarding the employed supply uncertainty budget, the deviations represent the difference in the projected 2030 supply potentials between the most optimistic and the most pessimistic supply scenarios. In contrast to the demand uncertainty budgets, the supply uncertainty budgets are constructed on an annual basis (i.e., an endogenously determined supply cut applies to the entire year). As detailed above, the supply cost curves for the six largest gas producers<sup>3</sup> are modeled in a piece-wise fashion, resulting in a merit order-style supply stack. Each individual supply stack consists of five individual segments. For EU producers, we assume a simplified per-unit cost. As illustrated in Figure D.1 in D, the endogenous realization of a supply drop given

<sup>3</sup> Russia, Norway, LNG, Caspian region, Algeria, Ukraine

the uncertainty budget of  $\Gamma^S = 10$  entails cutting supply from the five supply fields, which results in the worst-case scenario (i.e., the highest possible increase in the system’s operational costs).

5.3.3.3 Investment options: Projects of Common Interest

As indicated above, our analysis focuses on the economic viability of proposed gas infrastructure projects awarded the status of PCI. To qualify as PCI, projects must demonstrate significant improvement in market integration in at least two EU countries, enhance competition in energy markets, and contribute to the energy security [191]. PCI are eligible to receive public funding from the Connecting Europe Facility (CEF), which can cover up to 50% of project-specific investments. The most recent PCI list—the fourth such list, approved at the beginning of 2020—includes 32 gas-related infrastructure projects, most of which focus on enhancing regional infrastructure in Central and Southeastern Europe. According to European Commission [191], the completion of these 32 projects will facilitate a well-interconnected and shock-resilient gas network, providing all EU member states with access to at least three gas supply sources or the global LNG market.

In this analysis, we focus on the cross-border pipelines and regasification projects from the fourth PCI list. The individual projects are incorporated as discrete investment decisions (i.e., they constitute separate connections between the countries under consideration). Thus, the projects spanning multiple countries are split up into their constituent cross-border connections. The investment options comprise 26 pipeline arcs (13 bi-directional cross-border pipeline connections) and four LNG regasification terminals. Data on project-specific investments and the associated capacities of the considered PCI was obtained from various publicly available sources [192–196].

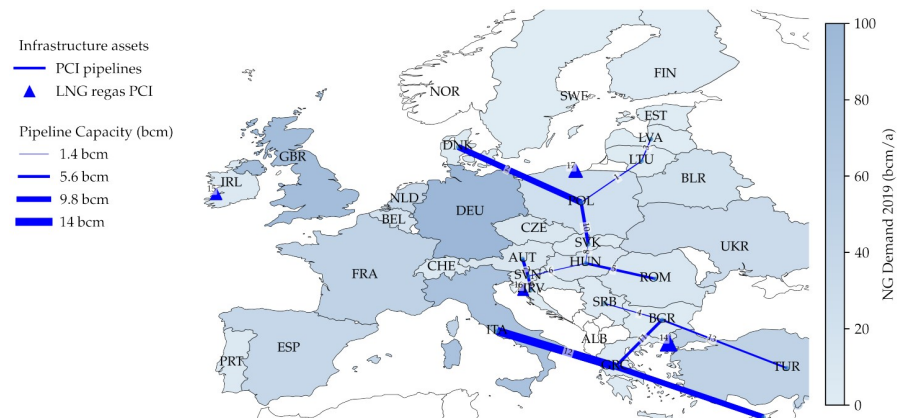


Figure 5.6: PCI included in the analysis: 26 pipelines and four LNG regasification terminals

Authors’ illustration.



The projects included in the analysis are illustrated in Figure 5.6. A table with information relevant to the individual pipeline and regasification terminal projects can be found in Appendix E.

#### 5.3.3.4 *Other input data*

Network data for the model (i.e., existing cross-border pipelines and regasification terminals in Europe) is primarily sourced from the ENTSO-G [197]. For the purposes of this analysis, we assume that the Nord Stream 2 project is completed and at full operational capacity in 2030 and that the terms of the recently negotiated Russia-Ukraine transit deal, in which there is a set minimum capacity obligation of 40 bcm/year through 2024, are extended. The analysis assumes that gas flows from Russia via Ukraine are restricted to this minimum volume [198].

Transmission costs are calculated using linear functions of pipeline length, pipeline type (on-shore/offshore), and transmission cost factor per unit of gas volume and unit of distance. The transmission cost factor is based on the natural gas modeling literature [116, 124]. The production costs of the largest suppliers are modeled based on a piece-wise approximation of the Golombek logarithmic cost function, which stems from Egging and Holz [124] and Riepin and Musgens [119]. For smaller domestic producers, we assume a constant per-unit production cost. Similarly, we model the representative LNG supply cost curve in a piece-wise linear manner to reflect the LNG supply structure for Europe. The constructed LNG cost curves include liquefaction and regasification costs. LNG shipping costs are calculated as a capacity-weighted function of distance between nodes. The supply cost curves for Europe in 2030 are calibrated based on BEIS [199].

Data concerning country-specific storage capacities as well as maximum monthly injection and withdrawal rates are sourced from the Gas Infrastructure Europe [113]. The data are aggregated at the national level (i.e., each country has one representative storage node). Since the optimization problem focuses on a single year, storage levels at the beginning and end of the year are fixed. We do not explicitly consider the demand-side response in our analysis, as data on country-specific potentials are generally unavailable, and the role of demand-side response as a flexibility tool in the European gas market is limited European Commission [115]. Thus, we incorporate an option for gas demand shedding at a penalty cost.

## 5.4 RESULTS AND DISCUSSION

The results section is organized as follows. Section 5.4.1 focuses on the robust expansion plan of European gas infrastructure considering the PCI and the worst-case realizations of cold-winter demand spikes under increasing uncertainty budgets. Afterward, Section 5.4.2 ex-

pands this analysis by assuming that the solution space is not limited to the set of **PCI** and including the option to expand all existing arcs in the EU. Section 5.4.3 evaluates the realization of **PCI** investments when incorporating uncertainty budgets representing both demand spikes and supply shortages. Finally, Section 5.4.4 examines the extent to which the composition of robust investments changes when introducing an investment budget.

It should be noted that the analysis and visualization of each scenario entail some modifications to the model solution space (i.e., the set of possible investment options) and uncertainty budgets ( $\Gamma_D$  and  $\Gamma_S$ ). We explain these modifications at the start of each subsection. Neither the **ARO** model nor the solution algorithm are changed across the considered scenarios.

In all cases, the results are computed in **GAMS**<sup>4</sup> using CPLEX solver on a computer with an Intel Core i7 – 8750 CPU at 2.20 GHz and 16 GB of RAM. The **ARO** model for all of the following scenarios is successfully converged (i.e.,  $UB - LB = 0$ ).

#### 5.4.1 Robust expansion considering cold-winter gas demand spikes

This section investigates how the optimal (in terms of system robustness) investment plan changes with respect to different values of the demand uncertainty budget  $\Gamma_D$ . The analysis is based on the following assumptions:

1. Investment decisions are made from the set of **PCI** (see Appendix E).
2. Uncertainty budget  $\Gamma_D$  is fixed to  $[0, 10, 30, 60]$ . Note that the worst-case realizations of unknown parameters are determined endogenously by the model algorithm. Empirically, a unit of uncertainty budget for demand entails one month of peak demand in a specific node (see Section 5.3.3.2 for further details). As this subsection focuses on gas demand uncertainty, supply uncertainty is not considered, meaning  $\Gamma_S$  is fixed to 0 (i.e., available supply is based on the reference scenario).
3. No limits are enforced on investment budget availability (i.e., constraint C.1c in C is relaxed).

Figure 5.7 presents the results of this analysis. The choropleth maps illustrate gas demand spikes associated with the worst-case demand realization under the uncertainty budget  $\Gamma_D$ . The realized investments are displayed as lines connecting two countries (pipelines) and triangles (regasification terminals). Note that for each scenario, the projects

<sup>4</sup> <https://www.gams.com/>

built represent the optimal expansion plan for the respective uncertainty budget. Above the choropleth maps, summary tables offer a quick comparison of investments across all scenarios.

The bottom row of Figure 5.7 represents an *estimated CAPEX* scenario, which assumes that project investors do not receive financial grants from the EU. This scenario can be viewed as an analysis of whether PCI are beneficial from a societal perspective. The results show that only two projects are built: the HU–SI pipeline ( $\Gamma_D = [0, 10, 30, 60]$ ) and the PL–SK pipeline ( $\Gamma_D = 60$ ). The HU–SI pipeline notably appears in the optimal solution under all uncertainty budgets, indicating the high value of this project to the gas system. According to the European Commission, the connection between the gas markets in SI and HU aims to diversify the gas supply in the region. The pipeline will improve diversification of gas sources (LNG sources from the Adriatic region), which are available in SI and enable access to gas storages in HU for SI users [200]. The PL–SK pipeline aims to create a north–south gas corridor in Eastern Europe and boost gas supply security throughout the region [201]. The model results suggest that the project provides value to the system amid increased demand uncertainty (scenario  $\Gamma_D = 60$  entails demand spikes in Poland).

The top row of Figure 5.7 represents a *subsidized CAPEX* scenario, which assumes that, due to their PCI status, the projects receive financial support from the CEF. This scenario can be viewed as an analysis of whether PCI are profitable from a business perspective (i.e., whether their value exceeds lower, subsidized investment costs). The results are notably different, as the optimal expansion plan includes a minimum of three projects built in  $\Gamma_D = 0$  and as many as eight projects under the uncertainty budget  $\Gamma_D = 80$ . The two projects built across all of the uncertainty budgets are the regasification terminals in Ireland and Croatia. The latter of these two, the KrK LNG terminal in Croatia, is the first LNG project of its kind in the country with an initial capacity of 2.6 bcm/a, which is equivalent to the annual gas demand in Croatia. With increasing uncertainty budget values, seven further projects are realized, resulting in stronger interconnection among the Baltic states (LV–LT), a new physical connection between the Baltic states and Poland (LT–PL), the north–south gas corridor (PL–SK), a regasification terminal in Greece (GR–LNG), greater supply diversification in the Balkan region (BG–SB, GR–BG, HR–SL), and increased access to LNG through terminals in Greece and Croatia.

One interesting observation in the *subsidized CAPEX* scenario is that the optimal expansion plan captures all of the PCI that are in the final realization stage. It should be noted that the LNG terminal in Croatia is operational starting January 2021 and four other projects that are currently under construction (LT–PL, BG–SB, PL–SK, GR–BG) have received significant financial support through grants and low-interest loans (see Appendix E). The results of the ARO model suggest that

real-world construction efforts have been targeted toward the most promising projects from a systems perspective. These projects appear to be well-situated to ensure supply security amid increasing demand uncertainty. Nevertheless, from a societal perspective (i.e., absent of subsidies), the results indicate that the vast majority of PCI are not economically viable under our model assumptions—even when the system is stressed by the ARO algorithm with regard to cold-winter gas demand spikes.

The results demonstrate a general trend toward an increasing number of investments alongside greater system stress (i.e., an increasing demand uncertainty budget). Additional projects are built to hedge against increasing levels of demand uncertainty, either by connecting countries in which demand spikes materialize to other countries or by interconnecting regions to diversify their supply and alleviate system congestion.

#### 5.4.2 *Robust expansion considering cold-winter gas demand spikes and investment options beyond the PCI list*

The expansion options considered in the above section were discrete expansion options limited to the set of PCI. This section evaluates whether the expansion of other existing infrastructure assets would be preferable from a systems perspective to hedge against the worst-case realization of demand across Europe. The analysis incorporates the following assumptions:

1. Investment decisions are made from the union of two sets: (i) PCI and (ii) 20% capacity increase on any arc in the gas infrastructure network (pipelines or regasification terminals) located in the EU.<sup>5</sup>
2. Uncertainty budgets are fixed:  $\Gamma_D = [0, 10, 30, 60]$ ,  $\Gamma_S = 0$ .
3. No limits are enforced on investment budget availability (i.e., constraint C.1c in C is relaxed).

Figure 5.8 illustrates the results. The choropleth maps follow the example of the previous section, illustrating the gas demand realizations and the respective investments under a range of uncertainty budgets.

One notable observation from the *subsidized CAPEX* scenario (top row of Figure 5.8) is that, despite expanding the investment options to more than 100 projects (17 PCI and 92 non-PCI projects), the solution of the ARO model comprises nine projects—the majority of which are

<sup>5</sup> The capacity of new investment options—a total of 92 arcs—is parametrized to a 20% increase in existing infrastructure items; the average capacity is comparable to the average size of the PCI projects. The CAPEX of the new investment options is parametrized based on the 75th percentile of the PCI' investment per bcm of capacity. The factors per bcm applied are computed separately for pipelines and LNG projects.

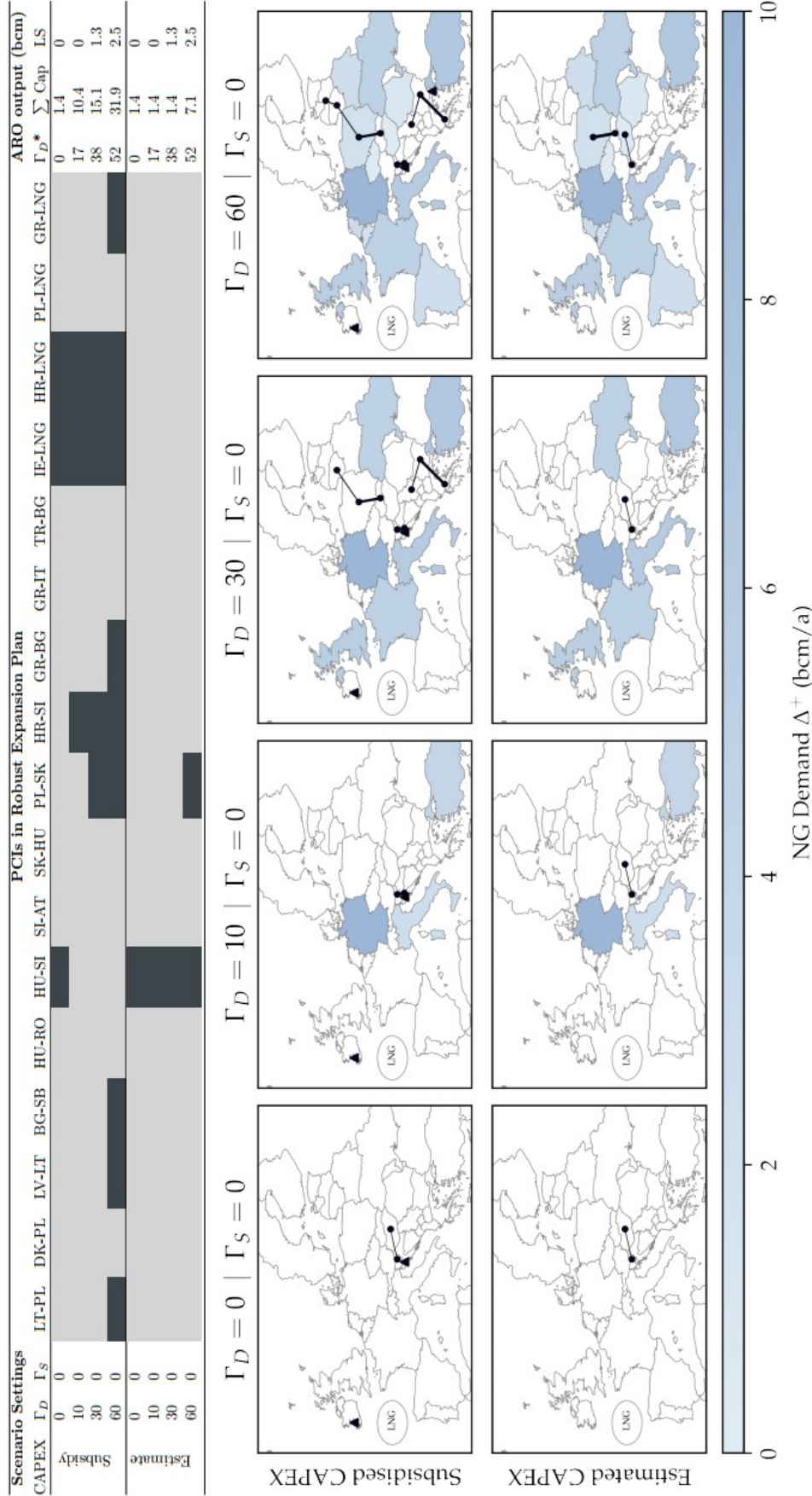


Figure 5.7: Robust expansion plan considering a set of PCIs under four uncertainty budgets for gas demand (columns). The horizontal axis aggregates demand spike values per country on an annual basis. Scenarios include two CAPEX assumptions (rows)

PCI. Hence, our modeling exercise confirms the estimates of national TSOs on gas flows under the system stress and the promising projects from to address that stress. This result suggests that, despite the high degree of interconnectivity in the European gas network, certain PCI are promising from a business perspective (i.e., in a presence of subsidy) in the face of the worst-case demand realization.

The new non-PCI projects that are realized as a part of the optimal expansion plan include one pipeline (UA–PL) and two regasification terminals in Belgium and France.

Interestingly, even though the UA–PL pipeline is not listed on the PCI list, the interconnector is highly likely to assume operations by the end of 2022, as the Ukrainian and Polish TSOs signed an agreement in 2016 to advance the construction of the project [202]. The project was conferred a code in the TYNDP 2020<sup>6</sup>. Although a relatively small addition in terms of transmission capacity, expansion of the pipeline would facilitate the further integration of Ukrainian storage facilities into the European gas system. The project is solely realized under a relatively large uncertainty budget of  $\Gamma_D = 60$ , which indicates the potential flexibility that it would provide the system amid widespread cold-winter demand peaks.<sup>7</sup>

Another observation that stands out in Figure 5.8 is the partial substitution of PCI by non-PCI projects. In particular, the two new LNG terminals reroute flows to Central Europe, compromising the economic viability of the LNG terminal in Greece and the two PCI pipelines previously built to bring gas north from the Adriatic region (the GR–BG and BG–SB pipe-lines are not built in this scenario). This result can be understood in the context of the system-wide optimization that the model entails.

The results are markedly different in the *estimated CAPEX* scenario (bottom row of Figure 5.8). As with the results in Section 5.4.1, the HU–SI pipeline appears in the optimal solution under all uncertainty budgets. However, the other two projects built under high uncertainty budgets (UA–PL and FR–LNG) are not from the PCI set. It is unsurprising to see the UA–PL pipeline appearing in the model solution in this scenario, as, in reality, the project is also completed without the subsidy. Overall, these results reflect the importance of efficient trade and storage utilization in a system as complex as the European gas market.

The results of this section provide further insight into robust gas infrastructure expansion under uncertainty budgets. The insights (i) confirm that, without financial support, most of the PCI are unlikely

6 In the TYNDP 2020, the project is listed under the code “TRA-A-621” for the Polish section and the code “TRA-A-561” for the Ukrainian section [197]

7 The integration of Ukrainian storage facilities into the European gas system brings further benefits not explicitly captured by our model (e.g., allowing vast Ukrainian storage capacity to be used by Polish companies that face strategic storage obligations).

to be realized; (ii) point toward the system benefits of the HU–SI and UA–PL pipelines; and (iii) indicate that, in a subsidized setting, PCI provide more system value in guarding against demand uncertainty than the infrastructure expansion options beyond the PCI list; this finding aligns with the strategic aims of the project list. The observation made in Section 5.4.1 that the ARO solution entails more investments under higher  $\Gamma_D$  values holds for this case as well.

#### 5.4.3 Robust expansion considering cold-winter demand spikes and supply shortages

Moving beyond an isolated analysis of 2030 demand uncertainty, this section investigates the optimal robust expansion plan considering the worst-case realizations of both gas demand and supply within the uncertainty budgets. The analysis is based on the following assumptions:

1. Investment decisions are made from the set of PCI projects.
2. Uncertainty budgets are fixed as follows:  $\Gamma_D = [0, 10, 30, 60]$ ,  $\Gamma_S = [1, 2]$ .<sup>8</sup> Empirically, a unit of the uncertainty budget entails a shortage in one production field in a specific node over the entire modeled year (see Section 5.3.3.2 for further details).
3. Investment costs are based on the subsidized CAPEX scenario.
4. No limits are enforced on investment budget availability (i.e., constraint C.1c in C is relaxed).

The results of this analysis are reported in Figure 5.9. The choropleth maps now illustrate the worst-case realizations of both demand and supply under the uncertainty budgets. As with the results in the previous sections, the  $\Gamma_D$  steps are visualized as columns, while the  $\Gamma_S$  steps form two rows for each CAPEX scenario.

Figure 5.9 demonstrates several interesting features of the robust solution.

First, the supply uncertainty budget of  $\Gamma_S = 1$  eliminates some projects from the solution space. These include pipelines in the Baltic states and Central Europe (LT–PL, LV–LT, PL–SK). The projects aimed at facilitating supply diversification in the Balkan region as well as two regasification terminals in Ireland and Croatia remain a part of the optimal expansion plan. Furthermore, this scenario includes (i) one additional investment (LNG terminal in Greece), which brings greater regasification capacity to the Adriatic region, and (ii) the construction of the GR–BG pipeline, which supports the GR–LNG terminal. As the resulting worst-case supply realization under  $\Gamma_S = [1]$  constitutes a supply drop of ca. 50 bcm/a from Russia, this solution is aimed at a cost-optimal substitution of the missing supply.

<sup>8</sup> A model run with  $\Gamma_S = [0]$  is discussed in Section 5.4.1.

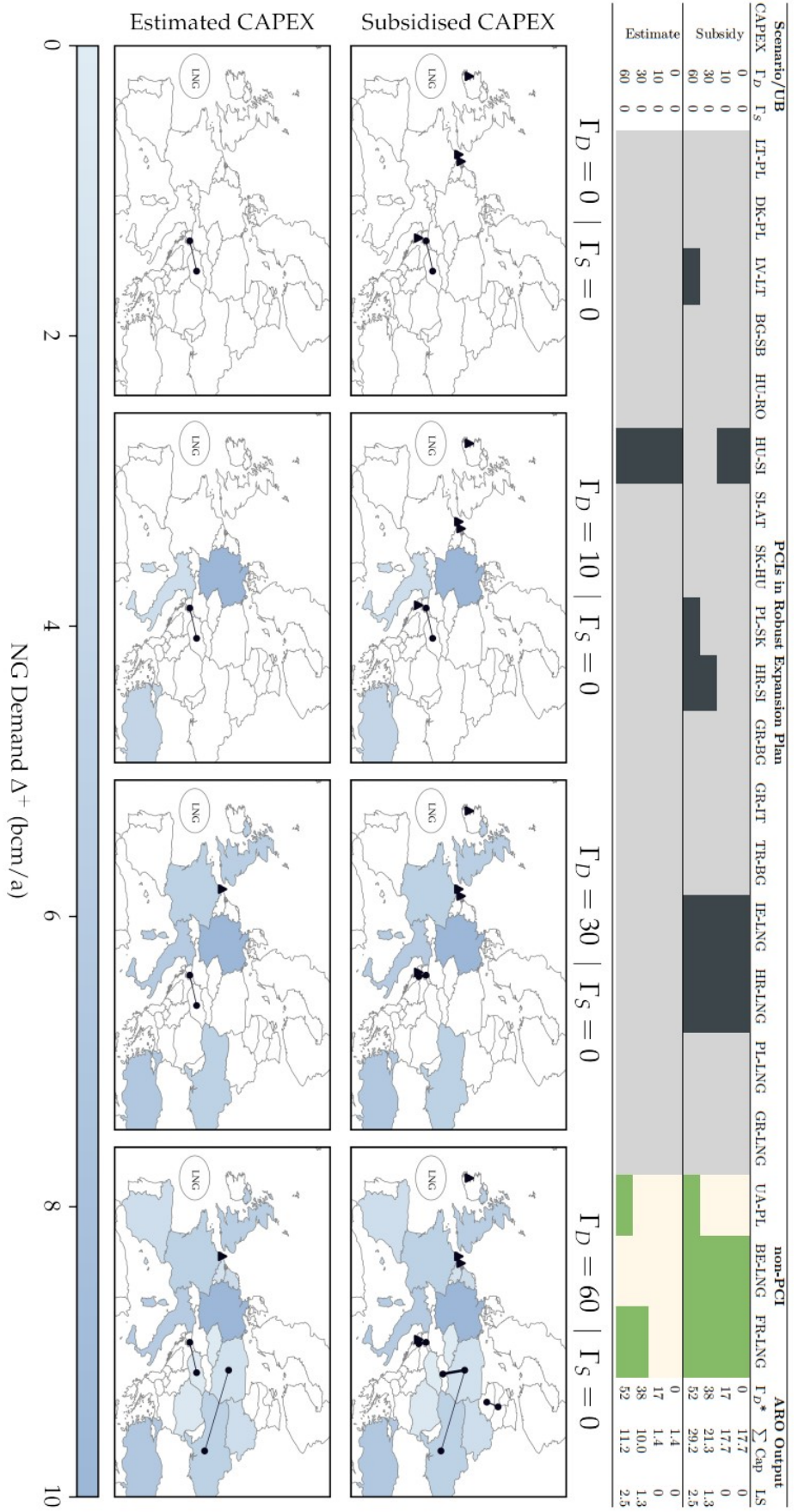


Figure 5.8: Robust expansion plan considering a set of PCIs and a 20% capacity increase option for any arc in the network (pipeline or regasification terminal) located in the EU. Scenarios include four uncertainty budgets for gas demand (columns) and two CAPEX assumptions (rows). The horizontal axis aggregates demand spike values per country on an annual basis



Second, the supply uncertainty budget of  $\Gamma_S = 2$  yields a situation in which an additional 45 bcm/a of LNG supply is unavailable. This further decreases the number of realized projects. As expected, new regasification projects are not viable in this scenario due to a shortage of available LNG supply. This has a reverberating effect, as the projects aimed at bringing gas north by connecting the Adriatic region with Central Europe (GR–BG, HR–SI, BG–SB) do not appear in the robust solution. The sole realized project is the HU–SL interconnector. This can be explained by its central location and the importance of access to gas storage in Hungary for consumers in Slovenia and neighboring countries.

Third, the results of this section highlight the general trend of investment dynamics when supply drops are incorporated into the uncertainty budget—the ARO solution generally entails fewer investments. This outcome stems from the fact that investment decisions associated with the robust solution under supply uncertainty entail interplay between capital costs, load-shedding costs, and network topology. The results demonstrate that additional LNG projects may be viable to hedge against pipeline supply shortages (e.g., GR–LNG, supply drops in Russia); however, if the supply of both Russian pipeline gas and LNG fall into the uncertainty budget, the economic viability of projects is compromised due to the system’s overall supply shortage. This is indicated by load-shedding volumes of ca. 65 bcm/a.

#### 5.4.4 Robust expansion considering an investment budget

This section evaluates how budget availability can influence the composition of investment decisions in the robust solution. The analysis is conducted with the following assumptions:

1. Investment decisions are made from the set of PCI projects.
2. Uncertainty budgets are fixed as follows:  $\Gamma_D = 60$ ,  $\Gamma_S = 0$ .
3. Investment costs are based on the subsidized CAPEX scenario.
4. An annualized investment budget has an upper limit that takes values of 20, 40, and 60 MEUR (i.e., constraint C.1c in C is binding).

The robust solution considering assumptions 1 and 2 and neglecting a budget constraint is detailed in Section 5.4.1. The model configuration yields the results reported in Figure 5.7 (row with  $\Gamma_D = 60$ ). The composition of investments obtained in the model configuration entails an annualized investment of 62.8 MEUR. Using this value as a reference, we construct a set of sensitivity cases in which the annualized investment budget is assumed to be 20, 40, and 60 MEUR.

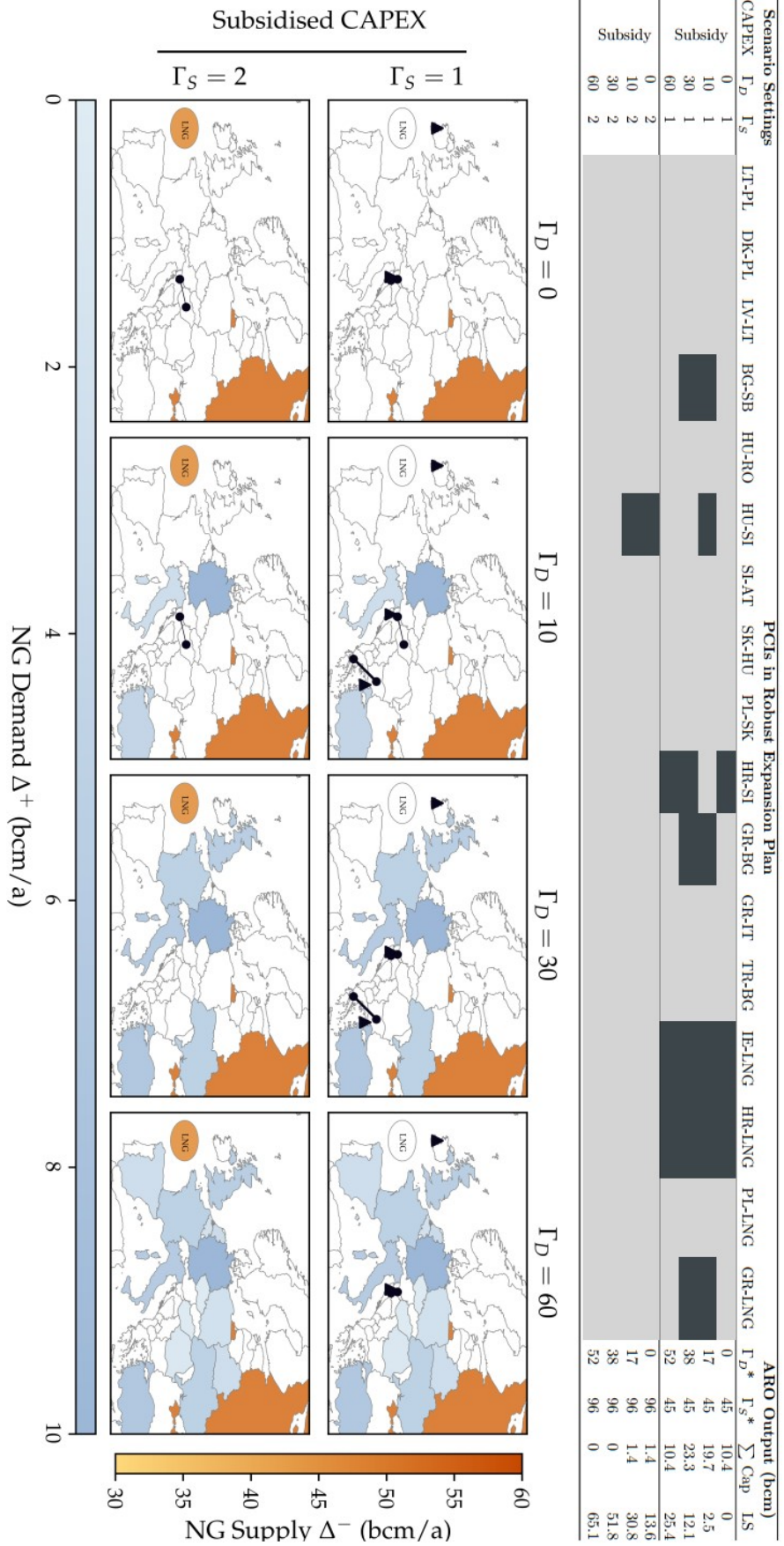


Figure 5.9: Robust expansion plan considering a set of PCIs under different uncertainty budgets for gas demand (columns) and supply (rows). Horizontal axis aggregates demand spike values on an annual basis per country. Vertical axis presents annual supply cut per country

Figure 5.10 illustrates the optimal investments for each budget scenario. Note the new columns with solution information relevant to this section.  $IB^*$  reports the cost of an annualized investment budget in MEUR per scenario. Each value is less than the budget limit set by the constraint due to the discrete nature of the investment decisions.  $\Delta IC$  reports the difference between the most expensive investment mix (with no constraint imposed on  $IB$ ) and the optimal solution in each scenario.  $\Delta TC$  reports the difference between the total cost (objective value of the subproblem) of each scenario and the total cost of the solution absent the investment budget. The optimization framework of the ARO model ensures that (a)  $\Delta TC \geq \Delta IC$  (i.e., investment decisions must have a positive (or no) impact on the objective value and that (b) the model setup void of an investment budget yields, by definition, the lowest objective value.

In the absence of an investment budget (the reference case, row  $IB = inf$  in Figure 5.10), the ARO model prefers nine PCI, among them three regasification terminals and six pipelines. When adding a budget restriction, the ARO model reduces the number of investments to avoid violating the budget.

With a budget of 20 MEUR, four projects are realized: LT–PL to establish a physical connection between the Baltic states and Poland; LV–LT to strengthen interconnection among the Baltic states; and HR–LNG and HR–SI to provide the Balkan region with access to LNG. This result aligns well with the current project status of the PCI, as the four projects built in the robust solution are either already operational or in the final stage of development. With a budget of 40 MEUR, a regasification terminal in Ireland is added to the investment mix. Increasing the budget to 60 MEUR adds a regasification terminal in Greece as well as two pipeline projects, GR–BG and BG–SB, which connect the Greek regasification terminal to the Balkan region. Eliminating the budget yields a single additional project—the PL–SK pipeline.

Figure 5.10 depicts how decreasing the investment budget results in a gradual increase in total costs. The behavior takes place due to an incremental increase in the operational costs. Under the model optimization framework, the investment decision is based on the equality of the investment costs and the benefits (i.e., a decrease in operational costs) of using the new infrastructure item. For this reason, no other PCI is realized despite the unlimited investment budget—an increase in the annual investment payment  $\Delta IC$  would not compensate for the decrease in the total costs.

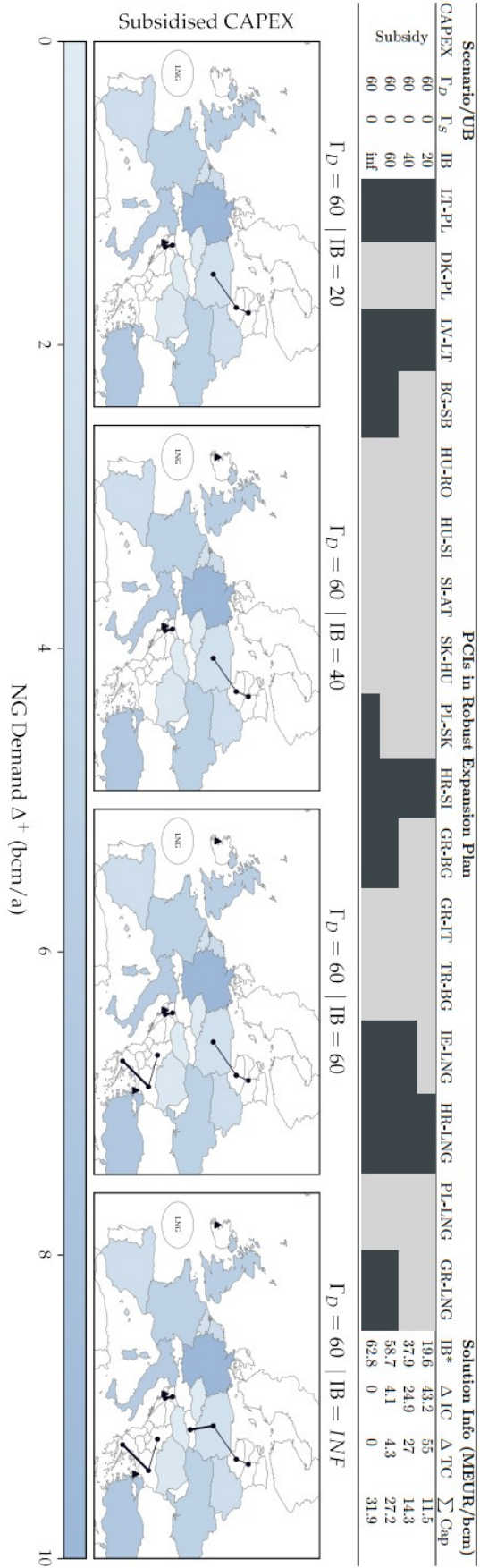


Figure 5.10: Robust expansion plan considering a set of PCIs subject to investment budgets. Scenarios entail four annualized budgets (columns)

## 5.5 SUMMARY AND OUTLOOK

The European natural gas market is subject to evolving market conditions and energy and climate policy dynamics that intensify uncertainty regarding the long-term projections of both demand and supply. This paper addresses this matter by suggesting an adaptive robust optimization framework for gas infrastructure expansion planning under these uncertainties. In particular, we analyze the value of Projects of Common Interests—gas infrastructure projects supported by EU public funds—in ensuring supply security in 2030. Methodologically, our analysis contributes to the literature by demonstrating the first application of adaptive robust optimization for gas infrastructure expansion planning considering long-term uncertainties.

In terms of demand uncertainty, we draw the conclusion that increasing levels of uncertainty, represented by the increasing value of uncertainty budgets, lead to additional investments. These investments aim to hedge against demand uncertainty, either by interconnecting regions to diversify their supply and alleviate system congestion or by connecting countries in which cold-winter demand spikes materialize to neighboring countries with large storage facilities (e.g., PL-UA pipeline).

There is a clear distinction in the incidence of project realization between scenarios with subsidized CAPEX and scenarios with estimated CAPEX. Without a substantial level of financial support, only a small subset of proposed projects are built. This finding coincides with recent analysis suggesting the superfluous nature of the projects proposed in the fourth Projects of Common Interest list [151].

The results of the scenario run considering a possibility of expanding the capacity of existing transmission infrastructure assets reveal that the subsidized investments in the Projects of Common Interest remain predominantly represented in the robust solution. These investments are complemented by the expansion of LNG infrastructure in Northwest Europe and by construction of UA–PL pipeline that enables the use of large Ukrainian storage facilities when hedging against demand spikes in Central Europe. The HU–SI and UA–PL pipelines are built even in a non-subsidized setting, which highlights the system benefits of these projects. Overall, these results reflect the importance of efficient trade and storage utilization in a system as complex as the European gas market.

An interesting observation is that introducing an investment budget result in the prioritization of a particular set of Projects of Common Interest—those that are either already operational or in the final stage of development. This result suggest that real-world construction efforts have been targeted toward the most promising projects from a systems perspective.

When supply drops are incorporated into the model, the general trend of investment dynamics is that the robust solution entails fewer investments with increasing supply uncertainty budget. This observation stems from the fact that investment decisions entail interplay between capital costs, load-shedding costs, and network topology. Specifically, the robust expansion plan utilizes the group of projects associated with facilitating access to Adriatic LNG supplies to hedge against supply drop from Russia. However, increasing the value of the uncertainty budget further, both Russian pipeline gas and LNG fall into the uncertainty budget. In this case, the economic viability of LNG projects is compromised due to the system overall supply shortage.

Our analysis contributes to the extant research on modeling uncertainty in the European gas market. In terms of methodology, our work can serve as the foundation for future research aimed at quantifying the value of gas infrastructure projects. However, our analysis must be considered in the proper context. Due to the scope of our analysis and the complexity of adaptive robust optimization, the employed linear model fails to incorporate demand elasticity and neglects strategic behaviors in gas markets. Furthermore, the aggregated nature of the transport model abstracts from physical gas flows and the associated non-linearities. The model application also entails certain simplifications (e.g., designating a central European LNG supplier instead of explicitly modeling gas liquefaction and regasification terminals).

Several questions remain for further research. In particular, demand uncertainty sets can be configured to incorporate regional correlation regarding cold-winter peaks. In our analysis, the worst-case demand realizations were assessed at the system level. Given that the impacts of extreme cold are likely to manifest regionally, uncertainty sets can be formulated to reflect spatial correlations. Future investigations could focus on storage assets from the Projects of Common Interests list, which were not within the scope of our analysis. Furthermore, it would be interesting to see research that, while inspired by our methodology, focuses on the markets for other products (e.g., hydrogen).

**DATA & CODE AVAILABILITY:** Datasets related to this article and a source code for the entire project are available in the public GitHub repository: <https://github.com/Irieo/ARO-GasInfrastructure>. The code reproduces the results presented in the paper.

**CREDIT AUTHORSHIP CONTRIBUTION STATEMENT** **Igor Riepin:** Conceptualization, Methodology, Software, Validation, Investigation, Writing - Original Draft, Project administration. **Matthew Schmidt:** Conceptualization, Data Curation, Validation, Visualization, Investigation, Writing - Original Draft. **Luis Baringo:** Methodology, Validation, Writing - Review & Editing. **Felix Müsgens:** Validation, Writing - Review & Editing, Supervision.

Part III

APPENDIX

# A

## LOGARITHMIC PRODUCTION COST FUNCTIONS

Production costs, as proposed by Golombek, Gjelsvik, and Rosendahl [203] and elaborated by Huppmann [204], are determined by a logarithmic function related to capacity utilization. The increasing marginal cost function can be expressed as follows:

$$TPC'(q) = \alpha + \beta \cdot q + \gamma \cdot \ln\left(1 - \frac{q}{Cap}\right) \quad (\text{A.1a})$$

$$\alpha, \beta \geq 0, \gamma \leq 0, q < Cap \quad (\text{A.1b})$$

In equation A.1,  $q$  is production quantity,  $Cap$  is available production capacity,  $\alpha$  is the minimum marginal unit cost term,  $\beta$  is the per-unit linearly increasing cost term, and  $\gamma$  is a logarithmic term. Note that marginal production costs increase sharply when production nears full capacity. The logarithmic term ensures that if capacity is expanded, marginal production costs for the same quantity of gas decrease (and vice versa). Fig. A.1 illustrates this approach for two selected nodes: Russia and the Netherlands.

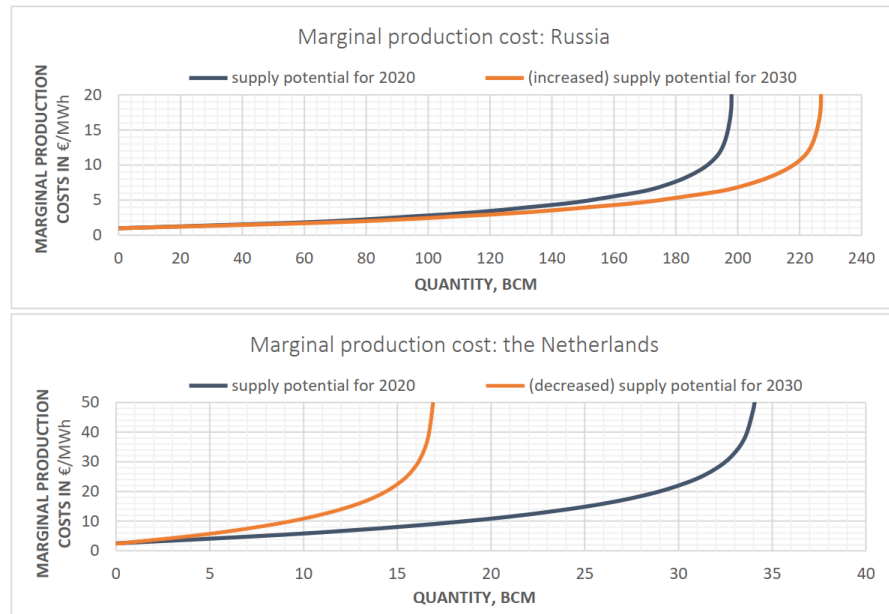


Figure A.1: Marginal production cost functions for two selected nodes

In order to keep the model formulation linear, we use piecewise approximations to logarithmic cost functions. Thus, we obtain a merit-order type of linear production costs function for each node.



## GEOGRAPHICAL COVERAGE OF THE GAS MARKET MODEL

---

Node names, compound regions, and individual countries.

---

### Countries in the EU<sup>a</sup>

Austria (AT)	Italy (IT)
Belgium (BE)	Netherlands (NL)
Czech Republic (CZ)	Poland (PL)
Denmark (DK)	Romania (RO)
France (FR)	Slovakia (SK)
Germany (DE)	Sweden (SE)
Hungary (HU)	

### Regions in the EU

Balkan node	Bulgaria (BG)
	Greece (EL)
	Croatia (HR)
	Slovenia (SI)
	Serbia <sup>b</sup> (RS)
Baltic node	Estonia (EE)
	Latvia (LV)
	Lithuania (LT)
Iberian node	Spain (ES)
	Portugal (PT)

### Major gas suppliers to the EU

Algeria (DZ)	Qatar (QA)
Libya (LY)	Russia (RU)
Nigeria (NG)	United States (US)
Norway (NO)	

---

<sup>a</sup>The EU members that are not represented in the model are Cyprus, Finland, Luxembourg, and Malta.

<sup>b</sup>As of May 2020, Serbia is not a member of the EU; however, the country is included in the model as a part of the Balkan node.

# C

## DETAILED FORMULATION OF MODEL APPLICATION

This Appendix provides the detailed formulation of the transmission expansion planning problem for the European natural gas market.

### Nomenclature (1/3)

Element	Description
<b>Indices</b>	
$d$	Demands
$p$	Producers
$l$	Arcs (pipeline and LNG routes)
$n$	Nodes
$s$	Storages
$t$	Time steps (months)
<b>Sets</b>	
$\Psi_n^D$	Demands located at node $n$
$\Psi_n^P$	Producers located at node $n$
$\Psi^T$	Time steps in modelling horizon
$\Psi^{l+}$	Prospective transmission infrastructure assets (PCI)
$\Psi^l$	Existing transmission infrastructure assets
$r(l)/s(l)$	Receiving/sending-end node of the $l$ th arc
<b>Scalars</b>	
$M$	Large scalar value
<b>Parameters</b>	
$C_d^{LS}$	Load-shedding cost of demand $d$ [€/kcm]
$C_p^P$	Production cost of producer $p$ [€/kcm]
$C_l^L$	Transport costs across of the $l$ th arc [€/kcm]
$C_l^{IC}$	Annualized cost of of the $l$ th arc [€]
$\bar{C}^I$	Annualized investment budget [€]

Nomenclature (2/3)

Element	Description
<b>Parameters</b>	
$\tilde{G}_{dt}^D$	Reference level of demand $d$ [bcm/m]
$\tilde{G}_p^P$	Reference capacity of producer $p$ [bcm/a]
$\hat{G}_{dt}^D$	Max deviation from level of reference demand $d$ [bcm/m]
$\hat{G}_p^P$	Max deviation from reference capacity of producer $p$ [bcm/m]
$\bar{G}_d^{SI} / \bar{G}_d^{SW}$	Injection/withdrawal capacity of storage mapped to demand $d$ [bcm/m]
$\underline{G}_{dt}^S / \bar{G}_{dt}^S$	Lower/upper bound on working gas volume of storage mapped to demand $d$ [bcm]
$\eta_d^{SI} / \eta_d^{SW}$	Injection/withdrawal efficiency of storage mapped to demand $d$ [%]
$E_d^{S0}$	Storage level at the first period of modelling horizon [bcm]
$\Gamma^D$	Uncertainty budget for demand
$\Gamma^P$	Uncertainty budget for supply
<b>Primal Variables</b>	
$g_{dt}^{LS}$	Load shed by demand $d$ [bcm/m]
$g_{pt}^P$	Production by producer $p$ [bcm/m]
$g_{lt}^L$	Gas transport across $l$ th arc [bcm/m]
$\bar{g}_{dt}^D$	Uncertain level of demand $d$ [bcm/m]
$\bar{g}_{pt}^P$	Uncertain capacity of producer $p$ [bcm/m]
$wg_{dt}^S$	Working gas volume of storage mapped to demand $d$ [bcm]
$g_{dt}^{SI}$	Gas injection in storage mapped to demand $d$ [bcm/m]
$g_{dt}^{SW}$	Gas withdrawal from storage mapped to demand $d$ [bcm/m]
<b>Dual Variables</b>	
(·)	Dual variables are provided after the corresponding equalities or inequalities separated by a colon

## Nomenclature (3/3)

Element	Description
<b>Binary Variables</b>	
$x_l^L$	Binary investment decision in prospective transmission asset $l$
$z_{dt}^D$	Binary variable representing deviation from reference monthly demand level $\tilde{G}_{dt}^D$
$z_p^P$	Binary variable representing deviation from reference annual supply level $\tilde{G}_p^P$
<b>Auxiliary Variables</b>	
$\tilde{\lambda}_{nt}$	Auxiliary variable to linearize $z_{d(n)t}^D \cdot \lambda_{nt}$
$\tilde{\phi}_{pt}^P$	Auxiliary variable to linearize $z_p^P \cdot \bar{\phi}_{pt}^P$

## C.1 DETERMINISTIC MODEL

The transmission expansion planning model for the European natural gas market can be formulated as the following deterministic MILP:

$$\begin{aligned} \min_{\Phi^D} \quad & \sum_{l \in \Psi^{L+}} x_l^L \cdot C_l^{IC} + \\ & \left( \sum_{pt} g_{pt}^P \cdot C_p^P + \sum_{lt} g_{lt}^L \cdot C_l^L + \sum_{dt} g_{dt}^{LS} \cdot C_d^{LS} \right) \end{aligned} \quad (\text{C.1a})$$

subject to

$$x_l^L = \{0, 1\} \quad \forall l \in \Psi^{L+} \quad (\text{C.1b})$$

$$\sum_{l \in \Psi^{L+}} x_l^L C_l^{IC} \leq \bar{C}^I \quad (\text{C.1c})$$

$$\begin{aligned} \sum_{p \in \Psi_n^P} g_{pt}^P + \sum_{d \in \Psi_n^D} (g_{dt}^{SW} - g_{dt}^{SI}) - \sum_{l|s(l)=n} g_{lt}^L + \sum_{l|r(l)=n} g_{lt}^L = \\ \sum_{d \in \Psi_n^D} (\tilde{G}_{dt}^D - g_{dt}^{LS}) : \lambda_{nt} \quad \forall n, \forall t \end{aligned} \quad (\text{C.1d})$$

$$0 \leq g_{lt}^L \leq \bar{G}_{lt}^L : \bar{\phi}_{lt}^L \quad \forall l, \forall t \quad (\text{C.1e})$$

$$0 \leq g_{pt}^P \leq \frac{\tilde{G}_p^P}{|\Psi^T|} : \bar{\phi}_{pt}^P \quad \forall p, \forall t \quad (\text{C.1f})$$

$$0 \leq g_{dt}^{LS} \leq \tilde{G}_{dt}^D : \bar{\phi}_{dt}^D \quad \forall d, \forall t \quad (\text{C.1g})$$

$$0 \leq g_{dt}^{SI} \leq \bar{G}_d^{SI} : \bar{\phi}_{dt}^{SI} \quad \forall d, \forall t \quad (\text{C.1h})$$

$$0 \leq g_{dt}^{SW} \leq \bar{G}_d^{SW} : \bar{\phi}_{dt}^{SW} \quad \forall d, \forall t \quad (\text{C.1i})$$

$$wg_{dt}^S = wg_{d,t-1}^S + g_{dt}^{SI} \eta_d^{SI} - \frac{g_{dt}^{SW}}{\eta_d^{SW}} : \mu_{d,t}^S \quad \forall d, \forall t \in \Psi^T \setminus \{t1\} \quad (\text{C.1j})$$

$$wg_{d(t1)}^S = E_d^{S0} + g_{d(t1)}^{SI} \eta_d^{SI} - \frac{g_{d(t1)}^{SW}}{\eta_d^{SW}} : \mu_{d(t1)}^S \quad \forall d, \{t1\} \quad (\text{C.1k})$$

$$\underline{G}_{dt}^S \leq wg_{dt}^S \leq \overline{G}_{dt}^S : \underline{\phi}_{dt}^S, \overline{\phi}_{dt}^S \quad \forall d, \forall t \quad (\text{C.1l})$$

where variables in set  $\Phi^D = \{x_l^L; g_{pt}^P; g_d^{LS}; g_{lt}^L; wg_{dt}^S; g_{dt}^{SW}; g_{dt}^{SI}\}$  denote the optimization variables of the deterministic optimization problem. The deterministic optimization problem (C.1) assumes perfect (and optimistic) foresight regarding realizations of natural gas demand and supply levels— $\tilde{G}_{dt}^D$  and  $\tilde{G}_p^P$ , respectively.

The objective function (C.1a) consists of two distinct parts. The first part constitutes investments in infrastructure assets, including pipelines and LNG terminals. Binary variable ( $x_l^L$ ) represents a discrete investment option of each asset. The second part of the objective function entails the operational costs for existing infrastructure, including production, transportation, and storage costs.

The objective function also includes associated costs for unserved demand. The objective function is subject to a range of constraints. The first such constraint is energy balance (C.1d), which entails the market-clearing condition (i.e., the gas flows entering and exiting a node must balance out). Supply constraints (C.1f) confine the monthly supply volumes of natural gas in each production node. The transmission constraint (C.1e) limits the monthly volume of natural gas transported via pipelines or LNG arcs. Finally, storage constraints (C.1i - C.1l) limit storage operation and define working gas volume in storage facilities across the time horizon of the model.

## C.2 ADAPTIVE ROBUST OPTIMIZATION MODEL

As noted above, the adaptive robust optimization problem takes the form of the following *min-max-min* problem:

$$\begin{aligned} & \min_{\Phi^1} \sum_{l \in \Psi^{L+}} x_l^L \cdot C_l^{IC} \\ & + \max_{\Phi^2 \in \Omega} \min_{\Phi^3 \in \Xi(\cdot)} \\ & \left[ \sum_t \left( \sum_p g_{pt}^P \cdot C_p^P + \sum_l g_{lt}^L \cdot C_l^L + \sum_d g_{dt}^{LS} \cdot C_d^{LS} \right) \right] \end{aligned} \quad (\text{C.2a})$$

subject to

$$\text{Constraints (C.1b) - (C.1c)} \quad (\text{C.2b})$$

where variables in sets  $\Phi^1 = \{x_l^L, \forall l \in \Psi^{L+}\}$ ,  $\Phi^2 = \{\bar{g}_{dt}^D, \bar{g}_{pt}^P\}$ , and  $\Phi^3 = \{g_{pt}^P, g_d^{LS}, g_{lt}^L, w g_{dt}^S, g_{dt}^{SW}, g_{dt}^{SI}\}$  denote the optimization variables of the first, second, and third level optimizations problems, respectively. The three-tiered formulation incorporates the following nested optimization problems:

1. The first level involves the determination of cost-optimal expansion decisions (i.e., the variables in set  $\Phi^1$  that correspond to investments in pipelines and LNG infrastructure).
2. The second level corresponds to unfortunate realizations of uncertainty variables represented by uncertainty sets (i.e., variables in set  $\Phi^2$ ).
3. The third level consists of corrective dispatch decisions, made in response to perturbations elicited by the first- and second-level decisions, that ensure a feasible solution (i.e., variables in set  $\Phi^3$  that correspond to the production, transportation, and storage of natural gas as well as, if necessary, the shedding of demand).

In problem (C.2),  $\Omega$  and  $\Xi$  represent the uncertainty and feasibility sets, respectively.

### C.3 UNCERTAINTY SETS

As explained in section 5.3.1.2, uncertainty in the demand and supply of natural gas is expressed by constructing confidence bounds around the respective decision variables. This is implemented in the model using the following cardinality-constrained uncertainty set formulation [174]:

$$\Omega = \left\{ \bar{g}_{dt}^D = \tilde{G}_{dt}^D + z_{dt}^D \cdot \hat{G}_{dt}^D \quad \forall d, \forall t \right. \quad (\text{C.3a})$$

$$\bar{g}_p^P = \tilde{G}_p^P - z_p^P \cdot \hat{G}_p^P \quad \forall p \quad (\text{C.3b})$$

$$\sum_{d \in D, t \in T} z_{dt}^D \leq \Gamma^D \quad (\text{C.3c})$$

$$\sum_{p \in P} z_p^P \leq \Gamma^P \quad (\text{C.3d})$$

$$z_{dt}^D \in \{0, 1\} \quad \forall d, \forall t \quad (\text{C.3e})$$

$$z_p^P \in \{0, 1\} \quad \forall p \quad (\text{C.3f})$$

### C.4 FEASIBILITY SETS

Given the first- and second-level decision variables, the set  $\Xi$  models the feasible space of third-level optimization problem:

$$\Xi(g_{pt}^P, g_d^{LS}, g_{lt}^L, w g_{st}^S, g_{st}^{SW}, g_{st}^{SI}) =$$

$$\{\Phi^3 : \sum_{p \in \Psi_n^P} g_{pt}^P + \sum_{d \in \Psi_n^D} (g_{dt}^{SW} - g_{dt}^{SI}) - \sum_{l|s(l)=n} g_{lt}^L + \sum_{l|r(l)=n} g_{lt}^L = \sum_{d \in \Psi_n^D} (\bar{g}_{dt}^D - g_{dt}^{LS}) : \lambda_{nt} \quad \forall n, \forall t \tag{C.4a}$$

$$0 \leq g_{lt}^L \leq \bar{G}_{lt}^L : \bar{\phi}_{lt}^L \quad \forall l, \forall t \tag{C.4b}$$

$$0 \leq g_{pt}^P \leq \bar{g}_{pt}^P : \bar{\phi}_{pt}^P \quad \forall p, \forall t \tag{C.4c}$$

$$0 \leq g_{dt}^{LS} \leq \tilde{G}_{dt}^D : \bar{\phi}_{dt}^D \quad \forall d, \forall t \tag{C.4d}$$

$$0 \leq g_{dt}^{SI} \leq \bar{G}_d^{SI} : \bar{\phi}_{st}^{SI} \quad \forall d, \forall t \tag{C.4e}$$

$$0 \leq g_{dt}^{SW} \leq \bar{G}_d^{SW} : \bar{\phi}_{st}^{SW} \quad \forall d, \forall t \tag{C.4f}$$

$$wg_{dt}^S = wg_{d,t-1}^S + g_{dt}^{SI} \eta_d^{SI} - \frac{g_{dt}^{SW}}{\eta_d^{SW}} : \mu_{d,t}^S \quad \forall d, \forall t \in \Psi^T \setminus \{t1\} \tag{C.4g}$$

$$wg_{d(t1)}^S = E_d^{S0} + g_{d(t1)}^{SI} \eta_d^{SI} - \frac{g_{d(t1)}^{SW}}{\eta_d^{SW}} : \mu_{d(t1)}^S \quad \forall d, \{t1\} \tag{C.4h}$$

$$\underline{G}_{dt}^S \leq wg_{dt}^S \leq \bar{G}_{dt}^S : \phi_{dt}^S \quad \forall d, \forall t \tag{C.4i}$$

$$\}$$

The associated dual variables for the respective constraints are provided after the colon in each equation.

## C.5 SOLUTION PROCEDURE

We use the column-and-constraint generation algorithm detailed in section 5.3.2 to iteratively solve the master and subproblem of the ARO model. A formulation of the master and subproblem in the explicit form is described in the following.

### c.5.1 Master problem

The master problem at iteration  $v$  is as follows:

$$\min_{\Phi^M} \sum_{l \in \Psi^{L+}} x_l^L \cdot C_l^{LC} + \theta \tag{C.5a}$$

subject to

Constraints (C.1b) - (C.1c)

$$\theta \geq \left[ \sum_t \left( \sum_p g_{ptv'}^P \cdot C_p^P + \sum_l g_{ltv'}^L \cdot C_l^L + \sum_d g_{dvtv'}^{LS} \cdot C_d^{LS} \right) \right] \quad \forall v' \leq v \tag{C.5b}$$

$$\begin{aligned} \sum_{p \in \Psi_n^P} g_{ptv'}^P + \sum_{d \in \Psi_n^D} (g_{dt}^{SW} - g_{dt}^{SI}) - \sum_{l|s(l)=n} g_{ltv'}^L + \sum_{l|r(l)=n} g_{ltv'}^L = \\ \sum_{d \in \Psi_n^D} (\bar{g}_{dt}^{D(v')} - g_{dtv'}^{LS}) \quad \forall n, \forall t, \forall v' \leq v \end{aligned} \quad (\text{C.5c})$$

$$0 \leq g_{ltv'}^L \leq \bar{G}_{lt}^L \quad \forall l, \forall t, \forall v' \leq v \quad (\text{C.5d})$$

$$0 \leq g_{ptv'}^P \leq \frac{\bar{g}_p^P(v')}{|\Psi^T|} \quad \forall p, \forall t, \forall v' \leq v \quad (\text{C.5e})$$

$$0 \leq g_{dtv'}^{LS} \leq \bar{G}_{dt}^D \quad \forall d, \forall t, \forall v' \leq v \quad (\text{C.5f})$$

$$0 \leq g_{dtv'}^{SI} \leq \bar{G}_d^{SI} \quad \forall d, \forall t, \forall v' \leq v \quad (\text{C.5g})$$

$$0 \leq g_{dtv'}^{SW} \leq \bar{G}_d^{SW} \quad \forall d, \forall t, \forall v' \leq v \quad (\text{C.5h})$$

$$wg_{dtv'}^S = wg_{d,t-1,v'}^S + g_{dtv'}^{SI} \cdot \eta_d^{SI} - \frac{g_{dtv'}^{SW}}{\eta_d^{SW}} \quad \forall d, \forall t \in \Psi^T \setminus \{t1\}, \forall v' \leq v \quad (\text{C.5i})$$

$$wg_{d(t1)v'}^S = E_d^{S0} + g_{d(t1)v'}^{SI} \cdot \eta_d^{SI} - \frac{g_{d(t1)v'}^{SW}}{\eta_d^{SW}} \quad \forall d, \{t1\}, \forall v' \leq v \quad (\text{C.5j})$$

$$\underline{G}_{dt}^S \leq wg_{dtv'}^S \leq \bar{G}_{dt}^S \quad \forall d, \forall t, \forall v' \leq v \quad (\text{C.5k})$$

where set  $\Phi^M = \{\Phi^1; \theta; g_{ptv'}^P; g_{dtv'}^{LS}; g_{ltv'}^L; wg_{dtv'}^S; g_{dtv'}^{SI}; g_{dtv'}^{SW}\}$  are the optimization variables of master problem (C.5).

### C.5.2 Subproblem

At each iteration  $v$ , master problem (C.5) yields the expansion decisions. The subproblem formulated below takes these decisions as input and determines the worst-case uncertainty realization:

$$\max_{\Phi^2 \in \Omega} \min_{\Phi^3 \in \Xi(\cdot)} \left[ \sum_t \left( \sum_p g_{pt}^P \cdot C_p^P + \sum_l g_{lt}^L \cdot C_l^L + \sum_d g_{dt}^{LS} \cdot C_d^{LS} \right) \right] \quad (\text{C.6})$$

Subproblem (C.6) is a bilevel problem in which the lower-level problem is continuous and linear on its decisions variables. Thus, we follow Baringo, Boffino, and Oggioni [174] and replace the lower-level problem by its dual form. Furthermore, we can replace the objective function of the subproblem by the dual objective function using the strong duality theorem. This allows formulating the subproblem as the single-level problem:

$$\begin{aligned} \max_{\Phi^2, \Phi^3} \\ \sum_t \left[ \sum_{d \in \Psi_n^D} (\bar{G}_{dt}^D \lambda_{n(d)t} + \hat{G}_{dt}^D \tilde{\lambda}_{n(d)t}) + \sum_{l \in \Psi^L} -\bar{G}_{lt}^L \bar{\phi}_{lt}^L + \sum_{l \in \Psi^{L+}} -\bar{G}_{lt}^L X_l^{L(v)} \bar{\phi}_{lt}^L \right] \end{aligned}$$



$$\begin{aligned}
& + \sum_p \left( -\frac{\tilde{G}_p^P}{|\Psi^T|} \bar{\phi}_{pt}^P + \frac{\hat{G}_p^P}{|\Psi^T|} \tilde{\phi}_{pt}^P \right) + \sum_d \left( -\bar{G}_d^{SI-SI} \bar{\phi}_{dt}^{SI} - \bar{G}_d^{SW-SW} \bar{\phi}_{dt}^{SW} + \underline{G}_{dt}^S \underline{\phi}_{dt}^S - \bar{G}_d^{S-S} \bar{\phi}_{dt}^S \right) \\
& + \sum_d \left[ -\tilde{G}_d^D \bar{\phi}_d^D \right] + \sum_d \mu_{d,\{t1\}}^S E_d^{S0} \quad (C.7a)
\end{aligned}$$

subject to

$$\bar{g}_{dt}^D = \tilde{G}_{dt}^D + z_{dt}^D \cdot \hat{G}_{dt}^D \quad \forall d, \forall t \quad (C.7b)$$

$$\bar{g}_p^P = \tilde{G}_p^P - z_p^P \cdot \hat{G}_p^P \quad \forall p \quad (C.7c)$$

$$\sum_{d \in D, t \in T} z_{dt}^D \leq \Gamma^D \quad (C.7d)$$

$$\sum_{p \in P} z_p^P \leq \Gamma^P \quad (C.7e)$$

$$\lambda_{n(p)t} - \bar{\phi}_{pt}^P - c_p^P \leq 0 \quad \forall p, \forall t \quad (C.7f)$$

$$\lambda_{n(d)t} - \bar{\phi}_{dt}^D - c_d^{LS} \leq 0 \quad \forall d, \forall t \quad (C.7g)$$

$$-\lambda_{n(s(l))t} + \lambda_{n(r(l))t} - \bar{\phi}_{lt}^L - c_l^L \leq 0 \quad \forall l \in \Psi^L \cup \Psi^{L+} | X_l^{L(v)} = 1, \forall t \quad (C.7h)$$

$$\lambda_{n(d)t} - \bar{\phi}_{dt}^{SW} - \frac{1}{\eta_d^{SW}} \cdot \mu_{dt}^S \leq 0 \quad \forall d, \forall t \quad (C.7i)$$

$$-\lambda_{n(d)t} - \bar{\phi}_{dt}^{SI} + \eta_d^{SI} \mu_{dt}^S \leq 0 \quad \forall d, \forall t \quad (C.7j)$$

$$-\mu_{dt}^S + \mu_{d,t+1}^S + \underline{\phi}_{dt}^S - \bar{\phi}_{dt}^S = 0 \quad \forall d, \forall t = 1, \dots, \Psi_{|\Psi^T|}^T - 1 \quad (C.7k)$$

$$-\mu_{d,t}^S + \underline{\phi}_{d,t}^S - \bar{\phi}_{d,t}^S = 0 \quad \forall s, \forall t = \Psi_{|\Psi^T|}^T \quad (C.7l)$$

$$\bar{\phi}_{pt}^P \geq 0 \quad \forall p, \forall t \quad (C.7m)$$

$$\bar{\phi}_{dt}^D \geq 0 \quad \forall d, \forall t \quad (C.7n)$$

$$\bar{\phi}_{lt}^L \geq 0 \quad \forall l \in \Psi^L, \forall t \quad (C.7o)$$

$$\bar{\phi}_{lt}^L \geq 0 \quad \forall l \in \Psi^{L+} | X_l^{L(v)} = 1, \forall t \quad (C.7p)$$

$$\bar{\phi}_{dt}^{SW}, \bar{\phi}_{dt}^{SI}, \underline{\phi}_{dt}^S, \bar{\phi}_{dt}^S \geq 0 \quad \forall d, \forall t \quad (C.7q)$$

$$\mu_{dt}^S \text{ free} \quad \forall d, \forall t \quad (C.7r)$$

$$\lambda_{nt} \text{ free} \quad \forall n, \forall t \quad (C.7s)$$

$$z_{dt}^D \in \{0, 1\} \quad \forall d, \forall t \quad (C.7t)$$

$$z_p^P \in \{0, 1\} \quad \forall p \quad (C.7u)$$

Note that to omit a MINLP formulation, we use a linearization technique addressing the bilinear terms  $\lambda_{n(d)t} \cdot \bar{g}_{dt}^D$  and  $\bar{\phi}_{pt}^P \cdot \bar{g}_{pt}^P$  in the objective function of the problem (C.7). The following constraints are added to the problem rendering the subproblem into the equivalent MILP:

$$(-M) \cdot z_{d(n)t}^D \leq \tilde{\lambda}_{nt} \leq (M) \cdot z_{d(n)t}^D \quad (\text{C.8a})$$

$$(-M) \cdot (1 - z_{d(n)t}^D) \leq \lambda_{nt} - \tilde{\lambda}_{nt} \leq (M) \cdot (1 - z_{d(n)t}^D) \quad (\text{C.8b})$$

$$(-M) \cdot z_p^P \leq \tilde{\phi}_{pt}^P \leq (M) \cdot z_p^P \quad (\text{C.8c})$$

$$(-M) \cdot (1 - z_p^P) \leq \bar{\phi}_{pt}^P - \tilde{\phi}_{pt}^P \leq (M) \cdot (1 - z_p^P) \quad (\text{C.8d})$$

## DEMAND AND SUPPLY UNCERTAINTY BUDGETS

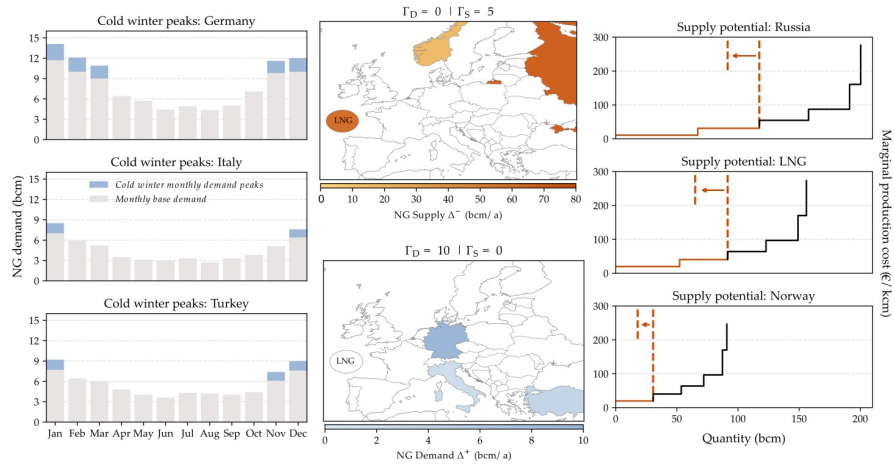


Figure D.1: Illustrative example of the worst-case demand and supply realizations subject to uncertainty budgets  $[\Gamma]$

Authors' illustration.

# E

## PROJECTS OF COMMON INTERESTS INCLUDED IN THE ANALYSIS

Table E.1: Projects of Common Interests included in the analysis (Chapter 5)

No.	PCI project	Capacity [bcm/a]	Start year	Estimated CAPEX <sup>1</sup> [MEUR]	Subsidy from CEF&EC [MEUR]	Status
1	Poland-Lithuania	2.4 (PL-LT)	2022-2023	558	276	U.C. <sup>3</sup>
2	Baltic Pipe	1.9 (LT-PL) 3.1 (PL-DK) 10.4 (DK-PL)	2022	784	267	U.C.
3	Latvia-Lithuania	1.9 (LT-LV) 2.0 (LV-LT)	2023	37		Proposed
4	Bulgaria-Serbia	1.8 (BG-SB) 0.2 (SB-BG)	2022	487	77	U.C.
5	Eastring Pipeline (a)	4.4 (RO-HU) 4.4 (HU-RO)	2025	547		Proposed
6	Eastring Pipeline (b)	3.3 (TR-BG) 3.3 (BG-TR)	2025	200		Proposed
7	Hungary-Slovenia	1.4 (HU-SI) 1.4 (SI-HU)	2025	104		Proposed
8	Slovenia-Austria	2.7 (AT-SI) 5.5 (SI-AT)	2023	218		Proposed
9	Croatia-Slovenia	5.0 (SI-HR) 5.0 (HR-SI)	2023	218		Proposed
10	Slovakia-Hungary <sup>2</sup>	3.8 (HU-SK) 1.0 (SK-HU)	2022	138		Proposed
11	Poland-Slovakia	4.7 (PL-SK) 5.7 (SK-PL)	2021	287	107	U.C.
12	Greece-Bulgaria	5.0 (GR-BG) 5.0 (BG-GR)	2021	287		Proposed
13	Poseidon Pipeline	14.0 (GR-IT) 14.0 (IT-GR)	2022-2025	2096		Proposed
14	Shannon LNG	2.8 (IE)	2022	500		Proposed
15	Krk LNG	2.6 (HR)	2021	234	107	Operation
16	Baltic Sea Coast LNG	4.0 (PL)	2022	196		Proposed
17	Alexandroupolis LNG	6.1 (GR)	2023	382		Proposed

<sup>1</sup> Information on PCI projects is collected from [www.gem.wiki](http://www.gem.wiki) web-page unless stated otherwise (Status: June 2021)

<sup>2</sup> PCI status pertains to the expansion of the interconnector

<sup>3</sup> Under Construction (U.C.)

LITERATURE REVIEW OF NATURAL GAS MODELS  
AND REPRESENTATION OF UNCERTAINTY

Table F.1: Overview of natural gas studies and their respective representation of uncertainty

Author/year	Problem type	Uncertainty addressed
Zwart and Mulder [205]	deterministic	supply, demand, capital costs
Lochner and Bothe [206]	deterministic	pipeline capacities
Zhuang and Gabriel [95]	stochastic	LTCs, spot market
Zwart [207]	deterministic	resource constraints
Neumann, Viehrig, and Weigt [208]	deterministic	supply, demand, infrastructure
Lochner, Dieckhoener, and Lindenberger [209]	deterministic	supply, demand, infrastructure
Abada and Massol [178]	deterministic	supply interruptions
Abada and Juvet [210]	stochastic	demand
Dieckhoener [179]	deterministic	infrastructure projects
Dieckhoener, Lochner, and Lindenberger [211]	deterministic	demand, supply, pipeline capacities
Egging [175]	stochastic	production, market structure
Chyong and Hobbs [116]	deterministic	demand, South Stream pipeline, transit fees
Flouri et al. [212]	Monte Carlo simulation	supply disruptions
Egging and Holz [180]	stochastic	demand, supply disruptions, resource basis
Fodstad et al. [68]	stochastic	demand
Holz, Richter, and Egging [129]	deterministic	demand
Kiss, Selei, and Tóth [213]	deterministic	infrastructure projects
Baltensperger et al. [181]	deterministic	LNG supply disruptions
Hecking and Weiser [214]	deterministic	LNG supply, Nord Stream 2 pipeline
Egging et al. [215]	stochastic	shale gas exploration
Xunpeng, Variam, and Tao [216]	deterministic	supply, demand
Deane, Ó Ciaráin, and Ó Galachóir [67]	deterministic	supply disruptions
Abrell, Chavaz, and Weigt [217]	deterministic	infrastructure projects
Eser, Chokani, and Abhari [132]	deterministic	infrastructure projects
Sesini, Giarola, and Hawkes [218]	deterministic	supply disruptions
Hauser [176]	stochastic	demand, supply disruptions
Riepin, Möbius, and Müsgens [177]	stochastic	demand



## BIBLIOGRAPHY

---

- [1] IRENA. *Renewable Energy Capacity Statistics*. 2020. URL: <https://www.irena.org/publications/2020/Mar/Renewable-Capacity-Statistics-2020>.
- [2] IEA. *World Energy Outlook*. 2019. URL: <https://www.iea.org/reports/world-energy-outlook-2019>.
- [3] European Commission. *A Clean Planet for all: A European Long-term Strategic Vision for a Prosperous, Modern, Competitive Climate Neutral Economy – In-Depth Analysis in Support of the Commission Communication COM/2018/773*. 2018. URL: <https://www.eumonitor.eu/9353000/1/j9vvik7m1c3gyxp/vktvm72o8kyq>.
- [4] Jonathan Bosch, Iain Staffell, and Adam D. Hawkes. “Temporally-explicit and spatially-resolved global onshore wind energy potentials.” In: *Energy* 131 (2017), pp. 207–217. ISSN: 0360-5442. DOI: [10.1016/j.energy.2017.05.052](https://doi.org/10.1016/j.energy.2017.05.052).
- [5] Doug Arent, Patrick Sullivan, Donna Heimiller, Anthony Lopez, Kelly Eurek, Jake Badger, Hans Ejsing Jorgensen, Mark Kelly, Leon Clarke, and Patrick Luckow. *Improved Offshore Wind Resource Assessment in Global Climate Stabilization Scenarios*. Tech. rep. NREL/TP-6A20-55049. Oct. 2012. DOI: [10.2172/1055364](https://doi.org/10.2172/1055364).
- [6] David Toke. “The UK offshore wind power programme: A sea-change in UK energy policy?” In: *Energy Policy* 39.2 (2011), pp. 526–534. DOI: [10.1016/j.enpol.2010.08.043](https://doi.org/10.1016/j.enpol.2010.08.043).
- [7] Richard Green and Nicholas Vasilakos. “The economics of offshore wind.” In: *Energy Policy* 39.2 (2011). Special Section on Offshore wind power planning, economics and environment, pp. 496–502. ISSN: 0301-4215. DOI: [10.1016/j.enpol.2010.10.011](https://doi.org/10.1016/j.enpol.2010.10.011).
- [8] PWC. *Unlocking Europe’s Offshore Wind Potential. Moving Towards a Subsidy Free Industry*. Tech. rep. 2018. URL: <https://store.pwc.de/en/publications/unlocking-europe-s-offshore-wind-potential-moving-towards-a-subsidy-free-industry>.
- [9] Aurora Energy Research. *The New Economics of Offshore Wind*. Tech. rep. 2018. URL: <https://auroraer.com/country/europe/great-britain/the-new-economics-of-offshore-wind/>.
- [10] NewEnergyUpdate. *Offshore Wind Developers See Ripe Conditions for Zero-subsidy Bids*. 2018. URL: <http://newenergyupdate.com/wind-energy-update/offshore-wind-developers-see-ripe-conditions-zero-subsidy-bids>.

- [11] Felix Creutzig, Peter Agoston, Jan Christoph Goldschmidt, Gunnar Luderer, Gregory Nemet, and Robert C Pietzcker. "The underestimated potential of solar energy to mitigate climate change." In: *Nature Energy* 2.9 (2017), pp. 1–9. DOI: [10.1038/nenergy.2017.140](https://doi.org/10.1038/nenergy.2017.140).
- [12] Oliver Schmidt, Adam Hawkes, Ajay Gambhir, and Iain Staffell. "The future cost of electrical energy storage based on experience rates." In: *Nature Energy* 2.8 (2017), pp. 1–8. DOI: [10.1038/nenergy.2017.140](https://doi.org/10.1038/nenergy.2017.140).
- [13] Philip Heptonstall, Robert Gross, Philip Greenacre, and Tim Cockerill. "The cost of offshore wind: Understanding the past and projecting the future." In: *Energy Policy* 41 (2012), pp. 815–821. DOI: [10.1016/j.enpol.2011.11.050](https://doi.org/10.1016/j.enpol.2011.11.050).
- [14] M Vieira, Brian Snyder, Elsa Henriques, and Luis Reis. "European offshore wind capital cost trends up to 2020." In: *Energy Policy* 129 (2019). DOI: [10.1016/j.enpol.2019.03.036](https://doi.org/10.1016/j.enpol.2019.03.036).
- [15] David E Dismukes and Gregory B Upton Jr. "Economies of scale, learning effects and offshore wind development costs." In: *Renewable Energy* 83 (2015), pp. 61–66. DOI: [10.1016/j.renene.2015.04.002](https://doi.org/10.1016/j.renene.2015.04.002).
- [16] Mark Bolinger and Ryan Wiser. "Understanding wind turbine price trends in the US over the past decade." In: *Energy Policy* 42 (2012), pp. 628–641. DOI: [10.1016/j.enpol.2011.12.036](https://doi.org/10.1016/j.enpol.2011.12.036).
- [17] Ryan Wiser, Karen Jenni, Joachim Seel, Erin Baker, Maureen Hand, Eric Lantz, and Aaron Smith. "Expert elicitation survey on future wind energy costs." In: *Nature Energy* 1.10 (2016), pp. 1–8. DOI: [10.1038/nenergy.2016.135](https://doi.org/10.1038/nenergy.2016.135).
- [18] Cody Scott Hoffman. "Financial viability of offshore wind on the Texas Gulf Coast." PhD thesis. 2019. DOI: [10.26153/tsw/2090](https://doi.org/10.26153/tsw/2090).
- [19] Henrik Klinge Jacobsen, Pablo Hevia-Koch, and Christoph Wolter. "Nearshore and offshore wind development: Costs and competitive advantage exemplified by nearshore wind in Denmark." In: *Energy for Sustainable Development* 50 (2019), pp. 91–100. DOI: [10.1016/j.esd.2019.03.006](https://doi.org/10.1016/j.esd.2019.03.006).
- [20] Philipp Beiter, Walter Musial, Levi Kilcher, Michael Maness, and Aaron Smith. *An assessment of the economic potential of offshore wind in the United States from 2015 to 2030*. Tech. rep. National Renewable Energy Lab.(NREL), Golden, CO (United States), 2017. URL: [10.2172/1349721](https://doi.org/10.2172/1349721).



- [21] Tyler J. Stehly, Miriam Noonan, David Mora, Lena Kitzing, Gavin Smart, Volker Berkhout, and Yuka Kikuchi. "IEA Wind TCP Task 26: Offshore Wind Energy International Comparative Analysis." In: (Nov. 2018). URL: <https://www.osti.gov/biblio/1483473>.
- [22] Lazard. *Lazard's Levelized Cost of Storage Analysis—v.12.0*. 2018. URL: <https://www.lazard.com/perspective/levelized-cost-of-energy-levelized-cost-of-storage-and-levelized-cost-of-hydrogen/>.
- [23] Offshore Wind Programme Board. *Transmission Costs for Offshore Wind*. Tech. rep. Apr. 2016. URL: <https://ore.catapult.org.uk/app/uploads/2018/02/Transmission-Costs-for-Offshore-Wind.pdf>.
- [24] Algemene Rekenkamer. *Focus on the Cost of Offshore Wind Energy*. Tech. rep. 2018. URL: <https://english.rekenkamer.nl/publications/reports/2018/09/27/focus-on-the-cost-of-offshore-wind-energy>.
- [25] John Aldersey-Williams, Ian D. Broadbent, and Peter A. Strachan. "Better estimates of LCOE from audited accounts—A new methodology with examples from United Kingdom offshore wind and CCGT." In: *Energy policy* 128 (2019), pp. 25–35. DOI: [10.1016/j.enpol.2018.12.044](https://doi.org/10.1016/j.enpol.2018.12.044).
- [26] Lena Kitzing. "Risk Implications of Energy Policy Instruments." PhD thesis. 2014. URL: <https://orbit.dtu.dk/en/publications/risk-implications-of-energy-policy-instruments>.
- [27] EWEA. *Design Options for Wind Energy Tenders*. 2015. URL: <http://www.ewea.org/fileadmin/files/library/publications/position-papers/EWEA-Design-options-for-wind-energy-tenders.pdf>.
- [28] Oscar Fitch-Roy. "An offshore wind union? Diversity and convergence in European offshore wind governance." In: *Climate Policy* 16.5 (2016), pp. 586–605. DOI: [10.1080/14693062.2015.1117958](https://doi.org/10.1080/14693062.2015.1117958).
- [29] Oliver Grothe and Felix Müsgens. "The influence of spatial effects on wind power revenues under direct marketing rules." In: *Energy Policy* 58 (2013), pp. 237–247. DOI: [10.1016/j.enpol.2013.03.004](https://doi.org/10.1016/j.enpol.2013.03.004).
- [30] WindEurope. *Wind Energy in Europe in 2018 – Trends and Statistics*. 2018. URL: <https://windeurope.org/wp-content/uploads/files/about-wind/statistics/WindEurope-Annual-Statistics-2018.pdf>.

- [31] Felix Müsgens and Iegor Riepin. "Is offshore already competitive? Analyzing German offshore wind auctions." In: *2018 15th International Conference on the European Energy Market (EEM)*. IEEE. 2018, pp. 1–6. DOI: [10.1109/EEM.2018.8469851](https://doi.org/10.1109/EEM.2018.8469851).
- [32] Ian Partridge. "Cost comparisons for wind and thermal power generation." In: *Energy Policy* 112 (2018). DOI: [10.1016/j.enpol.2017.10.006](https://doi.org/10.1016/j.enpol.2017.10.006).
- [33] John Aldersey-Williams and Tim Rubert. "Levelised cost of energy—A theoretical justification and critical assessment." In: *Energy policy* 124 (2019), pp. 169–179. DOI: [10.1016/j.enpol.2018.10.004](https://doi.org/10.1016/j.enpol.2018.10.004).
- [34] Philip Heptonstall, Robert Gross, and Florian Steiner. "The costs and impacts of intermittency—2016 update." In: *London: UK Energy Research Centre* (2017).
- [35] Hans Cleijne. *Cost of offshore transmission*. 2019.
- [36] Giles Hundleby. "Dong's Borssele Costs—a landmark Dutch auction by Giles Hundleby. BVG 595." In: *BVG Associates* (2016). URL: <https://bvgassociates.com/dongs-borssele-costs/>.
- [37] Florian Egli, Bjarne Steffen, and Tobias S Schmidt. "A dynamic analysis of financing conditions for renewable energy technologies." In: *Nature Energy* 3.12 (2018), pp. 1084–1092. DOI: [10.1038/s41560-018-0277-y](https://doi.org/10.1038/s41560-018-0277-y).
- [38] BEIS. *Energy and Emissions Projections*. 2019. URL: <https://www.gov.uk/government/collections/energy-and-emissions-projections>.
- [39] Stefan Pfenninger and Ian Staffell. "Long-term patterns of European PV output using 30 years of validated hourly reanalysis and satellite data." In: *Energy* 114 (2016). DOI: [10.1016/j.energy.2016.08.060](https://doi.org/10.1016/j.energy.2016.08.060).
- [40] Ian Staffell and Stefan Pfenninger. "Using bias-corrected reanalysis to simulate current and future wind power output." In: *Energy* 114 (2016). DOI: [10.1016/j.energy.2016.08.068](https://doi.org/10.1016/j.energy.2016.08.068).
- [41] John Aldersey-Williams, Ian D Broadbent, and Peter A Strachan. "Analysis of United Kingdom offshore wind farm performance using public data: improving the evidence base for policymaking." In: *Util. Policy* 62 (2020). DOI: [10.1016/j.jup.2019.100985](https://doi.org/10.1016/j.jup.2019.100985).
- [42] Andrew Smith. *Offshore Wind Capacity Factors*. 2020. URL: <https://energynumbers.info/>.

- [43] Yves-Marie Saint-Drenan, Romain Besseau, Malte Jansen, Iain Staffell, Alberto Troccoli, Laurent Dubus, Johannes Schmidt, Katharina Gruber, Sofia G. Simões, and Siegfried Heier. “A parametric model for wind turbine power curves incorporating environmental conditions.” In: *Renewable Energy* 157 (2020), pp. 754–768. ISSN: 0960-1481. DOI: [10.1016/j.renene.2020.04.123](https://doi.org/10.1016/j.renene.2020.04.123).
- [44] Iain Staffell and Richard Green. “How does wind farm performance decline with age?” In: *Renewable energy* 66 (2014), pp. 775–786. DOI: [10.1016/j.renene.2013.10.041](https://doi.org/10.1016/j.renene.2013.10.041).
- [45] Jon Olauson, Per Edström, and Jesper Rydén. “Wind turbine performance decline in Sweden.” In: *Wind Energy* 20.12 (2017), pp. 2049–2053. DOI: [10.1002/we.2132](https://doi.org/10.1002/we.2132).
- [46] Fernando Porté-Agel, Majid Bastankhah, and Sina Shamsoddin. “Wind-turbine and wind-farm flows: a review.” In: *Boundary-Layer Meteorology* 174.1 (2020), pp. 1–59. DOI: [10.1007/s10546-019-00473-0](https://doi.org/10.1007/s10546-019-00473-0).
- [47] Zhenzhong Zeng, Alan D. Ziegler, Timothy Searchinger, Long Yang, Anping Chen, Kunlu Ju, Shilong Piao, Laurent ZX Li, Philippe Ciais, Deliang Chen, et al. “A reversal in global terrestrial stilling and its implications for wind energy production.” In: *Nature Climate Change* 9.12 (2019), pp. 979–985. DOI: [10.1038/s41558-019-0622-6](https://doi.org/10.1038/s41558-019-0622-6).
- [48] Daniel Hdidouan and Iain Staffell. “The impact of climate change on the levelised cost of wind energy.” In: *Renewable energy* 101 (2017), pp. 575–592. DOI: [10.1016/j.renene.2016.09.003](https://doi.org/10.1016/j.renene.2016.09.003).
- [49] Lisa Ziegler. “Assessment of monopiles for lifetime extension of offshore wind turbines.” PhD thesis. Thesis, Norwegian Univ. of Science and Technology, 2018.
- [50] Megan Geuss. *Offshore, Act Two: New owner repowers 20-year-old wind farm off Swedish coast*. 2018. URL: <https://arstechnica.com/information-technology/2018/12/offshore-act-two-new-owner-repowers-20-year-old-wind-farm-off-swedish-coast/>.
- [51] Patrick Smith, Marc Costa-Ros, Bernhard Lange, Henrik Stiesdal, and Fabio Pollicino. “Question of the Week: Are offshore projects built to last.” In: *Windpower monthly* (2014). URL: <https://www.windpowermonthly.com/article/1320109/question-week-offshore-projects-built-last>.
- [52] David Foxwell. *Research claims 30-year lifespan is within reach for offshore wind projects*. URL: <https://www.rivieramm.com/news-content-hub/research-claims-30-year-lifespan-is-within-reach-for-offshore-wind-projects-28324>.

- [53] Athanasios Kolios and María Martínez-Luengo. “The end of the line for today’s wind turbines.” In: *Renewable Energy Focus* 17.3 (2016), pp. 109–111. URL: <http://www.renewableenergyfocus.com/view/43817/the-end-of-the-line-for-today-s-wind-turbines/>.
- [54] Frauke Wiese, Ingmar Schlecht, Wolf-Dieter Bunke, Clemens Gerbaulet, Lion Hirth, Martin Jahn, Friedrich Kunz, Casimir Lorenz, Jonathan Mühlenpfordt, Juliane Reimann, et al. “Open Power System Data—Frictionless data for electricity system modelling.” In: *Applied Energy* 236 (2019), pp. 401–409. DOI: [10.1016/j.apenergy.2018.11.097](https://doi.org/10.1016/j.apenergy.2018.11.097).
- [55] ENTSO-E. *Transparency Platform*. 2019. URL: <https://transparency.entsoe.eu/>.
- [56] Pantelis Capros, A De Vita, N Tasios, P Siskos, M Kannavou, A Petropoulos, S Evangelopoulou, M Zampara, D Papadopoulos, Ch Nakos, et al. *EU Reference Scenario 2016-Energy, transport and GHG emissions Trends to 2050*. Tech. rep. 2016. DOI: [10.2833/9127](https://doi.org/10.2833/9127).
- [57] Paul Twomey and Karsten Neuhoff. “Wind power and market power in competitive markets.” In: *Energy policy* 38.7 (2010), pp. 3198–3210. DOI: [10.1016/j.enpol.2009.07.031](https://doi.org/10.1016/j.enpol.2009.07.031).
- [58] Thorsten Engelhorn and Felix Müsgens. “How to estimate wind-turbine infeed with incomplete stock data: A general framework with an application to turbine-specific market values in Germany.” In: *Energy Economics* 72 (2018), pp. 542–557. DOI: [10.1016/j.eneco.2018.04.022](https://doi.org/10.1016/j.eneco.2018.04.022).
- [59] National Grid ESO. *Future Energy Scenarios 2019*. 2019. URL: <https://www.nationalgrideso.com/sites/eso/files/documents/fes-2019.pdf>.
- [60] *Official Exchange Rate (LCU per US\$, Period Average, World Bank Database*. 2019.
- [61] *Inflation, GDP Deflator (Annual %), Period Average, World Bank Database*. 2019.
- [62] Cinzia Alcidi, Matthias Busse, and Daniel Gros. “Is there a need for additional monetary stimulus? Insights from the original Taylor Rule.” In: *Insights from the Original Taylor Rule (April 15, 2016)*. CEPS Policy Brief 342 (2016). URL: <https://www.ceps.eu/wp-content/uploads/2016/04/PB342TaylorRule.pdf>.
- [63] ENTSOs. *Investigation on the interlinkage between gas and electricity scenarios*. Tech. rep. 2019. URL: <https://www.entsog.eu/met-hodologies-and-modelling#consistent-and-interlinked-electricity-and-gas-model>.

- [64] Jan Abrell and Hannes Weigt. "The short and long term impact of Europe's natural gas market on electricity markets until 2050." In: *Energy Journal* 37.SpecialIssue3 (2016), pp. 125–146. DOI: [10.5547/01956574.37.SI3.jabr](https://doi.org/10.5547/01956574.37.SI3.jabr).
- [65] Rudolf Gerardus Egging. "Multi-Period Natural Gas Market Modeling - Applications, Stochastic Extensions and Solution Approaches." In: (2010). URL: <https://drum.lib.umd.edu/handle/1903/11188>.
- [66] Adriaan Hendrik van der Weijde and Benjamin F. Hobbs. "The economics of planning electricity transmission to accommodate renewables: Using two-stage optimisation to evaluate flexibility and the cost of disregarding uncertainty." In: *Energy Economics* 34.6 (2012), pp. 2089–2101. DOI: [10.1016/j.eneco.2012.02.015](https://doi.org/10.1016/j.eneco.2012.02.015). URL: <http://dx.doi.org/10.1016/j.eneco.2012.02.015>.
- [67] J. P. Deane, M. Ó Ciaráin, and B. P. Ó Gallachóir. "An integrated gas and electricity model of the EU energy system to examine supply interruptions." In: *Applied Energy* 193 (2017), pp. 479–490. DOI: [10.1016/j.apenergy.2017.02.039](https://doi.org/10.1016/j.apenergy.2017.02.039).
- [68] Marte Fodstad, Ruud Egging, Kjetil Midthun, and Asgeir Tomasgard. "Stochastic Modeling of Natural Gas Infrastructure Development in Europe under Demand Uncertainty." In: *The Energy Journal* 37 (2016), pp. 1–28. DOI: [10.5547/01956574.37.SI3.mfod](https://doi.org/10.5547/01956574.37.SI3.mfod).
- [69] ENTSOs. *TYNDP 2018 Scenario Report*. Tech. rep. ENTSO-G and ENTSO-E, 2018. URL: <https://tyndp.entsoe.eu/tyndp2018/scenario-report>.
- [70] Per Ivar Helgesen. "Top-down and Bottom-up: Combining energy system models and macroeconomic general equilibrium models." In: *Project: Regional Effects of Energy Policy (RegPol). CenSES working paper 1* (2013), p. 2013.
- [71] Seungwon An, Qing Li, and Thomas W Gedra. "Natural gas and electricity optimal power flow." In: *2003 IEEE PES Transmission and Distribution Conference and Exposition (IEEE Cat. No. 03CH37495)*. Vol. 1. IEEE, 2003, pp. 138–143.
- [72] Martin Geidl and Göran Andersson. "Optimal power flow of multiple energy carriers." In: *IEEE Transactions on power systems* 22.1 (2007), pp. 145–155. DOI: [10.1109/TPWRS.2006.888988](https://doi.org/10.1109/TPWRS.2006.888988).
- [73] Takaaki Ohishi and Oderson Dias de Mello. "An integrated dispatch model of gas supply and thermoelectric systems." In: *Proceedings of the 15th power systems computation conference (PSCC), Liège, Belgium* (2005).

- [74] Michael Bartels and Andreas Seeliger. "Interdependenzen zwischen Elektrizitätserzeugung und Erdgasversorgung unter Berücksichtigung eines europäischen CO<sub>2</sub>-Zertifikatehandels: Ausgewählte Ergebnisse einer iterativen Modellkopplung." In: *Zeitschrift für Energiewirtschaft* 29.2 (2005), pp. 135–143.
- [75] R Rubio, D Ojeda-Esteybar, O Ano, and A Vargas. "Integrated natural gas and electricity market: A survey of the state of the art in operation planning and market issues." In: *2008 IEEE/PES Transmission and Distribution Conference and Exposition: Latin America*. IEEE. 2008, pp. 1–8. DOI: [doi:10.1109/TDC-LA.2008.4641767](https://doi.org/10.1109/TDC-LA.2008.4641767).
- [76] Modassar Chaudry, Nick Jenkins, and Goran Strbac. "Multi-time period combined gas and electricity network optimisation." In: *Electric power systems Research* 78.7 (2008), pp. 1265–1279. DOI: [10.1016/j.epsr.2007.11.002](https://doi.org/10.1016/j.epsr.2007.11.002).
- [77] Dominik Möst and Holger Perlwitz. "Prospects of gas supply until 2020 in Europe and its relevance for the power sector in the context of emission trading." In: *Energy* 34.10 (2009), pp. 1510–1522. DOI: [doi:10.1016/j.energy.2009.06.045](https://doi.org/10.1016/j.energy.2009.06.045).
- [78] Martin Lienert and Stefan Lochner. "The importance of market interdependencies in modeling energy systems—the case of the European electricity generation market." In: *International Journal of Electrical Power & Energy Systems* 34.1 (2012), pp. 99–113. DOI: [10.1016/j.ijepes.2011.09.010](https://doi.org/10.1016/j.ijepes.2011.09.010).
- [79] Jan Abrell and Hannes Weigt. "Investments in a combined energy network model: substitution between natural gas and electricity?" In: *The Energy Journal* 37.4 (2016). DOI: [10.5547/01956574.37.4.jabr](https://doi.org/10.5547/01956574.37.4.jabr).
- [80] Bining Zhao, Antonio J. Conejo, and Ramteen Sioshansi. "Coordinated expansion planning of natural gas and electric power systems." In: *IEEE Transactions on Power Systems* 33.3 (2017), pp. 3064–3075. DOI: [10.1109/TPWRS.2017.2759198](https://doi.org/10.1109/TPWRS.2017.2759198).
- [81] Modassar Chaudry, Nick Jenkins, Meysam Qadrdan, and Jianzhong Wu. "Combined gas and electricity network expansion planning." In: *Applied Energy* 113 (2014), pp. 1171–1187. DOI: [doi:10.1016/j.apenergy.2013.08.071](https://doi.org/10.1016/j.apenergy.2013.08.071).
- [82] Hossein Ameli, Meysam Qadrdan, and Goran Strbac. "Value of gas network infrastructure flexibility in supporting cost effective operation of power systems." In: *Applied Energy* 202 (2017), pp. 571–580. DOI: [10.1016/j.apenergy.2017.05.132](https://doi.org/10.1016/j.apenergy.2017.05.132).
- [83] Stephen Clegg and Pierluigi Mancarella. "Integrated electrical and gas network flexibility assessment in low-carbon multi-energy systems." In: *IEEE Transactions on Sustainable Energy* 7.2 (2015), pp. 718–731. DOI: [10.1109/TSSTE.2015.2497329](https://doi.org/10.1109/TSSTE.2015.2497329).

- [84] George B. Dantzig. "Linear programming under uncertainty." In: *Management Science* 1 (1955), pp. 197–206. DOI: [10.1287/mnsc.1.3-4.197](https://doi.org/10.1287/mnsc.1.3-4.197).
- [85] Dominik Möst and Dogan Keles. "A survey of stochastic modelling approaches for liberalised electricity markets." In: *European Journal of Operational Research* 207.2 (2010), pp. 543–556. DOI: [doi:10.1287/mnsc.1.3-4.197](https://doi.org/10.1287/mnsc.1.3-4.197).
- [86] Felix Musgens and Karsten Neuhoff. "Modelling dynamic constraints in electricity markets and the costs of uncertain wind output." In: (2006). URL: <http://www.dspace.cam.ac.uk/handle/1810/131648>.
- [87] Wim Benoot, Denise Van Regemorter, Jan Duerinck, Erik Laes, Wouter Nijs, Luc Van Wortwinkel, Hanne Michielsen, Davy Vercaemmen, and Joris Morbee. *Treating Uncertainty and Risk in Energy Systems with Markal/TIMES*. Tech. rep. 2011. URL: [https://www.academia.edu/19337059/Treating\\_Uncertainty\\_and\\_Risk\\_in\\_Energy\\_Systems\\_with\\_Markal\\_TIMES](https://www.academia.edu/19337059/Treating_Uncertainty_and_Risk_in_Energy_Systems_with_Markal_TIMES).
- [88] Michaela Fürsch, Stephan Nagl, and Dietmar Lindenberger. "Optimization of power plant investments under uncertain renewable energy deployment paths: a multistage stochastic programming approach." In: *Energy Systems* 5.1 (2014), pp. 85–121. DOI: [10.1007/s12667-013-0094-0](https://doi.org/10.1007/s12667-013-0094-0).
- [89] Pernille Seljom and Asgeir Tomasgard. "Short-term uncertainty in long-term energy system models—A case study of wind power in Denmark." In: *Energy Economics* 49 (2015), pp. 157–167. DOI: [doi:10.1016/j.eneco.2015.02.004](https://doi.org/10.1016/j.eneco.2015.02.004).
- [90] Bin Xu, Ping-An Zhong, Renato C. Zambon, Yunfa Zhao, and William W.-G. Yeh. "Scenario tree reduction in stochastic programming with recourse for hydropower operations." In: *Water Resources Research* 51.8 (2015), pp. 6359–6380. DOI: [10.1002/2014WR016828](https://doi.org/10.1002/2014WR016828).
- [91] Thomas Möbius and Felix Müsgens. "Electricity market equilibria and intermittent renewables—A stochastic approach." In: *2017 14th International Conference on the European Energy Market (EEM)*. IEEE. 2017, pp. 1–5. DOI: [10.1002/2014WR016828](https://doi.org/10.1002/2014WR016828).
- [92] Hannes Schwarz, Valentin Bertsch, and Wolf Fichtner. "Two-stage stochastic, large-scale optimization of a decentralized energy system: a case study focusing on solar PV, heat pumps and storage in a residential quarter." In: *OR spectrum* 40.1 (2018), pp. 265–310. DOI: [10.1007/s00291-017-0500-4](https://doi.org/10.1007/s00291-017-0500-4).
- [93] Bin Xu, Feilin Zhu, Ping-an Zhong, Juan Chen, Weifeng Liu, Yufei Ma, Le Guo, and Xiaoliang Deng. "Identifying long-term effects of using hydropower to complement wind power un-

- certainty through stochastic programming." In: *Applied Energy* 253 (2019), p. 113535. DOI: [10.1016/j.apenergy.2019.113535](https://doi.org/10.1016/j.apenergy.2019.113535).
- [94] Jifang Zhuang. "A stochastic equilibrium model for the North American natural gas market." PhD thesis. Thesis (Ph.D.) - University of Maryland, College Park, 2005. DOI: [9780542258664](https://doi.org/9780542258664).
- [95] Jifang Zhuang and Steven A. Gabriel. "A complementarity model for solving stochastic natural gas market equilibria." In: *Energy Economics* 30.1 (2008), pp. 113–147. URL: <https://ideas.repec.org/a/eee/eneeco/v30y2008i1p113-147.html>.
- [96] Christos Ordoudis, Pierre Pinson, and Juan M. Morales. "An integrated market for electricity and natural gas systems with stochastic power producers." In: *European Journal of Operational Research* 272.2 (2019), pp. 642–654. DOI: [doi:10.1016/j.ejor.2018.06.036](https://doi.org/10.1016/j.ejor.2018.06.036).
- [97] Zhong-Hua Su, Ruud Egging, Daniel Huppmann, and Asgeir Tomasgard. "A multi-stage multi-horizon stochastic equilibrium model of multi-fuel energy markets." In: *CenSES Working paper 2* (2015). DOI: [978-82-93198-15-4](https://doi.org/978-82-93198-15-4).
- [98] Iegor Riepin, Thomas Möbius, and Felix Müsgens. "Integrated electricity and gas market modeling-Effects of gas demand uncertainty." In: *2018 15th International Conference on the European Energy Market (EEM)*. IEEE, 2018, pp. 1–5. DOI: [10.1109/EEM.2018.8469790](https://doi.org/10.1109/EEM.2018.8469790).
- [99] Bining Zhao, Antonio J. Conejo, and Ramteen Sioshansi. "Unit commitment under gas-supply uncertainty and gas-price variability." In: *IEEE Transactions on Power Systems* 32.3 (2016), pp. 2394–2405. DOI: [10.1109/TPWRS.2016.2602659](https://doi.org/10.1109/TPWRS.2016.2602659).
- [100] Clemens Gerbaulet and Casimir Lorenz. *dynELMOD: A dynamic investment and dispatch model for the future European electricity market*. Tech. rep. DIW Data Documentation, 2017.
- [101] Franziska Holz, Dawud Ansari, Ruud Egging, and Per Ivar Helgesen. "Hybrid modelling: linking and integrating top-down and bottom-up models." In: *Issue Paper of H2020 project SET-Nav*. Trondheim: NTNU (2016).
- [102] John R. Birge and Francois Louveaux. *Introduction to stochastic programming*. Springer Science & Business Media, 2011. URL: <https://link.springer.com/book/10.1007/978-1-4614-0237-4>.
- [103] John R. Birge. "The value of the stochastic solution in stochastic linear programs with fixed recourse." In: *Mathematical programming* 24.1 (1982), pp. 314–325. DOI: [10.1007/BF01585113](https://doi.org/10.1007/BF01585113).



- [104] Erik Laes and Johan Couder. "Probing the usefulness of technology-rich bottom-up models in energy and climate policies: Lessons learned from the Forum project." In: *Futures* 63 (2014), pp. 123–133. DOI: [10.1016/j.futures.2014.06.001](https://doi.org/10.1016/j.futures.2014.06.001).
- [105] Andreas Schröder, Friedrich Kunz, Jan Meiss, Roman Mendelvitich, and Christian Von Hirschhausen. *Current and prospective costs of electricity generation until 2050*. Tech. rep. DIW data documentation, 2013.
- [106] Open Power System Data. *Data Package National Generation Capacity. Version Version 2019-12-02*. 2020. DOI: [10.25832/national-generation-capacity/2019-12-02..](https://doi.org/10.25832/national-generation-capacity/2019-12-02..)
- [107] Eurostat. *Environment and energy statistics*. 2019. URL: <http://ec.europa.eu/eurostat/data/database>.
- [108] ENTSO-E. Transparency Platform. *Actual Generation per Production Type*. 2020. URL: <https://transparency.entsoe.eu/>.
- [109] Cambridge Economic Policy Associates. *Study on the estimation of the Value of Lost Load of electricity supply in Europe*. Tech. rep. July. 2018.
- [110] ENTSO-G. *Ten-Year Network Development Plan data 2018*. 2018. URL: <https://www.entsog.eu/tyndp>.
- [111] Anne Neumann, Sophia Rüster, and Christian von Hirschhausen. "Long-term contracts in the natural gas industry: Literature survey and data on 426 contracts (1965-2014)." In: *DIW Data Documentation* (2015).
- [112] ENTSO-G. *Capacity Map*. 2018. URL: <https://www.entsog.eu/maps>.
- [113] Gas Infrastructure Europe. *Data transparency platform*. 2019. URL: <https://www.gie.eu/>.
- [114] GIIGNL. *The annual report on the LNG industry*. 2016. URL: <http://giignl.org/publications>.
- [115] European Commission. "The role of gas storage in internal market and in ensuring security of supply." In: *EU publications* (2015). DOI: [10.2832/568590](https://doi.org/10.2832/568590). URL: <http://ec.europa.eu/energy/en/studies/>.
- [116] Chi Kong Chyong and Benjamin F Hobbs. "Strategic Eurasian natural gas market model for energy security and policy analysis: Formulation and application to South Stream." In: *Energy Economics* 44 (2014), pp. 198–211. DOI: [10.1016/j.eneco.2014.04.006](https://doi.org/10.1016/j.eneco.2014.04.006).
- [117] ACER. "Gas Transmission Tariffs in South and Central East Europe." In: *ECRB (The Energy Community Regulatory Board) report* (2018).

- [118] Howard Rogers. "The LNG Shipping Forecast: costs rebounding, outlook uncertain." In: *OIES Energy Insight* 27 (2018).
- [119] Iegor Riepin and Felix Musgens. "Seasonal Flexibility in the European Natural Gas Market." In: *The Energy Journal* 43.1 (2022). DOI: [10.5547/01956574.43.1.irie](https://doi.org/10.5547/01956574.43.1.irie).
- [120] REKK. "Measures To Increase The Flexibility And Resilience Of The European Natural Gas Market." In: (2014). URL: <https://rekk.hu/analysis-details/233>.
- [121] Anouk Honore. "The Dutch Gas Market: trials, tribulations, and trends." In: (2017). DOI: [10.26889/9781784670832](https://doi.org/10.26889/9781784670832).
- [122] Snam, IGU and BCG. *Global Gas Report 2018*. 2018. URL: <http://www.snam.it/en/Natural-gas/global-gas-report/>.
- [123] The Oil and Gas Authority. *National Report on Oil and Gas Reserves and Resources*. 2016. URL: <https://www.gov.uk/guidance/oil-and-gas-uk-field-data>.
- [124] Ruud Egging and Franziska Holz. *Global gas model: Model and data documentation v3.0 (2019)*. Tech. rep. DIW Data Documentation, 2019. DOI: <https://dx.doi.org/10.18723/diw-ddc:2019-100>.
- [125] Lars Mathiesen, Kjell Roland, and Knut Thonstad. "The European natural gas market: Degrees of market power on the selling side." In: *Natural Gas Markets and Contracts* (1987), pp. 27–58.
- [126] Steven A. Gabriel, Supat Kiet, and Jifang Zhuang. "A mixed complementarity-based equilibrium model of natural gas markets." In: *Operations research* 53.5 (2005), pp. 799–818. DOI: [10.2307/25146915](https://doi.org/10.2307/25146915).
- [127] Harald Hecking and Timo Panke. *COLUMBUS-A global gas market model*. Tech. rep. EWI Working Paper, 2012.
- [128] Franziska Holz. "Modeling the European natural gas market: static and dynamic perspectives of an oligopolistic market." In: (2009). DOI: [10.14279/depositonce-2089](https://doi.org/10.14279/depositonce-2089).
- [129] Franziska Holz, Philipp M. Richter, and Ruud Egging. "The role of natural gas in a low-carbon Europe: infrastructure and supply security." In: *The Energy Journal* 37.Sustainable Infrastructure Development and Cross-Border Coordination (2016). DOI: [10.5547/01956574.37.SI3.fhol](https://doi.org/10.5547/01956574.37.SI3.fhol).
- [130] Wietze Lise and Benjamin F. Hobbs. "A dynamic simulation of market power in the liberalised European natural gas market." In: *The Energy Journal* 30.Special Issue (2009). DOI: [10.5547/ISSN0195-6574-EJ-Vol30-NoSI-8](https://doi.org/10.5547/ISSN0195-6574-EJ-Vol30-NoSI-8).

- [131] Caroline Dieckhoner. “Simulating security of supply effects of the Nabucco and South Stream projects for the European natural gas market.” In: *The Energy Journal* 33.3 (2012). DOI: [10.5547/01956574.33.3.6](https://doi.org/10.5547/01956574.33.3.6).
- [132] Patrick Eser, Ndaona Chokani, and Reza Abhari. “Impact of Nord Stream 2 and LNG on gas trade and security of supply in the European gas network of 2030.” In: *Applied energy* 238 (2019), pp. 816–830. DOI: [10.1016/j.apenergy.2019.01.068](https://doi.org/10.1016/j.apenergy.2019.01.068).
- [133] András Kiss, Adrienn Selei, and Borbála Takácsné Tóth. “A top-down approach to evaluating cross-border natural gas infrastructure projects in Europe.” In: *The Energy Journal* 37 (Sustainable Infrastructure Development and Cross-Border Coordination 2016).
- [134] Beatrice Petrovich, Howard Rogers, Harald Heckling, and Florian Weiser. “European gas grid through the eye of the TIGER: investigating bottlenecks in pipeline flows by modelling history.” In: *OIES PAPERS: NG* 112 (2016).
- [135] Borbála Tokácsne Tóth, Adrienn Selei, Péter Kotek, Ákos Beothy, David Leython, Peter Cameron, and Abdul Jalil Jumriany. “Follow-up study to the LNG and storage strategy.” In: *European Commission, Directorate General for Energy, September 2017, 226 pp* (2017). URL: [https://ec.europa.eu/energy/sites/ener/files/documents/follow\\_up\\_study\\_lng\\_storage\\_final\\_01.pdf](https://ec.europa.eu/energy/sites/ener/files/documents/follow_up_study_lng_storage_final_01.pdf).
- [136] Felix Höffler and Madjid Kübler. “Demand for storage of natural gas in northwestern Europe: Trends 2005–30.” In: *Energy Policy* 35.10 (2007), pp. 5206–5219. DOI: [10.2139/ssrn.906992](https://doi.org/10.2139/ssrn.906992).
- [137] AF Correlje. “Seasonal flexibility in the Northwest European gas market: An outlook for 2015 and 2020.” In: *Clingendael Energy Paper* (2011).
- [138] Kjetil Trovik Midthun. *Optimization models for liberalized natural gas markets*. Fakultet for samfunnsvitenskap og teknologiledelse, 2007.
- [139] Alberto Herrán-González, Jesus M. De La Cruz, Bonifacio De Andrés-Toro, and José Luis Risco-Martín. “Modeling and simulation of a gas distribution pipeline network.” In: *Applied Mathematical Modelling* 33.3 (2009), pp. 1584–1600. DOI: [10.1016/j.apm.2008.02.012](https://doi.org/10.1016/j.apm.2008.02.012).
- [140] Yue Qiu, Sara Grundel, Martin Stoll, and Peter Benner. “Efficient numerical methods for gas network modeling and simulation.” In: *arXiv preprint arXiv:1807.07142* (2018). URL: <http://arxiv.org/abs/1807.07142>.
- [141] ENTSO-G. *Capacity Map*. 2017. URL: <https://www.entsog.eu/maps/transmission-capacity-map/2017>.

- [142] Team Consult. *Market study: A glimpse at the landscape of European LNG regasification infrastructure*. 2017.
- [143] Howard Rogers. "The LNG Shipping Forecast: costs rebounding, outlook uncertain." In: *OIES Energy Insight* 27 (2018).
- [144] CEER. "CEER Vision on the Regulatory Arrangements for the Gas Storage Market. Council of European Energy Regulators." In: *Public Consultation Paper Ref: C14-GWG-112-03* (2014).
- [145] Gasunie Transport Services. *Gas Extraction in Groningen to Dip below 10bcm next Gas Year*. 2020. URL: <https://www.gasunietransportservices.nl/en/news/gas-extraction-in-groningen-to-dip-below-10bcm-next-gas-year>.
- [146] Chris N Le Fevre. "Gas storage in Great Britain." In: NG72 (2013). DOI: [10.26889/9781907555657](https://doi.org/10.26889/9781907555657).
- [147] IEA. *Natural gas information 2019*. Tech. rep. Paris: International Energy Agency, 2019.
- [148] Mike Fulwood. *Energy Transition: Modelling the Impact on Natural Gas*. Tech. rep. July. Oxford: Oxford Institute for Energy Studies, 2021.
- [149] Yves SMEERS. "Gas models and three difficult objectives." In: *LIDAM Discussion Papers*, Université catholique de Louvain, Center for Operations Research and Econometrics (CORE) (2008). URL: <https://ideas.repec.org/p/cor/louvco/2008009.html>.
- [150] European Commission. *The European energy security strategy*. Tech. rep. Brussels, Belgium, 2014. DOI: [10.4324/9781315455297-11](https://doi.org/10.4324/9781315455297-11).
- [151] Artelys. *An updated analysis on gas supply security in the EU energy transition*. Tech. rep. Paris: Artelys Optimization Solutions, 2020.
- [152] Dimitris Bertsimas, Eugene Litvinov, Xu Andy Sun, Jinye Zhao, and Tongxin Zheng. "Adaptive Robust Optimization for the Security Constrained Unit Commitment Problem." In: *IEEE Transactions on Power Systems* 28.1 (2013), pp. 52–63. DOI: [10.1109/TPWRS.2012.2205021](https://doi.org/10.1109/TPWRS.2012.2205021).
- [153] Xiufeng Yue, Steve Pye, Joseph DeCarolis, Francis G.N. Li, Fionn Rogan, and Brian Gallachoir. "A review of approaches to uncertainty assessment in energy system optimization models." In: *Energy Strategy Reviews* 21.June (2018), pp. 204–217. ISSN: 2211467X. DOI: [10.1016/j.esr.2018.06.003](https://doi.org/10.1016/j.esr.2018.06.003).

- [154] Hao Cong, Yang He, Xu Wang, and Chuanwen Jiang. "Robust optimization for improving resilience of integrated energy systems with electricity and natural gas infrastructures." In: *Journal of Modern Power Systems and Clean Energy* 6.5 (2018), pp. 1066–1078. ISSN: 21965420. DOI: [10.1007/s40565-018-0377-5](https://doi.org/10.1007/s40565-018-0377-5).
- [155] Denis Aßmann, Frauke Liers, and Michael Stingl. "Decomposable robust two-stage optimization: An application to gas network operations under uncertainty." In: *Networks* 74.1 (2019), pp. 40–61. ISSN: 10970037. DOI: [10.1002/net.21871](https://doi.org/10.1002/net.21871).
- [156] Robert J. Lempert, Steven W. Popper, and Steven C. Bankes. *Shaping the Next One Hundred Years: New Methods for Quantitative, Long-Term Policy Analysis*. Vol. 4. 4. RAND, 2003. ISBN: 0833032755. DOI: [10.5465/amle.2005.19086797](https://doi.org/10.5465/amle.2005.19086797).
- [157] Tobias Junne, Mengzhu Xiao, Lei Xu, Zongfei Wang, Patrick Jochem, and Thomas Pregger. "How to assess the quality and transparency of energy scenarios: Results of a case study." In: *Energy Strategy Reviews* 26.July (2019). ISSN: 2211467X. DOI: [10.1016/j.esr.2019.100380](https://doi.org/10.1016/j.esr.2019.100380).
- [158] Peter Kall and Stein W. Wallace. *Stochastic Programming*. John Wiley and Sons Ltd, 1994. ISBN: 9780471951087.
- [159] Stein W. Wallace and Stein Erik Fleten. "Stochastic Programming Models in Energy." In: *Handbooks in Operations Research and Management Science* 10.C (2003), pp. 637–677. ISSN: 09270507. DOI: [10.1016/S0927-0507\(03\)10010-2](https://doi.org/10.1016/S0927-0507(03)10010-2).
- [160] Dominik Möst and Dogan Keles. "A survey of stochastic modelling approaches for liberalised electricity markets." In: *European Journal of Operational Research* 207.2 (2010), pp. 543–556. ISSN: 03772217. DOI: [10.1016/j.ejor.2009.11.007](https://doi.org/10.1016/j.ejor.2009.11.007).
- [161] Seán Collins, John Paul Deane, Kris Poncelet, Evangelos Panos, Robert C. Pietzcker, Erik Delarue, and Brian Pádraig Ó Gallachóir. "Integrating short term variations of the power system into integrated energy system models: A methodological review." In: *Renewable and Sustainable Energy Reviews* 76.January (2017), pp. 839–856. ISSN: 18790690. DOI: [10.1016/j.rser.2017.03.090](https://doi.org/10.1016/j.rser.2017.03.090).
- [162] Terje Aven. "On the meaning of a black swan in a risk context." In: *Safety Science* 57 (2013), pp. 44–51. ISSN: 09257535. DOI: [10.1016/j.ssci.2013.01.016](https://doi.org/10.1016/j.ssci.2013.01.016).
- [163] A L Soyster. "Programming with Set- Inclusive Constraints and Applications to Inexact Linear Programming." In: *Operations Research* 21.2 (1973), pp. 1154–1157. DOI: [10.1287/opre.21.5.1154](https://doi.org/10.1287/opre.21.5.1154).

- [164] Bo Zeng and Long Zhao. "Solving two-stage robust optimization problems using a column-and- constraint generation method." In: *Operations Research Letters* 41.5 (2013), pp. 457–461. ISSN: 01676377. DOI: [10.1016/j.orl.2013.05.003](https://doi.org/10.1016/j.orl.2013.05.003).
- [165] Nikolaos H. Lappas and Chrysanthos E. Gounaris. "Robust optimization for decision-making under endogenous uncertainty." In: *Computers and Chemical Engineering* 111 (2018), pp. 252–266. ISSN: 00981354. DOI: [10.1016/j.compchemeng.2018.01.006](https://doi.org/10.1016/j.compchemeng.2018.01.006).
- [166] Dimitris Bertsimas, David B. Brown, and Constantine Caramanis. "Theory and applications of robust optimization." In: *SIAM Review* 53.3 (2011), pp. 464–501. ISSN: 00361445. DOI: [10.1137/080734510](https://doi.org/10.1137/080734510).
- [167] Ihsan Yanikoglu, Bram L. Gorissen, and Dick den Hertog. "A survey of adjustable robust optimization." In: *European Journal of Operational Research* 277.3 (2019), pp. 799–813. ISSN: 03772217. DOI: [10.1016/j.ejor.2018.08.031](https://doi.org/10.1016/j.ejor.2018.08.031).
- [168] Alvaro Lorca, X. Andy Sun, Eugene Litvinov, and Tongxin Zheng. "Multistage adaptive robust optimization for the unit commitment problem." In: *Operations Research* 64.1 (2016), pp. 32–51. DOI: [10.1287/opre.2015.1456](https://doi.org/10.1287/opre.2015.1456).
- [169] Yizhou Zhou, Zhinong Wei, Guoqiang Sun, Kwok W. Cheung, Haixiang Zang, and Sheng Chen. "A robust optimization approach for integrated community energy system in energy and ancillary service markets." In: *Energy* 148 (2018), pp. 1–15. ISSN: 03605442. DOI: [10.1016/j.energy.2018.01.078](https://doi.org/10.1016/j.energy.2018.01.078).
- [170] Li Yao, Xiuli Wang, Tao Qian, Shixiong Qi, and Chengzhi Zhu. "Robust day-ahead scheduling of electricity and natural gas systems via a risk-averse adjustable uncertainty set approach." In: *Sustainability (Switzerland)* 10.11 (2018). ISSN: 20711050. DOI: [10.3390/su10113848](https://doi.org/10.3390/su10113848).
- [171] Carlos Ruiz and Antonio J. Conejo. "Robust transmission expansion planning." In: *European Journal of Operational Research* 242.2 (2015), pp. 390–401. ISSN: 03772217. DOI: [10.1016/j.ejor.2014.10.030](https://doi.org/10.1016/j.ejor.2014.10.030).
- [172] Raquel García-Bertrand and Roberto Mínguez. "Dynamic Robust Transmission Expansion Planning." In: *IEEE Transactions on Power Systems* 32.4 (2017), pp. 2618–2628. ISSN: 08858950. DOI: [10.1109/TPWRS.2016.2629266](https://doi.org/10.1109/TPWRS.2016.2629266).
- [173] Luis Baringo and Ana Baringo. "A stochastic adaptive robust optimization approach for the generation and transmission expansion planning." In: *IEEE Transactions on Power Systems* 33.1 (2018), pp. 792–802. ISSN: 08858950. DOI: [10.1109/TPWRS.2017.2713486](https://doi.org/10.1109/TPWRS.2017.2713486).

- [174] Luis Baringo, Luigi Boffino, and Giorgia Oggioni. "Robust expansion planning of a distribution system with electric vehicles, storage and renewable units." In: *Applied Energy* 265 (February 2020), p. 114679. ISSN: 03062619. DOI: [10.1016/j.apenergy.2020.114679](https://doi.org/10.1016/j.apenergy.2020.114679).
- [175] Ruud Egging. "Benders Decomposition for multi-stage stochastic mixed complementarity problems – Applied to a global natural gas market model." In: *European Journal of Operational Research* 226.2 (2013), pp. 341–353. ISSN: 0377-2217. DOI: [10.1016/j.ejor.2012.11.024](https://doi.org/10.1016/j.ejor.2012.11.024).
- [176] Philipp Hauser. "Does 'more' equal 'better'? – Analyzing the impact of diversification strategies on infrastructure in the European gas market." In: *Energy Policy* 153 (2021), p. 112232. ISSN: 0301-4215. DOI: [10.1016/j.enpol.2021.112232](https://doi.org/10.1016/j.enpol.2021.112232).
- [177] Iegor Riepin, Thomas Möbius, and Felix Müsgens. "Modelling uncertainty in coupled electricity and gas systems—Is it worth the effort?" In: *Applied Energy* 285 (2021), p. 116363. ISSN: 0306-2619. DOI: [10.1016/j.apenergy.2020.116363](https://doi.org/10.1016/j.apenergy.2020.116363).
- [178] Ibrahim Abada and Olivier Massol. "Security of supply and retail competition in the European gas market." In: *Energy Policy* 39.7 (2011), pp. 4077–4088. ISSN: 03014215. DOI: [10.1016/j.enpol.2011.03.043](https://doi.org/10.1016/j.enpol.2011.03.043).
- [179] Caroline Dieckhoener. "Simulating Security of Supply Effects of the Nabucco and South Stream Projects for the European Natural Gas Market." In: *The Energy Journal* 33.3 (2012), pp. 153–181. URL: <http://dx.doi.org/10.5547/019>.
- [180] Ruud Egging and Franziska Holz. "Risks in global natural gas markets: Investment, hedging and trade." In: *Energy Policy* 94 (2016), pp. 468–479. ISSN: 03014215. DOI: [10.1016/j.enpol.2016.02.016](https://doi.org/10.1016/j.enpol.2016.02.016).
- [181] Tobias Baltensperger, Rudolf M. Füchslin, Pius Krütli, and John Lygeros. "European Union gas market development." In: *Energy Economics* 66 (2017), pp. 466–479. ISSN: 0140-9883. DOI: [10.1016/J.ENERCO.2017.07.002](https://doi.org/10.1016/J.ENERCO.2017.07.002).
- [182] Bokan Chen. "Applications of optimization under uncertainty methods on power system planning problems." Doctoral Thesis. 2016. URL: <https://dr.lib.iastate.edu/handle/20.500.12876/30694>.
- [183] Rabih A. Jabr. "Robust Transmission Network Expansion Planning With Uncertain Renewable Generation and Loads." In: *IEEE Transactions on Power Systems* 28.4 (2013), pp. 4558–4567. DOI: [10.1109/TPWRS.2013.2267058](https://doi.org/10.1109/TPWRS.2013.2267058).

- [184] Roberto Mínguez and Raquel García-Bertrand. “Robust transmission network expansion planning in energy systems: Improving computational performance.” In: *European Journal of Operational Research* 248.1 (2016), pp. 21–32. ISSN: 03772217. DOI: [10.1016/j.ejor.2015.06.068](https://doi.org/10.1016/j.ejor.2015.06.068).
- [185] Ana Baringo, Luis Baringo, and José M. Arroyo. “Day-Ahead Self-Scheduling of a Virtual Power Plant in Energy and Reserve Electricity Markets Under Uncertainty.” In: *IEEE Transactions on Power Systems* 34.3 (2019), pp. 1881–1894. DOI: [10.1109/TPWRS.2018.2883753](https://doi.org/10.1109/TPWRS.2018.2883753).
- [186] Noemi G. Cobos, José M. Arroyo, and Alexandre Street. “Least-Cost Reserve Offer Deliverability in Day-Ahead Generation Scheduling Under Wind Uncertainty and Generation and Network Outages.” In: *IEEE Transactions on Smart Grid* 9.4 (2018), pp. 3430–3442. DOI: [10.1109/TSG.2016.2632622](https://doi.org/10.1109/TSG.2016.2632622).
- [187] Chaoyue Zhao, Jianhui Wang, Jean-Paul Watson, and Yongpei Guan. “Multi-Stage Robust Unit Commitment Considering Wind and Demand Response Uncertainties.” In: *IEEE Transactions on Power Systems* 28.3 (2013), pp. 2708–2717. DOI: [10.1109/TPWRS.2013.2244231](https://doi.org/10.1109/TPWRS.2013.2244231).
- [188] Antonio J. Conejo, Luis Baringo, Jalal Kazempour, and Afzal S. Siddiqui. *Investment in electricity generation and transmission: Decision making under uncertainty*. 2016, pp. 1–384. ISBN: 9783319295015. DOI: [10.1007/978-3-319-29501-5](https://doi.org/10.1007/978-3-319-29501-5).
- [189] ENTSO-G. *TYNDP 2020 Scenario Building Guidelines*. Tech. rep. June. ENTSO-G, 2020. URL: <https://2020.entsos-tyndp-scenarios.eu>.
- [190] Eurostat. *European Statistics: Energy, transport and environment indicators*. 2020. URL: <https://ec.europa.eu/eurostat/web/energy/data/database>.
- [191] European Commission. *Key cross border infrastructure projects*. Brussels, 2021. URL: [https://ec.europa.eu/energy/topics/infrastructure/projects-common-interest/key-cross-border-infrastructure-projects\\_en](https://ec.europa.eu/energy/topics/infrastructure/projects-common-interest/key-cross-border-infrastructure-projects_en).
- [192] ACER. *Consolidated Report on the Progress of Electricity and Gas Projects of Common Interest - 2019*. Tech. rep. Ljubljana: Agency for the Cooperation of Energy Regulators, 2019.
- [193] Oil Change International. *Gas and the European Investment Bank: Why New Gas Infrastructure Investment Is Incompatible with Climate Goals*. Tech. rep. Washington, D.C.: Oil Change International, 2019.
- [194] Three Seas Initiative. *Priority Interconnection Projects: 2019 Status Report*. Slovenia, 2019.



- [195] European Union. *Projects of common interest – Interactive map*. 2020. URL: [https://ec.europa.eu/energy/infrastructure/transparency\\_platform/map-viewer/main.html](https://ec.europa.eu/energy/infrastructure/transparency_platform/map-viewer/main.html).
- [196] Global Energy Monitor. *Global Fossil Infrastructure Tracker*. 2021. URL: <https://globalenergymonitor.org/projects/global-fossil-infrastructure-tracker/>.
- [197] ENTSO-G. *TYNDP 2020 Scenario Report*. Tech. rep. ENTSO-G, 2020. URL: <https://www.entsog.eu/tyndp#entsog-ten-year-network-development-plan-2020>.
- [198] Simon Pirani and Jack Sharples. “The Russia-Ukraine gas transit deal: opening a new chapter.” In: *Energy Insight* 64 (2020), pp. 1–9.
- [199] BEIS. *Fossil Fuel Supply Curves*. Tech. rep. London: UK Department for Business, Energy & Industrial Strategy, 2016. URL: <https://www.gov.uk/government/publications/fossil-fuel-price-assumptions-2016>.
- [200] European Commission. *Project of common interest 6.23. PCI fiche: Hungary – Slovenia - Italy interconnection*. Tech. rep. Feb. 2021. URL: [https://ec.europa.eu/energy/maps/pci\\_fiches/PciFiche\\_6.23.pdf](https://ec.europa.eu/energy/maps/pci_fiches/PciFiche_6.23.pdf).
- [201] Eustream. *Project of common interest (PCI) No. 6.2.1: Poland – Slovakia Interconnection, Eustream (Slovak Gas TSO)*. 2021. URL: [https://www.eustream.sk/en\\_transmission-system/en\\_pl-sk-interconnector/en\\_project-of-common-interest-pci](https://www.eustream.sk/en_transmission-system/en_pl-sk-interconnector/en_project-of-common-interest-pci).
- [202] Energy Community. *Gas 14: Gas interconnection Poland-Ukraine*. 2021. URL: <https://www.energy-community.org/regionalinitiatives/infrastructure/PLIMA>.
- [203] Rolf Golombek, Eystein Gjelsvik, and Knut Einar Rosendahl. “Effects of liberalizing the natural gas markets in Western Europe.” In: *The Energy Journal* 16.1 (1995). DOI: [10.5547/ISSN0195-6574-EJ-Vol16-No1-6](https://doi.org/10.5547/ISSN0195-6574-EJ-Vol16-No1-6).
- [204] Daniel Huppmann. “Endogenous investment decisions in natural gas equilibrium models with logarithmic cost functions.” In: *DIW Berlin Discussion Paper No. 1253* (2012). DOI: [10.2139/ssrn.2175648](https://doi.org/10.2139/ssrn.2175648).
- [205] Gijsbert Zwart and Machiel Mulder. *NATGAS: a model of the European natural gas market*. 2006.
- [206] Stefan Lochner and David Bothe. “From Russia with gas: an analysis of the Nord Stream pipeline’s impact on the European Gas Transmission System with the TIGER-Model.” In: *EWI Working Paper, No 07.02* 07.02 (2007), pp. 1–16.

- [207] Gijsbert T.J. Zwart. "European Natural Gas Markets: Resource Constraints and Market Power." In: *The Energy Journal* 30.2009 (2009), pp. 151–165. URL: [www.jstor.org/stable/41323201](http://www.jstor.org/stable/41323201).
- [208] Anne Neumann, Norman Viehrig, and Hannes Weigt. "InTra-Gas - A Stylized Model of the European Natural Gas Network." In: *SSRN Electronic Journal* (2009).
- [209] Stefan Lochner, Caroline Dieckhoener, and Dietmar Lindenberger. *Model-based Analysis of Infrastructure Projects and Market Integration in Europe with Special Focus on Security of Supply Scenarios*. Tech. rep. Institute of Energy Economics at the University of Cologne (EWI), 2010.
- [210] Ibrahim Abada and Pierre-André Jouvét. "A stochastic generalized Nash-Cournot model for the northwestern European natural gas markets: The S-GaMMES model." Paris, 2012. URL: <https://ideas.repec.org/p/cec/wpaper/1308.html>.
- [211] Caroline Dieckhoener, Stefan Lochner, and Dietmar Lindenberger. "European natural gas infrastructure: The impact of market developments on gas flows and physical market integration." In: *Applied Energy* 102.2013 (2013), pp. 994–1003. ISSN: 03062619. DOI: [10.1016/j.apenergy.2012.06.021](https://doi.org/10.1016/j.apenergy.2012.06.021).
- [212] Maria Flouri, Charikleia Karakosta, Charikleia Kladouchou, and John Psarras. "How does a natural gas supply interruption affect the EU gas security? A Monte Carlo simulation." In: *Renewable and Sustainable Energy Reviews* 44 (2015), pp. 785–796. ISSN: 18790690. DOI: [10.1016/j.rser.2014.12.029](https://doi.org/10.1016/j.rser.2014.12.029).
- [213] András Kiss, Adrienn Selei, and Borbála Takácsné Tóth. "A Top-Down Approach to Evaluating Cross-Border Natural Gas Infrastructure Projects in Europe." In: *The Energy Journal* 37.3 (2016), pp. 61–79. DOI: [doi.org/10.5547/0195655](https://doi.org/10.5547/0195655).
- [214] Harald Hecking and Florian Weiser. *Impacts of Nord Stream 2 on the EU natural gas market*. Tech. rep. ewi Energy Research & Scenarios, 2017. URL: <https://www.ewi.uni-koeln.de/en/publications/impacts-of-nord-stream-2-on-the-eu-natural-gas-market>.
- [215] Ruud Egging, Alois Pichler, Øyvind Iversen Kalvø, and Thomas Meyer Walle-Hansen. "Risk aversion in imperfect natural gas markets." In: *European Journal of Operational Research* 259.1 (2017), pp. 367–383. ISSN: 03772217. DOI: [10.1016/j.ejor.2016.10.020](https://doi.org/10.1016/j.ejor.2016.10.020).
- [216] Shi Xunpeng, Hari Malamakkavu Padinjare Variam, and Jacqueline Tao. "Global impact of uncertainties in China's gas market." In: *Energy Policy* 104.October 2016 (2017), pp. 382–394. ISSN: 03014215. DOI: [10.1016/j.enpol.2017.02.015](https://doi.org/10.1016/j.enpol.2017.02.015).

- [217] Jan Abrell, Léo Chavaz, and Hannes Weigt. *Dealing with Supply Disruptions on the European Natural Gas Market: Infrastructure Investments or Coordinated Policies?* 1155002547. 2019. ISBN: 1155002547. DOI: [10.2139/ssrn.3425739](https://doi.org/10.2139/ssrn.3425739).
- [218] Marzia Sesini, Sara Giarola, and Adam D. Hawkes. "The impact of liquefied natural gas and storage on the EU natural gas infrastructure resilience." In: *Energy* 209 (2020), p. 118367. ISSN: 03605442. DOI: [10.1016/j.energy.2020.118367](https://doi.org/10.1016/j.energy.2020.118367).